Universidade de Aveiro Departamento de Química
2010

ANABEL TABARE DE OLIVEIRA

DESSULFURAÇÃO DE COMBUSTÍVEIS UTILIZANDO LÍQUIDOS IÓNICOS

DESULFURIZATION OF FUELS USING IONIC LIQUIDS

Universidade de Aveiro Departamento de Química
2010

ANABEL TABARE DE OLIVEIRA

DESSULFURAÇÃO DE COMBUSTÍVEIS UTILIZANDO LÍQUIDOS IÓNICOS

DESULFURIZATION OF FUELS USING IONIC LIQUIDS

Dissertação apresentada à Universidade de Aveiro para cumprimento dos requisitos necessários à obtenção do grau de Mestre em Engenharia Química, realizada sob a orientação científica do Doutor João Araújo Pereira Coutinho, Professor Associado com Agregação do Departamento de Química da Universidade de Aveiro e co-orientação da Doutora Luciana Isabel Nabais Tomé, Estagiária de Pós-Doutoramento do Departamento de Química da Universidade de Aveiro.

Dedico este trabalho a todos os que me apoiaram incondicionalmente.

“Deus quer, o Homem sonha e a obra nasce”
Fernando Pessoa

o júri

presidente

Professora Doutora Ana Maria Rebelo Barreto Xavier
Professora auxiliar do Departamento de Química da Universidade de Aveiro

Professor Doutor João Manuel da Costa e Araújo Pereira Coutinho
Professor associado com agregação do Departamento de Química da Universidade de Aveiro

Doutora Luciana Isabel Nabais Tomé
Estagiária de Pós-Doutoramento do Departamento de Química da Universidade de Aveiro

Doutora Mara Guadalupe Freire Martins
Estagiária de Pós-Doutoramento no Instituto de Tecnologia Química e Biológica, ITQB2, Universidade Nova de Lisboa

agradecimentos

Chegar aqui após um longo e intenso ano traz-me uma imensa felicidade, já que este trabalho é o culminar de um percurso de cinco anos. Eis que chegou o momento de dividi-la com as pessoas que contribuíram para conquistar mais esta vitória tão importante para mim.

Em primeiro lugar, agradeço ao meu orientador Professor João Coutinho, pela oportunidade para desenvolver este trabalho e pelo apoio dado ao longo do ano.

À Luciana, pela competência com que orientou o meu trabalho, pelo tempo que generosamente me dedicou, transmitindo-me os melhores e mais úteis ensinamentos com paciência, pela motivação e confiança depositadas em mim mesmo quando as coisas pareciam não correr bem, tudo isto constituíram os pilares deste trabalho.

À Maria Jorge pela disponibilidade para fechar ampolas, à Ana Rute pelos dias dedicados a COSMOtolitar e ao Bernd pelos compostos virtuais gentilmente cedidos.

Aos membros do Path pelos convívios e espírito de inter-ajuda sempre presentes.

Aos meus colegas com quem convivi e estudei ao longo do curso: À Ana pelas longas conversas ao telefone em que nunca faltavam palavras de apoio mesmo quando estava mais desanimada. À Filipa pela energia positiva e pelo carinho demonstrados. À Noemi, Filipe, Cláudia, Ana Margarida, Sandra, Raquel e às minhas afilhadas Bianca e Catarina. A todos agradeço o convívio e amizade cultivados e o apoio mútuo que em especial se gerou durante este ano. Aos meus amigos pelos momentos de diversão e descontracção, que me fizeram acreditar que era possível chegar ao fim com sucesso. À Mena, Comandante e Judite agradeço-vos pelo carinho e apoio!

O meu maior agradecimento é dirigido aos meus Pais, pela formação que me puderam proporcionar e por terem sido o apoio contínuo: À minha mãe que sempre me aplaudiu nos momentos de glória e me encorajou nos momentos difíceis para lutar sempre. Ao meu pai que me cultivou a importância da construção de um carácter próprio para enfrentar a vida. Que este trabalho seja também uma vitória vossa, a prova de que o vosso esforço foi recompensado. Aos meus irmãos Aníbal e Angelo que sempre torceram por mim. Até a ti Sacana, pelas vezes que regressava a casa e estavas à janela e assim que me vias, corrias para mim. Mesmo quando te levava à rua, eram momentos de descontracção que eu disfrutava.

Aos meus tios, padrinhos e primos que me deram força, valorizando o meu potencial. À minha família Venezuelana, criadora do lençol mais bonito do dia do enterro, o qual exibi com muito orgulho e cujo apoio, apesar da distância, foi notável.

Aos pais do Tiago pelo carinho e apoio sentidos: os belos petiscos e sobremesas (ai aquela mousse au chocolat...) que tanta energia (e kilinhos…) me transmitiram.

A ti Tiago, meu querido amigo e namorado, agradeço-te pelo apoio genuíno, pela tua presença constante nos momentos mais complicados, incluindo aqueles em que pacientemente suportaste dias trocados por noites sempre ao meu lado nas crises (especialmente informáticas…), por aquele abraço… Obrigada por existires na minha vida, e pelos momentos de alegria que faço questão de dividir contigo!

A todos, o meu MUITO OBRIGADA, do fundo do coração!!

"Aqueles que passam por nós, não vão sós, não nos deixam sós.
Deixam um pouco de si, levam um pouco de nós."
Antoine de Saint-Exupéri

palavras-chave

Dessulfuração, líquidos iónicos, equilíbrio líquido-líquido, compostos sulfurados, COSMO-RS

resumo

Actualmente, é crucial a redução do conteúdo de compostos sulfurados nos combustíveis, uma vez que os organismos governamentais estão a implementar legislações cada vez mais rígidas para diminuir impactos ambientais negativos. Por esta razão, torna-se fundamental desenvolver processos de dessulfuração apropriados e eficientes, no sentido de se corresponder às regulamentações actuais e futuras.

O processo mais utilizado para a remoção de compostos sulfurados (S-compostos) tem sido a hidrodessulfuração, mas esta é ineficiente e dispendiosa, pelo que se torna importante desenvolver novas alternativas. Dentro das várias propostas sugeridas, a extracção líquido-líquido utilizando líquidos iónicos (LIs) provou ser uma das mais promissoras.

Para uma aplicação bem sucedida dos LIs como solventes nos procedimentos de dessulfuração, e para a concepção de processos e equipamento, é crucial que os dados de equilíbrio líquido-líquido (ELL) de sistemas envolvendo LIs, aromáticos e hidrocarbonetos (HCs) estejam disponíveis, para que se possa identificar as melhores condições e os LIs mais convenientes. Estes devem ter algumas características definidas, tais como imiscibilidade com HCs, assim como uma boa capacidade e selectividade para os compostos aromáticos sulfurados.

Embora os dados de ELL em sistemas binários e ternários envolvendo LIs, S-compostos e HCs, assim como a informação sobre os efeitos da natureza destes componentes estejam disponíveis na literatura, os dados de solubilidade continuam a ser muito escassos e o número de LIs considerados é reduzido. Tendo em conta as necessidades actuais, torna-se relevante desenvolver estudos adicionais.

O objectivo deste trabalho é identificar LIs com potencial para serem aplicados na dessulfuração de combustíveis. Neste sentido, diagramas de fase de sistemas binários envolvendo LIs baseados no catião imidazólio e tiofeno (considerado como modelo de S-composto) foram determinados experimentalmente e previstos com o modelo COSMO-RS (modelo para solventes reais). Os diagramas de fase para sistemas ternários compreendendo LIs, S-compostos e hidrocarbonetos (representativo dos componentes do combustível) foram também calculados utilizando este modelo.

Os dados de ELL permitiram avaliar o efeito das características estruturais dos LIs nas solubilidades mútuas e concluir sobre os factores que influenciam a selectividade dos LIs e a sua capacidade de extracção dos S-compostos aromáticos a partir das suas misturas com HC nos processos de dessulfuração. Através da comparação dos diagramas de fase de LLE utilizando COSMO-RS com dados experimentais disponíveis, foi possível testar a capacidade do modelo para descrever e prever o comportamento de fase para este tipo de sistemas.

keywords Desulfurization, ionic liquids, liquid-liquid equilibrium, thiophene-derivatives, COSMO-RS

abstract

Nowadays, the reduction of the sulfur content in fuels is mandatory since governments are implementing increasingly rigid legislations to decrease negative environmental impacts. For this reason, it is crucial to develop appropriate and efficient desulfurization processes in order to meet the current and upcoming regulations.

The process most used for the removal of sulphur compounds (S-compounds) has been hydrodesulfurization, but it is inefficient and expensive, being thus important to develop new alternatives. Among the several approaches proposed, the liquid-liquid extraction using ionic liquids (ILs) has proved to be one of the most promising.

For the successful application of ILs as solvents in desulfurization procedures and for the correct design of processes and equipment, it is vital that data on the liquid-liquid equilibrium (LLE) of systems involving ILs, aromatics and hydrocarbons (HCs) are available, in order to identify the best conditions and more convenient ILs to be used. These should have some defined characteristics like immiscibility with the HCs and a good extraction capability and selectivity for the sulphur aromatic compounds.

Although LLE data on binary and ternary systems involving ILs, S-compounds and HCs, as well as information on the effects of the nature of these components, are available in literature, the solubility data are still quite scarce and the number of ILs considered is reduced. Regarding the current demands, it is therefore important to develop further studies.

The objective of the present work is to identify ILs with potential to be applied in the desulfurization of fuel oils. For this purpose, phase diagrams of binary systems comprising imidazolium-based ILs and thiophene (taken as model S-compound) were experimentally determined and predicted with the COSMO-RS model (conductor-like screening model for real solvents). The phase diagrams of ternary systems containing ILs, S-compounds and HCs (representative of the components of the fuel) were also calculated using this model.

The LLE data enabled to evaluate the effect of the structural characteristics of the ILs, S-compounds and HCs on the mutual solubilities between these compounds and conclude about the factors that influence the selectivity of the ILs and their extraction capability of aromatic S-compounds from their mixtures with HC in desulfurization processes. By comparing the LLE phase diagrams calculated using COSMO-RS with available experimental data, it was possible to test the ability of this model to describe and predict the phase behaviour of this type of systems.

Contents

List of figures

List of tables

Nomenclature

List of Symbols

a_{eff}	effective contact area between two surface segments, (Å^2)
A_S	total surface area, (Å^2)
A^{X_i}	total surface area of molecule X_i , (Å^2)
c_{HB}	hydrogen bond strength coefficient, ((kJ.Å^4)/(mol.e^2))
E_{HB}	hydrogen bonding energy, (kJ/mol)
E_{misfit}	electrostatic misfit energy, (kJ/mol)
E_{vdW}	van der Waals energy, (kJ/mol)
K_S	sulfur partition coefficient, mol(S) kg(IL)$^{-1}$/mol(S) kg(oil)$^{-1}$
$p_S(\sigma)$	sigma profile of a solvent
$p^{X_i}(\sigma)$	sigma profile of a solute *i*
$p'_S(\sigma)$	normalised sigma profile of a solvent
R	ideal gas constant, kJ/(mol. K)
S	solvent
T	Temperature, K
x_i	mole fraction of compound *i*
X_i	*i* molecule considered as solute
x_{IL}	ionic liquid mole fraction

Greek letters

α'	electrostatic misfit interactions coefficient, kJ/(mol.Å^2)
$\mu_S(\sigma)$	chemical potential of a surface segment, kJ/(mol.Å^2)
$\mu_S^{X_i}$	pseudo-chemical potential of the component X_i in a solvent, kJ/(mol.Å^2)
$\mu_{C,S}^{X_i}$	combinatorial contribution term of different sizes and shapes of the molecules, kJ/(mol.Å^2)
σ	polarization charge density, e/Å^2
σ'	polarization charge density, e/Å^2
$\sigma_{acceptor}$	polarization charge of an hydrogen bonding acceptor, e/Å^2
σ_{donor}	polarization charge of an hydrogen bonding donor, e/Å^2
σ_{HB}	hydrogen bonding threshold, e/Å^2
τ_{vdW}, τ'_{vdW}	element-specific van der Waals coefficients, kJ/(mol.Å^2)

Abbreviations

3-MT	3-methylthiophene
4-MDBT	4-methyldibenzothiophene
4,6-DMDBT	4,6-dimethyldibenzothiophene
BDS	biodesulfurization
BT	benzothiophene
COSMO-RS	conductor-like screening model for real solvents
DBT	dibenzothiophene
EDS	extractive desulfurization
EoS	equation of state
GCMs	structure-interpolating group-contribution methods
HCs	hydrocarbons
HDS	hydrodesulfurization
ILs	ionic liquids
LCST	lower critical solution temperature
LLE	liquid-liquid equilibrium
N-compounds	nitrogen compounds
NMR	nuclear magnetic resonance
NRTL	non-Random Two Liquid model
ppm	parts-per-million
Py	pyridine
TP	thiophene
S-compounds	sulfur compounds
SLE	solid-liquid equilibrium
VOCs	volatile organic compounds
UNIQUAC	universal quasichemical model
UCST	upper critical solution temperature
[amim][PF_6]	1-allyl-3-methylimidazolium hexafluorophosphate
[C_1mim][$MeSO_4$]	1,3-dimethylimidazolium methylsulfate
[C_1mim][$DMPO_4$]	1,3-dimethylimidazolium dimethylphosphate
[C_1mim][MP]	1,3-dimethylimidazolium methylphosphonate
[C_2mim][BF_4]	1-ethyl-3-methylimidazolium tetrafluoroborate

$[C_2mim]Cl$	1-ethyl-3-methylimidazolium chloride
$[C_2mim][NTf_2]$	1-ethyl-3-methylimidazolium bis(trifluoromethylsulfonyl)imide
$[C_2mim][N(CN)_2]$	1-ethyl-3-methylimidazolium dicyanamide
$[C_2mim][DEPO_4]$	1-ethyl-3-methylimidazolium diethylphosphate
$[C_2mim][SCN]$	1-ethyl-3-methylimidazolium thiocyanate
$[C_2mim][MeSO_4]$	1-ethyl-3-methylimidazolium methylsulfate
$[C_2mim][DMPO_4]$	1-ethyl-3-methylimidazolium dimethylphosphate
$[C_2mim][EtSO_4]$	1-ethyl-3-methylimidazolium ethylsulfate
$[C_2C_2im][EtSO_4]$	1,3-diethylimidazolium ethylsulfate
$[C_2C_2im][DEPO_4]$	1,3-diethylimidazolium diethylphosphate
$[C_4mim][SCN]$	1-butyl-3-methylimidazolium thiocyanate
$[C_4mim]Cl$	1-butyl-3-methylimidazolium chloride
$[C_4mim][BF_4]$	1-butyl-3-methylimidazolium tetrafluoroborate
$[C_4mim][N(CN)_2]$	1-butyl-3-methylimidazolium dicyanamide
$[C_4mim][NTf_2]$	1-butyl-3-methylimidazolium bis(trifluoromethylsulfonyl)imide
$[C_4mim][OcSO_4]$	1-butyl-3-methylimidazolium octylsulfate
$[C_4mim][PF_6]$	1-butyl-3-methylimidazolium hexafluorophosphate
$[C_4mim][MeSO_4]$	1-butyl-3-methylimidazolium methylsulfate
$[C_4mim][Cu_2Cl_3]$	1-butyl-3-methylimidazolium chlorocuprate
$[C_4mim][FeCl_4]$	1-butyl-3-methylimidazolium tetrachloroferrate
$[C_4mim][DBPO_4]$	1-butyl-3-methylimidazolium dibutylphosphate
$[C_4C_2im][EtSO_4]$	1-butyl -3-ethylimidazolium ethylsulfate
$[C_4C_2mim][DBPO_4]$	1-butyl -3-ethylimidazolium dibutylphosphate
$[C_6mim][NTf_2]$	1-hexyl-3-methylimidazolium bis(trifluoromethylsulfonyl)imide
$[C_6mim][SCN]$	1-hexyl-3-methylimidazolium thiocyanate
$[C_8mim][BF_4]$	1-octyl-3-methylimidazolium tetrafluoroborate
$[C_8mim][NTf_2]$	1-octyl-3-methylimidazolium bis(trifluoromethylsulfonyl)imide
$[C_4{}^3mpy][BF_4]$	1-butyl-3-methylpyridinium tetrafluoroborate
$[C_6{}^3mpy][BF_4]$	1-hexyl-3-methylpyridinium tetrafluoroborate
$[C_8{}^3mpy][BF_4]$	1-octyl-3-methylpyridinium tetrafluoroborate

$[C_6^{3,5}dmpy][NTf_2]$	1-hexyl-3,5-dimethylpyridinium bis(trifluoromethylsulfonyl)imide
$[C_4^4mpy][NTf_2]$	1-butyl-4-methylpyridinium bis(trifluoromethylsulfonyl)imide
$[C_4^4mpy][TOS]$	1-butyl-4-methylpyridinium tosylate
$[Et_3S][NTf_2]$	triethylsulphonium bis(trifluoromethylsulfonyl)imide

1. Introduction

1.1. Scopes and Objectives

Governmental regulations on the sulfur content of fuels are becoming increasingly strict in order to reduce the emissions of sulfur oxides and other sulfur compounds (S-compounds) to the atmosphere and mitigate negative environmental impacts. For this reason, it is crucial to develop suitable and efficient desulfurization processes in order to meet the current and upcoming regulations. Among the several approaches proposed, the liquid-liquid extraction using ionic liquids (ILs) has proved to be one of the most promising.

Due to the huge number of possible combinations of cations and anions in ILs, experimental measurements become impracticable and, for this reason, it is necessary the use of a predictive model for their study, like the COSMO-RS (conductor-like screening model for real solvents). This model is a convenient tool, as it requires the molecular structure as the only information and it does not require adjusted parameters to the experimental data.

This work aims at identifying ILs with potential to be applied in the desulfurization of fuel oils. For this purpose, phase diagrams of binary systems comprising imidazolium-based ILs and thiophene (taken as a model S-compound) were determined experimentally and predicted with the COSMO-RS

This model was also applied to describe the liquid-liquid equilibrium (LLE) of ternary systems containing imidazolium and pyridinum-based ILs, aromatic S- and N-compounds, and hydrocarbons (HCs) (representative of the components of the fuel).

The analysis of the LLE phase diagrams enabled to evaluate the effect of the structural characteristics of the ILs, aromatics and HCs on the mutual solubilities between these compounds and conclude about the factors that influence the selectivity of the ILs and their extraction potential of aromatic compounds from fuels. By comparing the LLE phase diagrams calculated using COSMO-RS with available experimental data, it was possible to test the ability of this model to describe and predict the phase behaviour of this type of systems.

1.2. General Context

The Earth´s climate is changing gradually, largely as a result of human and industrial activities which are often hazardous and made in large proportions, overwhelming the delicate balance of nature on Earth.

Currently, energy production is mostly based on non-renewable energy sources. These have widespread in technology, but have a high environmental impact. Fossil fuels are still the main choice of supply in the transport sector and will certainly continue to be extensively used in the near future. Therefore, harmful emissions to the atmosphere are expected to increase during the next decades, being thus crucial to develop and adopt several environmental policies in order to avoid an irreversible climate change.

The S-content in fossil fuels is a very serious environmental concern because, upon combustion, S-compounds are converted to sulfur oxides (SO_x). These compounds are the major source of acid rain and air pollution and contribute to global warming [1-3]. Besides causing changes in climate, SO_x also affects the human health, causing respiratory problems and being particularly irritating to the lungs. In addition, SO_x irreversibly poisons the noble metal catalysts for the conversion of NO_x, CO, and particulate matter for exhaust gas treatment in vehicles [4-5].

During the last few decades, the deep desulfurization of transportation fuels has thus become an increasingly important subject due to more stringent governmental regulations established in many countries for environmental protection purposes [6]. The sulfur limit (S-limit) on diesel oil was fixed in 2010 in a value of 15 ppm in USA, in 2009 in a value of 10 ppm in the European Union and Japan, and 50 ppm in Brazil while globally, the average S-content in crude oils has increased about 60 % from 1981 to 2001 [3, 7-9]. The future tendency will be to produce S-free gasoline, diesel and other fuels like those used in agriculture tractors and nonroad mobile machinery, forcing intensive research on alternative technologies [10-12].

Sulfur is found in concentrations that depend on the source of the crude feedstock, methods of refining and the degree and nature of blending. Desulfurization technologies are selected and their suitability evaluated according to the requirements of the produced fuels.

1.3. Ionic Liquids

ILs are commonly defined as salts melting at temperatures below 100ºC, typically formed by the combination of large organic cations and organic or inorganic anions of variable nature[14-15]. Since, unlike common salts, they cannot easily form an ordered crystalline structure and they are liquid at or near room temperature and at atmospheric pressure.

The ILs most studied and reported in literature are those containing anions such as tetrafluoroborate, hexafluorophosphate, bis(trifluoromethylsulfonyl)imide, halogenates, or trifluoromethanesulfonate, combined with ammonium, phosphonium, sulfonium, pyridinium, imidazolium or pyrrolidinium cations. The structures of some of the most common cations and anions composing ILs are illustrated in Figure 1.1.

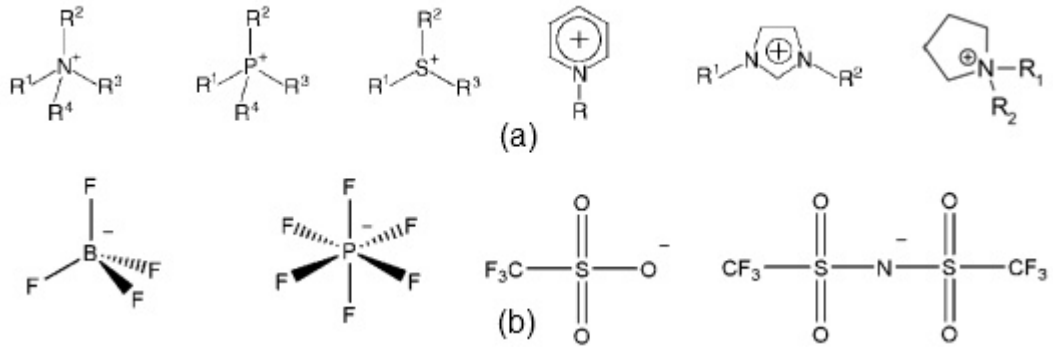

Figure 1.1: Structure of common (a) cations and (b) anions of ionic liquids**.**

For the IL to be liquid at room temperature, the cation should preferentially be unsymmetrical, *e.g.* R_1 and R_2 (Figure 1.1) should be of different alkyl groups in the dialkylimidazolium cation. The relatively large size of one or both ions in ILs and the low symmetry of the cation contribute for the lower melting points of these compounds [16]. The nature of the anion is also largely responsible for its chemical properties [17-18].

These compounds present remarkable and advantageous thermophysical properties, such as low vapour pressure under atmospheric conditions, large liquidus temperature range, high ionic conductivity, high solvation ability for organic, inorganic, organometallic and polymeric materials, non-flammability, high chemical and thermal stability and reusability [17, 19-23]. Due to these unique features, ILs have been the subject of an enormous research effort from the scientific community and are currently suggested as promising and environmentally benign alternatives for conventional volatile and toxic organic solvents in a wide range of applications such as liquid/liquid extraction [24], gas separation and

purification [25], chemical synthesis [26], electrochemistry [27], catalysis [28], chromatographic methods [29], liquid membranes [30], among others. Although ILs are recognized as "green solvents", it is relevant to study their environmental impact and other properties such as toxicity, biodegrability or bioaccumulation [2, 31-32]. For example, imidazolium and pyridinium-based ILs have usually a low toxicity, which is largely driven by the size of the cation chain [33]. In general, the shorter the length of the alkyl chain of the cation, the lower the toxic effect is [33]. The anion may also influence the toxicity but its effect is not as significant [14, 33-34].

The key feature of these solvents is that their properties can be tuned through the use of different selected combinations of anions and cations and/or functional groups [15]. By manipulating their structure, a unique set of properties can be explored for specific applications [20, 35-36]. Due to this versatility, they are named "designer solvents" [16].

The first report on ionic liquids dates back to 1914 when Walden [37] synthesised ethylammonium nitrate, $[EtNH_3][NO_3]$, a salt with a melting point of 12 ºC. Some years after, in 1952, ILs were first considered for their application as electrolytes in electrochemistry [38], when Hurley and Wier used the first room-temperature ILs with chloroaluminate ions as bath solutions for electroplating aluminum. However, this kind of ILs did not receive considerable attention owing to their reactivity to moisture and many chemicals. The true emergence of ILs as broadly functional solvents occurred with the development of the air- and moisture-stable imidazolium-based ILs in 1992 [21].

In recent years, the number of possible stable combinations of cations and anions has increased significantly (it is estimated that there could be up to 10^{18} ILs [39]) and therefore many and extensive studies have been carried out to get information on these solvents. As it can be seen in Figure 1.2, there has been an impressive increase in the number of publications on ILs in the past decade, which is indicative of the tremendous interest in this field.

In the last decades, ILs have proved to be suitable for a growing number of applications: as solvents for a variety of chemical reactions and separation processes [16, 38-39], as sensors, lubricants, electrolytes in fuel cells, batteries, plasticizers, ionogels, capacitors, liquid crystals, heat transfer fluids and even embalming fluids, to name just a few [14, 17, 39].

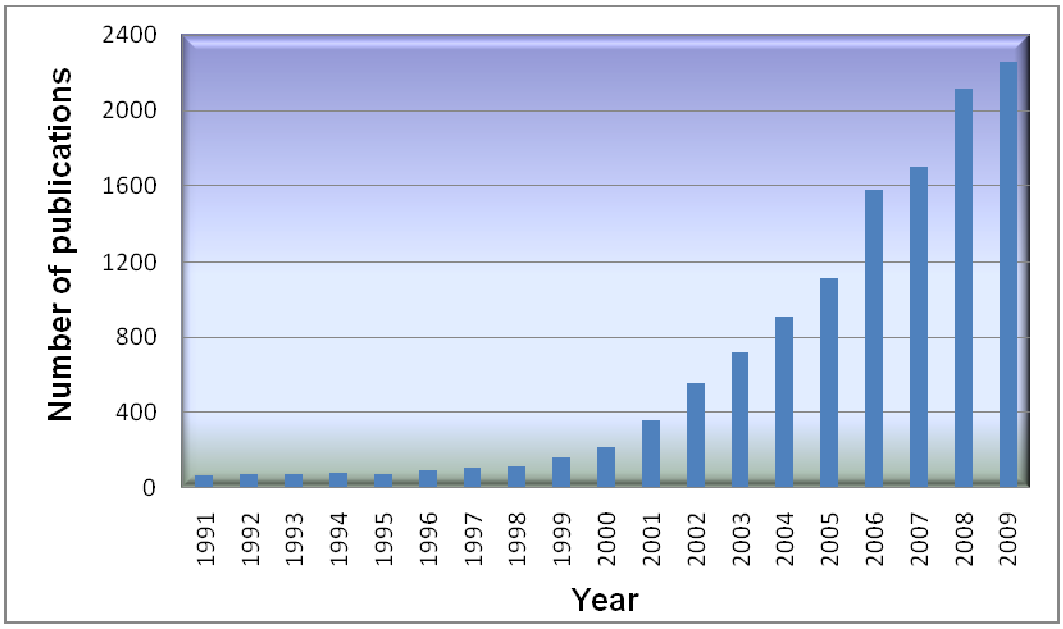

Figure 1.2: Number of publications involving ionic liquids between 1991 and 2009 [13].

Some innovative applications, such as the use of ILs for the production of energy [40] (for example in the capture and conversion of solar energy into electricity) or as pharmaceutical salts [41], are still rising. Recently, a promising field of research has been the use of ILs as solvents for the extraction of S-compounds from transportation fuels [1, 12, 22, 42-52].

1.4. Current technology for desulfurization of fuels

Conventionally, the removal of S-compounds from crude oil-derived fuels-gasoline, diesel and jet-fuels is made through catalytic hydrodesulfurization (HDS). This process is carried out industrially in petroleum refineries and conducted at temperatures around 350ºC, at hydrogen pressures of 3-10 MPa, and using traditional commercial catalysts such as Co–Mo/Al_2O_3, Ni–Mo/Al_2O_3 or Ni–W/Al_2O [10, 47]. The principle of this prevailing technology is the reaction of S-compounds with hydrogen (H_2) to convert them to hydrogen sulfide (H_2S) and HCs [53]. H_2S is subsequently removed, generally via classic Claus process, to produce elemental sulfur [48]. The hydrocarbon part is recovered and remains in the refinery streams [48]. HDS is successful for a variety of S-containing compounds that exhibit varying reactivities towards desulfurization. Reactivity depends on the local environment of the sulfur atom in the molecule, and on the overall shape of the molecule [12, 54]. This method has been widely employed throughout the world for over 60

years and generally enables the elimination of aliphatic/paraffinic S-containing compounds like thiols, thioethers, sulfides and disulfides quite efficiently, according to the present S-content regulations [5, 54-56]. However, it is difficult to achieve ultralow sulfur levels because some refractory S-containing aromatics, namely thiophene (TP), benzothiophene (BT), multiple alkylated derivatives of dibenzothiophene (DBT) and especially high molecular weight substituted DBTs are highly resistant to hydrotreatment and are difficult to convert into H_2S due to the sterically hindered adsorption of these compounds on the catalyst surface and the lack of high performance catalysts specific to such series [48, 53, 57-62]. Thus, the rate of HDS superproportionally decreases with the increase of the degree of desulfurization because many S-compounds, particularly sterically hindered DBT derivatives, are much less reactive to HDS [12]. The structures of typical S-compounds that are found in transportation fuels are depicted in Figure 1.3.

Moreover, undesired side reactions such as the saturation of more olefins will also be induced, resulting in a decrease in the octane/cetane number of fuels. The H_2, which is fed into the HDS-reactor jointly with preheated oil is merely consumed to a small extent in the trickle bed reactor and needs to be separated from the desulfurized oil and recycled into the reactor. Normally, recycle-rates of up to 50 are needed, which results in high (re)compression costs [63]. The operation at higher temperature also leads to increased cracking, coke formation and thus subsequent catalyst deactivation. For example, either about four times more active catalyst or an increase of 38 ºC in reaction temperature are the conditions needed to meet the required S-reduction of diesel products from 500 to 50 ppm [64] when using a Co-Mo catalyst. In addition, to decrease the S-content from 500 to less than 15 ppm, the reactor volume must be at least three times larger than those presently used in refining industry [65]. The use of slurry reactors in HDS could be a promising alternative to the conventional reactors used in this process (fixed bed reactors) because of their uniform temperature profile, high catalyst efficiency, and online removal and addition of catalyst [7].Other improvements in this technology are focused on the development of high activity catalysts, advanced reactor design of multiple bed systems within one reactor, and new internals or structured catalysts to realize counter-current flow [58, 61].

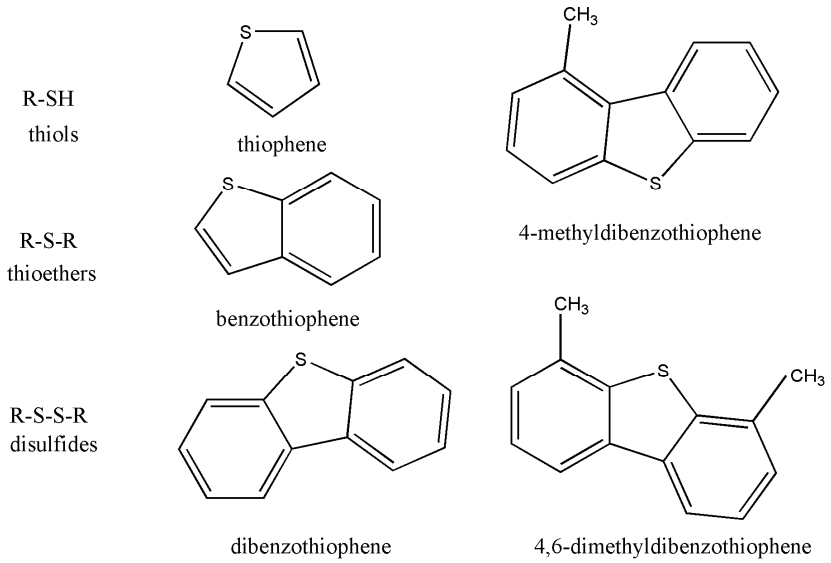

Figure 1.3**:** Structures of typical organosulfur compounds found in transportation fuels.

While the efforts to counter the main drawbacks and improve the efficiency of HDS are ongoing, the search for alternative, efficient and less-energy-demanding processes for the deep desulfurization of transportation fuels has been recently intensified. Many non-HDS approaches [58] that provide potential solutions to obtain S-free clean fuels, and that are able to eliminate undesirable S-containing compounds or to convert them into more innocuous forms, are under development: for example, selective adsorption [4, 6, 54, 66-67], biodesulfurization (BDS) [68-70], precipitation [71], oxidation with molecular solvents [72-76], oxidation with ILs [5, 11, 56-57, 77-85], and extraction with ILs [1, 12, 22, 42-52]. All the processes mentioned, considered individually or in combination with HDS, may be new economically viable solutions for desulfurization. Figure 1.4 shows a scheme of the integration of a liquid-liquid extraction step using ILs in the desulfurization of diesel oil as a complement of HDS, in order to separate unconverted DBT-derivatives from the pre-desulfurized products of HDS. It also includes a small up-stream N-extraction unit for the selective separation of nitrogen compounds (N-compounds). The addition of this unit is advantageous, because it relieves the HDS unit. N-compounds strongly inhibit the HDS reactions and the partition coefficient for the extraction of N-compounds by ILs is so high that the IL/oil ratio needed for extraction would be very small.

Other alternative methods that have been used for desulfurization are reactive distillation [86], several ultrasonic treatments [87-88], alkylation-precipitation and photo-oxidation. However, these two last options mentioned have some disadvantages, such as

the use of expensive alkylation reagents and slow reaction rates [89-90]. In contrast, fuel oil desulfurization by membrane process, such as pervaporation, is a newly emerging technology with several potential advantages over distillation, molecular sieves or extraction [91-92].

A combination between oxidative desulfurization (ODS) and extraction has also attracted much interest, and it is considered one of the most promising strategies to achieve low S-content fuel. In this method, S-compounds are oxidized into their corresponding sulfones and/or sulfoxides, which are then removed by selective extraction with polar solvents [63, 77, 80, 85, 93].

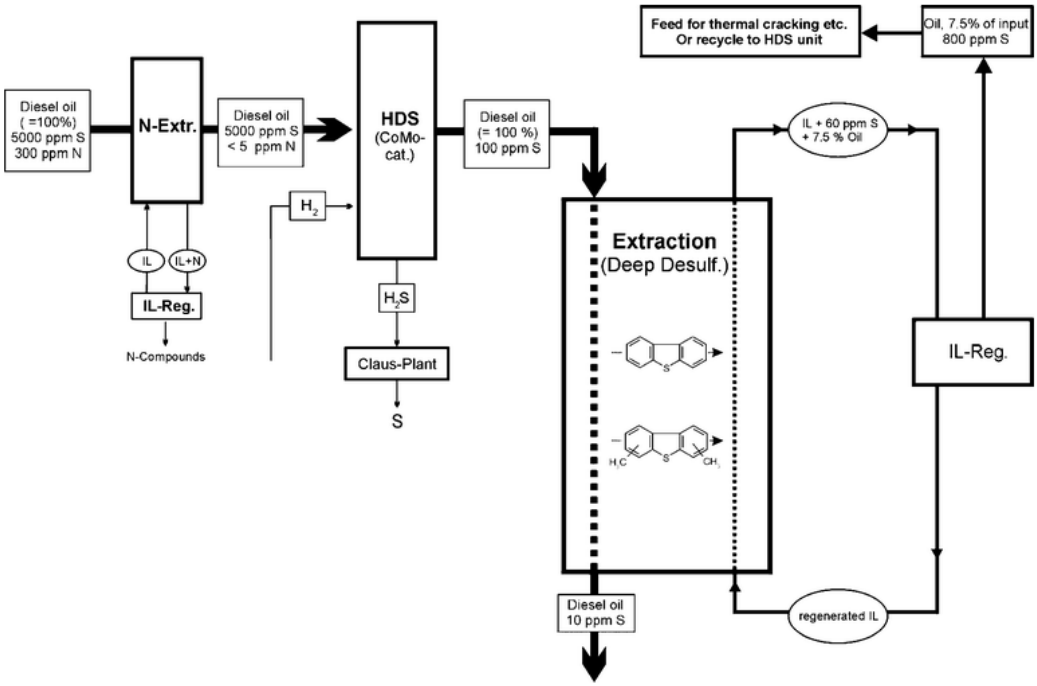

Figure 1.4: Integration of IL-extraction into an existing refinery network for desulfurization of diesel oil (data based on mass balance for $[C_8mim][OcSO_4]$ as extracting agent, cross-solubility of oil: 5 %, mass ratio IL to oil: 1.5, K_S = 0.8 and 6 theoretical plates) [12].

.

This method can effectively remove S-compounds, but one of the prime concerns is that a large amount of flammable and volatile organic compounds (VOCs) such as acetonitrile [82], dimethyl sulfoxide (DMSO) [84], and dimethylformamide (DMF) [78], are employed as extractants. The application of VOCs raises further environmental and safety concerns like wastewater emission and fire hazards [85]. Therefore, it is highly desirable to look for suitable extractants such as ILs to meet the demands of green technology [78].

One of the most promising approaches is liquid-liquid extractive desulfurization (EDS). It is an easy process with relatively high efficiency that is carried out at mild conditions (ambient pressure and relative low temperatures), without the need for H_2 and catalysts. Moreover, unlike HDS, it does not need drastic reaction conditions or special equipments and does not change the chemical structure of the fuel components. The key to the success and safety of EDS is the selection of an adequate solvent. ILs have been extensively suggested and employed as extracting agents in many desulfurization processes due to their advantageous characteristics, such as environmentally harmless, low cost, nonvolatibility and thermal stability over a wide range of temperatures (which results in an easiness of regeneration for the used extractant by distillation). Moreover, the possibility of designing ILs with adequate solubility, high affinity to S-containing compounds, in particular, to sterically hindered S-compounds and virtual immiscibility with fuel oils (which eliminates the potential cross-contamination to fuel oil) constitutes a further advantage [46]. In EDS, it is desired to remove the S-compounds without removing aromatics because these are important for maintaining the octane number in transportation fuels. The regeneration and subsequent recycling of ILs is also of vital importance in the extraction processes of a refinery stream using these solvents. Hydrophilic, moisture-insensitive ILs can be dissolved in water, with S-compounds separating or precipitating. Water can then be removed by evaporation under a stream of nitrogen at 110 ºC, due to the negligible vapor pressure of most ILs. This procedure requires a large amount of heat for water evaporation, and would be difficult to incorporate in a continuous process on a multi-ton scale. Efficient techniques for separating water and ILs need further studies. In the case of hydrophobic ILs, S-compounds can be removed by distillation. Once more, the distillation requires heat, and it is only viable with low-boiling sulfur compounds like TP. With high-boiling S-compounds like DBT or 4,6-DMDBT, distillation is less effective. The use of re-extraction with $scCO_2$ needs further research on the applicability of the process on a multi-ton scale considering the large scale usage of energy [53].

Other molecular solvents such as polyalkyleneglycol, polyalkyleneglycol ether, pyrrolidones, imidazolidinones, pyrimidinones and dimethyl sulfoxide have been employed as extractants for the removal of S-compounds from fuels, but their performance is not satisfactory, and sometimes their solubility in fuel or vice versa is noticeable leading to cross-contamination problems [46, 50]. So, ILs seem to be more appropriate than

molecular solvents since they meet the majority of the required criteria mentioned above [45, 50, 94], having, additionally, high extraction ratios and greater selectivity. A wide range of ILs have been tested for the extraction of S-compounds from model diesel oil [12], model fuel and commercial gasoline [22, 42-44, 46].

1.5. The role of ILs on the desulfurization of fuel oils

The use of imidazolium-based ILs for the selective extraction of S-compounds from diesel fuel was described for the first time by Bösmann and co-workers [42] , when these authors investigated the performance of mixtures of [C_2mim]Cl and [C_4mim]Cl with aluminium trichloride ($AlCl_3$) as extractive solvents. Since then, due to their easiness of synthesis and attractive physical properties, this family of ILs has been the most frequently applied for extraction purposes.

Due to their excellent extraction capability, $AlCl_3$- and aluminium tetrachloride-based ILs ($AlCl_4$-based ILs) were initially widely employed in the removal of S-containing compounds [12, 42, 95], yet they have disadvantages that discourage their use and limit their practical utility. For instance, the occurrence of side reactions when contacting with compounds that contain thiols leads to the formation of dark precipitates which darken the color of processed fuels [22, 96]. Moreover, these ILs are sensitive to moisture generating hydrochloric acid and are unstable in air [97]. The use of completely halogen-free ILs for desulfurization has been tested since then, and most of the following studies are focused on imidazolium-based ILs [42].

The extraction of S-compounds with imidazolium-based ILs containing $[PF_6]^-$ or $[BF_4]^-$ anions were studied broadly. [$C_n$mim][BF_4] ILs, for instance with n = 2, 4, 8 proved to be efficient solvents for desulfurization processes [10, 23, 36, 44]. This family of ILs has a high extraction ability of thiophene ([TP]), dibenzothiophene ([DBT]) and other S-compounds, which increases with the increase of the length of the alkyl chain of the cation [10, 23, 36, 44]. In the case of [C_8mim][BF_4] it was observed nearly a 80 % extraction in three stages [10]. These ILs are thermally stable, readily regenerated for reuse and, unlike $AlCl_3$-based ILs, are more insensitive to the presence of water.

The water soluble [C_4mim][BF_4] was found to be a more effective solvent when compared to the water-immiscible [C_4mim][PF_6], using octane and dodecane as model oils [42, 98]. The interpretation given lies on more favorable interactions established by DBT

with $[C_4mim][BF_4]$ than with $[C_4mim][PF_6]$, owing to the fact that the anion $[PF_6]^-$ is larger than $[BF_4]^-$ [98].

Zhang and co-workers [22, 44, 99] determined and compared the extraction ability of $[C_2mim][BF_4]$, $[C_4mim][PF_6]$ and $[C_4mim][BF_4]$ for some model S-compounds, and further elucidated the structural effects of ILs on the absorption capability for TP by multinuclear NMR spectroscopy. Although all these ILs show remarkable selectivity for S- and N-containing molecules, higher absorption ability was found for $[C_4mim][PF_6]$ and $[C_4mim][BF_4]$ than for $[C_2mim][BF_4]$. The efficiency of the ILs in extraction processes was proved to be dependent on the size and structure of both cations and anions of the ILs and on the molecular structure of the S-compounds [22, 44, 99]. A high density of aromatic π electrons is favourable for the absorption. As an example, TP with its five-membered ring establishes stronger interactions with the ILs than the nonaromatic isobutylthiol. An interesting aspect is that ILs were also used as solvents in the desulfurization of actual fuel and it was found that about 30 wt % of sulfur was preferentially removed with little alteration in the content of the aromatics [22].

Imidazolium-based ILs comprising other types of anions like $[C_2C_2im][EtSO_4]$, $[C_4C_2im][EtSO_4]$, $[C_2mim][EtSO_4]$, $[C_2mim][MeSO_4]$, $[C_4mim][MeSO_4]$ and $[C_1mim][MeSO_4]$ have also been used to extract DBT from model diesel fuel [97]. It was observed a linear increase in the extraction yield of DBT with an increase in the length of the alkyl chain of the IL cation [97]. Having the longest alkyl chain, $[C_4C_2im][EtSO_4]$ proved to be the most efficient IL. It was also reported a good selectivity of this IL, as well as of two other ILs $[C_2C_2im][EtSO_4]$ and $[C_4mim][MeSO_4]$ for DBT over diphenylsulfide and diphenyldisulfide [97]. In further studies on the effect of the co-solvent [97], it was concluded that the nature of solvent does not have a significant influence. In addition, an increase in the mass ratio of the IL to the model fuel can increase the extraction yield up to 70 % after one round of extraction. After five rounds the S-content might decrease noticeably, for example, from 1000 to 350 ppm [97].

Other promising solvents for the extraction of DBT and its derivatives are $[C_2mim][EtSO_4]$ and $[C_4mim][OcSO_4]$. These ILs are halogen-free, water stable and available from relatively cheap starting materials [12].

Studies on the LLE of different fuel components and S-containing compounds were carried out to further evaluate the efficiency of $[C_2mim][EtSO_4]$ as extractive solvent [3,

[100]. The use of S-containing ILs for desulfurization can sound inappropriate but leaching of IL into the oil phase is in any case unwanted. Nevertheless, certain degree of cross-solubility of hydrocarbons in the IL was observed [12]. For [C_4mim][$OcSO_4$], it was obtained a partition coefficient (K_S) two times higher than for [C_2mim][$EtSO_4$] but the cross-solubility is 4–16 times higher [12].

CuCl-based ILs like [C_4mim][Cu_2Cl_3] exhibit noticeable extraction ability for the desulfurization of gasoline, due to the π-complexing interaction of TP and Cu-anionic species. No side reactions occur and this type of ILs have the advantage of being moisture-insensitive and stable in air [43].

Many other ILs, for instance, $FeCl_3$-based ILs [50, 101], [C_8mim][NTf_2] [22, 36, 42, 94, 102-104], [amim][PF_6] [44] or [C_4mim][$FeCl_4$] [98], have been employed as extracting solvents, showing variable desulfurization capabilities.

Phosphoric ILs have been providing encouraging results having the additional advantage of being easy to manufacture in a commercial scale with very high yield. In investigations focused on [C_1mim][$DMPO_4$], [C_4mim][$DBPO_4$] and [C_2mim][$DEPO_4$] [46], it was found that the desulfurization ability follows the order [C_4mim][$DBPO_4$] > [C_2mim][$DEPO_4$] >> [C_1mim][$DMPO_4$], and for a specified IL, the K_S decreases in the order DBT > BT > 3-MT. However fuel solubility in ILs is noticeable and its magnitude follows the same tendency. Due to the relatively high S-removal ability, low fuel dissolvability and small influence on the gasoline treated, as well as the easiness of being reclaimed by dilution with water, [C_2mim][$DEPO_4$] was the IL recommended for the desulfurization of gasoline via an EDS process [1, 46]. Other phosphoric IL suggested for the extraction of DBT, BT and 3-MT was [C_2C_2im][$DEPO_4$] prevailing over [C_2mim][$DMPO_4$] and [C_4C_2mim][$DBPO_4$] due to its higher S-extractive ability, lower solubility in fuel (and thus negligible influence on the composition of the fuel) and easy recuperation [45]. Nie and co-workers [52] studied the influence of the length of the alkyl group of these cations in alkylphosphate-ILs, showing that the longer the alkyl substitutent of the anion or cation, the higher is the value of the K_S for the IL considered.

Recently, the extractive capability of ILs based on the dicyanamide anion ($[N(CN)_2]^-$) for TP and DBT from model fuel oils was investigated [105], revealing that [C_2mim][$N(CN)_2$] and [C_4mim][$N(CN)_2$] were the most efficient ones for desulfurization purposes.

Gao and co-workers [47, 51] studied alkyl- and alkylmethyl-pyridinium-based ILs, but best results were achieved with $[alkyl\text{-}dmpy]^+$. The extractive performance follows the order $[C_8{}^3mpy][BF_4] > [C_6{}^3mpy][BF_4] > [C_4{}^3mpy][BF_4]$, and the selectivity of the ILs for the S-compounds decreases in the order DBT > BT > TP > 4,6-DMDBT under the same conditions, except for the $[C_8{}^3mpy][BF_4]$ for which followed the order of DBT > BT> 4,6-DMDBT> TP [47]. These results indicate that the extraction is more favorable for those aromatic heterocyclic S-compounds having higher aromatic π-electrons density. The mechanism that has been suggested for the extraction of S-compounds with 3-methylpyridinium-based ILs is the formation of liquid clathrates due to the π-π interaction between the aromatic groups of S-compounds and the pyridinium ring system. This phenomenon, has been also supported by Holbrey [106]. Zhang [22, 44] and Su and co-workers [99] also concluded that the cation and anion sizes of imidazolium-based ILs, play an important role in determining the interaction between TP and ILs.

Good extraction performances are also observed for imidazolium and pyridinim-based ILs containing acetate ($[CH_3CO_2]^-$) and thiocyanate ($[SCN]^-$) anions suggesting that more benign and cheaper anions can be employed as alternatives to the perfluorinated $[NTf_2]^-$ and $[BF_4]^-$, especially when attached to cations such as $[C_4{}^3mpy]^+$ [35, 47, 51, 107].

Other studies [35] revealed that $[C_4{}^4mpy][TOS]$, is not the best IL for the separation of aromatic compounds from aliphatic compounds as proved by the relatively low selectivity values obtained. Being a polyaromatic specie, the tosylate anion presents a high affinity for polyaromatic S-compounds. However, $[TOS]^-$-based ILs are also technically limited by their higher melting temperatures. Generally, better results are obtained for $[NTf_2]^-$ [35].

Holbrey and co-workers [107] investigated the extraction of DBT from dodecane using a series of ILs comprising several combinations of different cation families (imidazolium, pyridinium, pyrrolidinium, and quinolinium) and anion types. The K_S values of DBT in the ILs, ranged from 0.8 to 9, revealing an evident dependence on the cation class [107]. The ILs containing $[CH_3CO_2]^-$ and $[SCN]^-$ had the best extraction performances within all the anions considered [107]. ILs comprising these two anions in combination with the pyridinium cations showed high extraction abilities, with 81–83 % of the DBT removed in one contact. Polyaromatic quinolinum-based ILs were found to be the most efficient extractors [107]. However, the use of these and other polyaromatic cations, such as 1,3-

dibenzimidazolium is technically limited by the high melting points of the correspondent ILs and barely tend to form low-melting point ILs when combined with highly flexible perfluorinated anions such as $[NTf_2]^-$ [107]. The effect of the cation in the ILs desulfurization ability follows the sequence methylpyridinium ≥ pyridinium ≈ imidazolium ≈ pyrrolidinium, with a much less significant variation with anion type. It was found that ILs containing 1-butyl-*n*-methylpyridinium cations (*n* = 3 or 4) provide good DBT extraction yields, independently of the anion present [107].

Although there is already a considerable amount of studies about the application of ILs on the desulfurization of fuels, the number of ILs considered is still reduced regarding the present demands and the current importance of the topic, and there are still important issues to clarify. Therefore, research remains open and intense.

2. Modeling

2.1. COSMO-RS predictive model

Computational methods and fluid thermodynamics are important tools for the quantitative estimation of structures, properties and interactions of molecules, relevant to overcome chemical and biochemical engineering problems. A recent and useful predictive methodology used to describe thermophysical properties of fluids and/or complex liquid mixtures is COSMO-RS. This simulation model is based on unimolecular quantum calculations of individual molecules in a system and was proposed by Klamt and co-workers [108-113]. It combines the electrostatic advantages and the computational efficiency of the quantum chemical dielectric continuum solvation model, COSMO, with a statistical thermodynamics approach for local interaction of surfaces, which contemplate local deviations from dielectric behaviour as well as hydrogen-bonding. The calculation procedure of COSMO-RS considers fundamentally two major stages: quantum chemical COSMO calculations for the molecular species involved, where the information about both solvents and solutes is extracted and COSMO-RS statistical thermodynamic calculations performed within the COSMOtherm software [114-115] .

Regarding the first step, the calculations are embedded in a perfect conductor, i.e, the model is applied in order to reproduce a virtual conductor environment for the solute molecules which induces a polarization charge density (σ), on the interface between the molecule and the conductor [108]. These charges act back on the solute and generate a more polarized electron density than in vacuum. Throughout the quantum chemical self-consistency algorithm cycle, the solute molecule is therefore converged to its energetically optimal state in a conductor with respect to electron density, which is the reference state for the following COSMO-RS calculations. The molecular geometry can be optimized using conventional methods for calculations in vacuum. The calculations end up with the self-consistent state of the solute in the presence of a virtual conductor that surrounds the solute outside the cavity. Although time-consuming, one advantage of this procedure is that the quantum chemical calculations have to be performed just once for each molecule under consideration and then can be stored in a database [116].

In the COSMO-RS iteractively approach, the most important energetic contributions are considered, the electrostatic misfit energy (E_{misfit}) and hydrogen-bonding (E_{HB}) and are described as functions of the polarization charges of the two interacting segments,

(σ,σ') or $(\sigma_{acceptor},\sigma_{donor})$, if the segments belongs to hydrogen bond donor or acceptor atom, as described in Equation 2.1 and Equation 2.2 . The less specific van der Waals energy (E_{vdW}) is also considered but in an approximate mode and dependent only on the elements of the atoms involved and is described by Equation 2.3.

$$E_{misfit}(\sigma,\sigma') = a_{eff}\frac{\alpha'}{2}(\sigma+\sigma')^2 \qquad \text{Equation 2.1}$$

$$E_{HB} = a_{eff}c_{HB}\min(0;\min(0;\sigma_{donor}+\sigma_{HB})\times\max(0;\sigma_{acceptor}-\sigma_{HB})) \qquad \text{Equation 2.2}$$

$$E_{vdW} = a_{eff}(\tau_{vdW}+\tau'_{vdW}) \qquad \text{Equation 2.3}$$

According to Equation 2.1 to Equation 2.3, there are five adjustable parameters, fitted to the individual atoms properties and are the following: an interaction parameter, α' , the effective contact area between two surface segments, a_{eff} , the hydrogen bond strength, c_{HB} , the threshold for hydrogen bonding, σ_{HB} , and lastly, the element-specific van der Waals interaction coefficients, τ_{vdW} and τ'_{vdW} .

The 3D polarization density distribution on the surface of each molecule X_i is converted into a distribution function called σ-profile, $p^X(\sigma)$ that describes the relative amount of surface segment with polarity σ. For the statistical thermodynamics is expedient to consider a normalized ensemble and, in this sense, the combination of the molecular σ-profiles and the pure or mixture solvents S σ-profiles results in the mole fraction weighted sum of σ-profiles of its compounds, $p_S(\sigma)$, and normalized by the total surface area, A_S, enables to obtain the normalised σ-profile of the overall system, $p'_S(\sigma)$, as defined in Equation 2.4, where x_i is the mole fraction of component *i*, $p^{X_i}(\sigma)$ is the corresponding σ-profile and A^{X_i} is surface area of the solute molecule X_i.

$$p'_S(\sigma) = \frac{p_S(\sigma)}{A_S} = \frac{\sum_i x_i p^{X_i}(\sigma)}{\sum_i x_i A^{X_i}} \qquad \text{Equation 2.4}$$

The most important descriptor used in COSMO-RS is in fact *σ*, which would be induced on the molecular surface if the molecule would be in a virtual conductor environment. This descriptor can be calculated by quantum chemical calculations using the

COSMO, and it is an extremely valuable descriptor for the local polarity of molecular surface and it is the only descriptor determining the interaction energies. Thus, the ensemble of surface pieces characterising a liquid system S is described by the distribution function, $p_S(\sigma)$, that depicts the amount of surface in the ensemble having a screening charge density between σ and $\sigma + d\sigma$. Therefore, the σ-profile of a particular compound is derived from the quantum chemical COSMO output for that molecule, applying some local averaging algorithm that take into account that only screening charge densities averaged over an effective contact area are of physical meaning in COSMO-RS [114-115].

As $p'_S(\sigma)$ describes totally the molecular interactions (Equation 2.4) and as the chemical potential result from these interactions, the chemical potentials are calculated with an exact statistical thermodynamics algorithm for independently pair-wise interacting surfaces, *i.e.*, they are obtained by solving iteratively Equation 2.5 obtained by combining $p'_S(\sigma)$ with the energies associated to the molecular interaction [111].

$$\mu_S(\sigma) = -\frac{RT}{a_{eff}} \ln\left[\int p_S(\sigma') \exp\left(\frac{1}{RT}\left(a_{eff}\mu_S(\sigma') - E_{misfit}(\sigma,\sigma') - E_{HB}(\sigma,\sigma')\right)\right) d\sigma'\right] \quad \text{Equation 2.5}$$

$\mu_S(\sigma)$, the term of σ-potential, is the chemical potential of a surface segment with screening charge density σ and measures the affinity of a solvent to surface segment with polarity σ. The term of vdW energy, which does not become visible in Equation 2.5, can be added to the reference energy in solution.

Integrating Equation 2.5, it is possible to calculate the pseudo-chemical potential of the component X_i in a solvent S, over the surface of the compound [108], where the $\mu_{C,S}^{X_i}$ is a combinatorial contribution term of different sizes and shapes of the molecules in the system which depends of the area and volume.

$$\mu_S^{X_i} = \mu_{C,S}^{X_i} + \int p^{X_i}(\sigma)\mu_S(\sigma) d\sigma \quad \text{Equation 2.6}$$

The COSMO-RS method depends only on a small number of adjustable parameters (predetermined from known properties of individual atoms) and that are not specific for functional groups or type of molecules.

As it can be seen from Equation 2.6, the COSMO-RS is a reliable approach, since the statistical thermodynamics enables the determination of the chemical potential of all the components of an arbitrary mixture at a given temperature and from these, several thermodynamic properties can be derived, such as activity coefficients, partition coefficients, solubilities, VLE/LLE phase behaviour, among many other properties [108, 111, 113, 117].

3. LLE in Binary Systems

3.1. Introduction

The knowledge of the physical, chemical and thermodynamic properties of ILs is essential to identify the most suitable IL for any particular application.

In desulfurization processes, the most suitable ILs are those which exhibit immiscibility with HCs and high extraction capability and selectivity for the S-compounds. Solid-liquid equilibrium (SLE) and LLE data are thus fundamental for the successful use of ILs as solvents in liquid–liquid extraction issues and for the correct design of desulfurization processes. This thermodynamic information can be obtained experimentally, but, due to the infinite number of possible combinations of cations and anions in ILs, experimental measurements become time consuming, expensive and, eventually, impracticable and so it is necessary to develop alternative methodologies like correlations and predictive models which are able to describe ILs properties and phase behaviour based on experimental measurements on selected systems. COSMO-RS has been extensively applied to model the phase equilibria of ILs and of several types of molecular compounds like alcohols, hydrocarbons, ethers, ketones, and water [117-122], with excellent agreement with experimental data. This model has also proved to be a powerful and convenient tool in the prediction of properties of systems involving ILs [108, 111, 113, 117], having advantages over traditional approaches such as structure-interpolating group-contribution methods (GCMs), equations of state (EoS), and other correlations that require a large experimental database prior to their effective use, which is a restrictive factor considering the huge number of possible ILs. In addition, it does not require adjusted parameters to experimental data, being therefore possible to be applied to an unlimited number of ILs. The performance of this predictive method has been analysed in the description of the LLE of binary systems involving ILs and has proved to be, at least qualitatively, an *a priori* method of selection for predicting the phase behaviour of those systems [117-122]. Surprisingly, LLE data on binary systems involving ILs and S-compounds are still very scarce. There is only one study concerning the LLE or SLE of (IL + TP) binary systems in which the data were correlated with the thermodynamic methodology non-random two liquid (NRTL) [35], providing a good description of the LLE experimental data.

In this work, liquid-liquid phase diagrams of (TP + IL) binary systems were experimentally measured and predicted using COSMO-RS. This model was further applied

to model LLE experimental data for (IL + TP) binary mixtures available in literature, which are summarized in Table 3.1.

Table 3.1: Experimental LLE data for IL-TP binary systems available in literature.

Ionic Liquids	**S-compound**	**Analytical tecnique**	**Model Applied**	**Reference**
$[C_2mim][SCN]$	Thiophene	Dynamic	NRTL	[35]
$[C_4mim][SCN]$				
$[C_6mim][SCN]$				
$[C_4{}^4mpy][NTf_2]$				
$[Et_3S][NTf_2]$				

In literature, [35] TP was taken as a model compound for organic sulfur-based compounds present in fossil fuels. Imidazolium-based ILs comprising cations with different alkyl chain lengths in combination with different anions were used to evaluate the effect of the cation alkyl chain, the effect of the cation family and of the nature of the anion on the solubility data and, consequently, on the selectivity of the ILs for the S-compounds.

3.2 Experimental section

3.2.1. Chemical Materials

The ILs used - 1-butyl-3-methylimidazolium bis(trifluoromethylsulfonyl)imide, $[C_4mim][NTf_2]$ and 1-hexyl-3-methylimidazolium bis(trifluoromethylsulfonyl)imide, $[C_6mim][NTf_2]$ were purchased from IoLitec with mass fraction purities > 99%. The molecular structures of the ILs are shown in Figure 3.1.

To reduce the water and volatile compounds content to negligible values, ILs individual samples were dried under constant agitation at vacuum (0.1 Pa) and moderate temperature (353 K) for a minimum of 48 h. After this procedure, their purity was checked by ^1H, ^{19}F and ^{13}C NMR spectra. TP (Figure 3.2) was dried using molecular sieves.

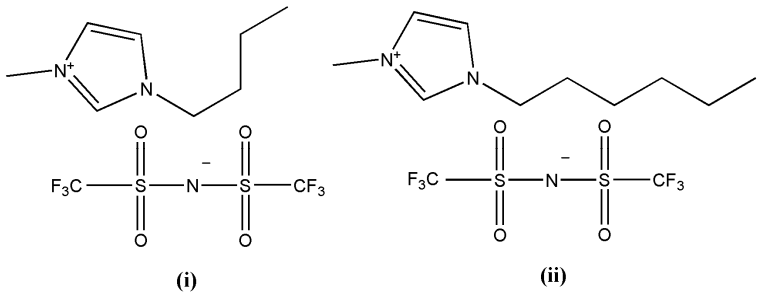

Figure 3.1: Chemical structure of the ILs studied: (i) $[C_4mim][NTf_2]$; (ii) $[C_6mim][NTf_2]$.

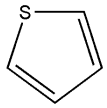

Figure 3.2: Chemical structure of thiophene.

3.2.2. Experimental Procedure

The phase diagrams for the binary systems ($[C_4mim][NTf_2]$ + TP) and ($[C_6mim][NTf_2]$ + TP) were measured by turbidimetry. The onset of the liquid-liquid immiscibility (cloud point temperature) was determined by visual observation of the phase demixing (turbidity followed by phase separation). Mixtures of TP and IL were gravimetrically prepared within an uncertainty of 10^{-4} g, and introduced in Pyrex-glass capillaries with a stirrer. The concentration range studied, $0.36 < x_{IL} < 0.51$, was restricted by experimental limitations (the visual method was not applicable at mole fractions of the IL out of this range, since the experimental setup is limited either for low or high temperatures) and was established on the basis of titrations carried out prior to the experiments. The sealed capillaries were placed in a thermostatted bath and were kept under continuous stirring during the whole experiment. Solutions presenting two phases at ambient temperature were heated into the homogeneous region and then slowly cooled until visual detection of phase demixing. The cooling rate was about 10 ºC for each 30 minutes. The temperature at which the first sign of turbidity appeared upon cooling was taken as the temperature of the liquid-liquid phase transition. For monophasic solutions at room temperature, the heating process was suppressed. The temperature was controlled with a calibrated U1252A, Handheld Digital Multimeter 4.5-digit associated to a calibrated Pt100 temperature sensor immersed in the thermostating liquid. This equipment has an uncertainty of ± 0.01 K. Three consistent measurements were carried out for each solution. Figure 3.3 shows the setup used to carry out the experimental measurements.

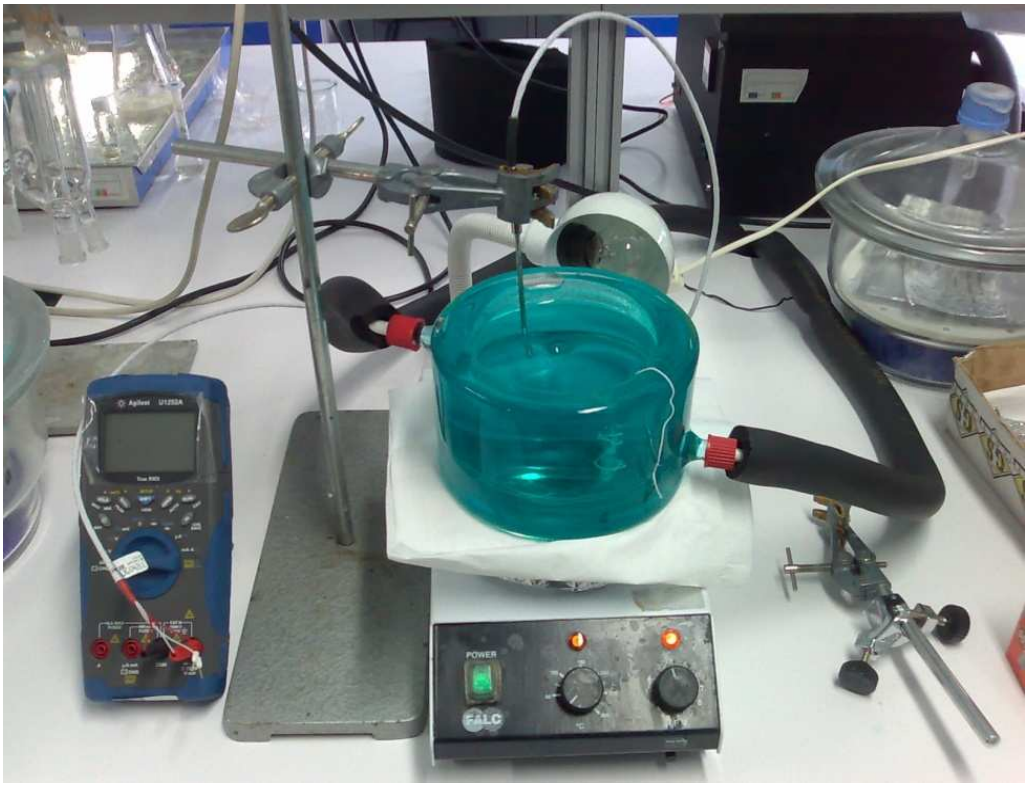

Figure 3.3: Experimental setup used to carry out the experimental measurements.

3.3 Modeling

The COSMO-RS calculations of the LLE of (IL + TP) binary systems were performed using the COSMOtherm program [114-115]. The Turbomole program package [123-124] using the BP density functional theory and the Ahlrichs-TZVP (triple-ζ valence polarized large basis set) [125] was used to create the optimized geometries. It was employed the parameter file BP_TZVP_C21_0110. A pseudobinary approach was used in the COSMOtherm program with the IL cation and anion inputted as separated compounds (or COSMO files).

The LLE was calculated for the (IL + TP) binary systems studied in the experimental section and, additionally, for (IL + TP) binary mixtures reported in literature [35] comprising ILs composed of imidazolium, pyridinium and sulphonium cations in combination with $[SCN]^-$ and $[NTf_2]^-$ anions, as depicted in Figure 3.4. TP was taken as the model S-compound present in fuels.

Since ILs are complex molecules, they can adopt different geometries originating conformers associated to distinct energy states. In a previous work, Freire et al.[117]

assessed the influence of the conformations of the ILs anions and cations and of other molecules on the COSMO-RS prediction of the liquid-liquid phase behaviour.

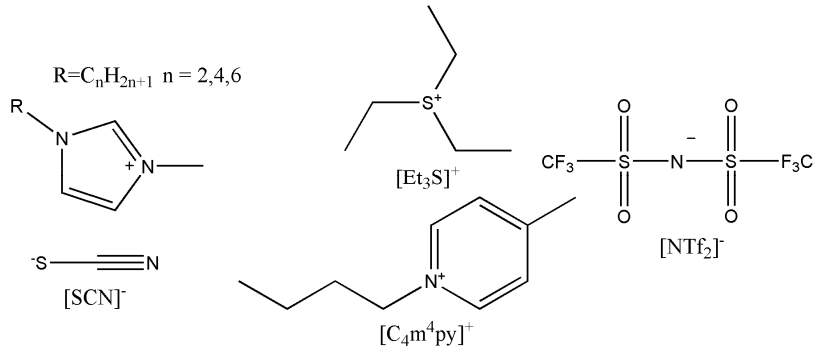

Figure 3.4: Chemical structure of the ILs studied.

It was concluded that the conformations considered in the calculations do have an effect on the results obtained and that improved results are achieved using the conformer with the lowest energy. For this reason, in this work the fully optimized geometries (at the same level of theory) of the lowest energy conformers of each cation and anion were used. Thiophene has no conformers.

3.4 Results and Discussion

The results of the experimental solubility measurements for the (IL + TP) binary systems are presented in Table 3.2, where the experimental LLE temperatures, *T*, *vs* mole fraction of the IL, x_{IL} are listed, and the corresponding experimental LLE phase diagrams illustrated in Figure 3.5. COSMO-RS results and the comparison between experimental and predictive data (both obtained in this work and that reported in literature [35]) are presented in Figure 3.5 to Figure 3.10.

From the analysis of the LLE data obtained it is clear that the phase behaviour of the binary systems (IL + TP) is dependent on the structural changes and nature of the cation and anion of the IL. To better evaluate and interpret these effects, they will be discussed separately below.

Table 3.2: Experimental LLE in the (IL + TP) binary systems.

[C_4mim][NTf_2]		[C_6mim][NTf_2]	
x_{IL}	T/K ± σ[a]	x_{IL}	T/K ± σ[a]
0.5105	272.20 ± 0.17	0.4427	271.72 ± 0.11
0.4996	287.96 ± 0.17	0.4354	276.94 ± 0.06
0.4957	290.58 ± 0.07	0.4225	288.82 ± 0.09
0.4897	300.26 ± 0.24	0.4139	294.11 ± 0.02
0.4868	303.4 ± 0.07	0.3923	313.44 ± 0.02
0.4706	336.50 ± 0.11	0.3882	320.80 ± 0.07
		0.3811	324.69 ± 0.02
		0.3639	336.32 ± 0.04

[a]Standard deviation

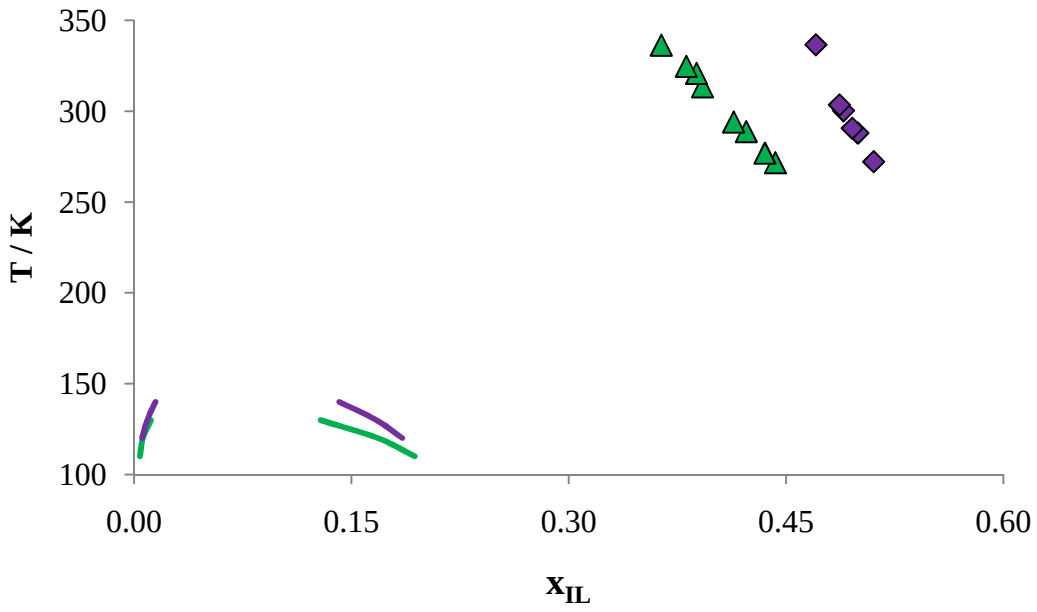

Figure 3.5:Liquid–liquid phase diagram for [C_4mim][NTf_2] (◆) and [C_6mim][NTf_2] (▲) with TP. The single symbols and the lines represent, respectively, the experimental data and the COSMO-RS calculations obtained in this work.

3.4.1. Effect of the alkyl chain length of the IL cation

The COSMO-RS predictions for the LLE phase diagrams of mixtures of [C_4mim][NTf_2] with TP and of [C_6mim][NTf_2] with TP presented in Figure 3.5, reveal an upper critical solution temperature (UCST) for both systems. Although the visual method was not applicable in the whole range of the IL mole fraction, the experimental points obtained for the systems also suggest this result. In fact, the experimental maximum of

both binodal curves occurs at very high temperatures (above 350 K), and therefore it was not possible to measure these points due to the experimental limitations.

The shape of the equilibrium curve is similar for both ([$C_n$mim][NTf_2] + TP) systems. Although the COSMO-RS results do not correspond quantitatively with the experimental points, the model can predict qualitatively the trends observed. From the data presented in Figure 3.5, it can be seen that an increase of the alkyl chain length of the IL cation from C_4 to C_6 originates an increase in the mutual solubility, and therefore, an increase in the IL selectivity for TP. The interaction established between the ILs and TP is mainly due to π-π interactions between the aromatic ring of TP and of the imidazolium cation of the IL. When the length of the alkyl chain of the IL cation increases, two factors have to be considered. On one hand, the coulombic interaction between the IL anion and cation decreases and the π-π interactions between TP and the imidazolium ring increases. On the other hand, because alkyl is an electron donating group, when the size of the alkyl chain of the cation increases the π-π interactions between TP and the imidazolium ring of the IL increases. This mechanism has been suggested before to explain the increase of the extractive performance of S-compounds of other imidazolium [44, 52] and pyridinium-based ILs [51] with the increase of the alkyl chain of their cations.

From the comparison of the measured and predicted equilibrium curves it can also be observed that the size of the immiscibility area and the predicted UCST for both IL systems were underestimated. COSMO-RS assumes high solubility at very low temperatures and big discrepancies concerning the experimental data and the correlation values are found. This might result from the fact that COSMO-RS does not properly account for the π-π interactions most responsible for these systems miscibility. Nevertheless, as mentioned above, this model provides an acceptable qualitative agreement.

To further analyse the performance of COSMO-RS model in the description of (IL + TP) binary mixtures, the results obtained with COSMO-RS in this work were compared to experimental LLE data on binary systems containing TP and imidazolium-based ILs comprising the $[SCN]^-$ available in literature [35]. As it can be seen from Figure 3.6, the experimental phase diagrams of all imidazolium $[SCN]^-$-ILs in TP exhibit an immiscibility area in the liquid phase with a LCST, but COSMO-RS predicts a different shape of the equilibrium curves, or, in other words, a different solubility behaviour, predicting an immiscibility area in the liquid phase with a UCST.

Although COSMO-RS incorrectly describes the shape of the equilibrium curves, the predicted trend for the solubility of TP in the ILs follows the order $[C_6mim][SCN]$ > $[C_4mim][SCN]$ > $[C_2mim][SCN]$, predicting the same cation alkyl chain length influence observed with $[NTf_2]^-$–based ILs.

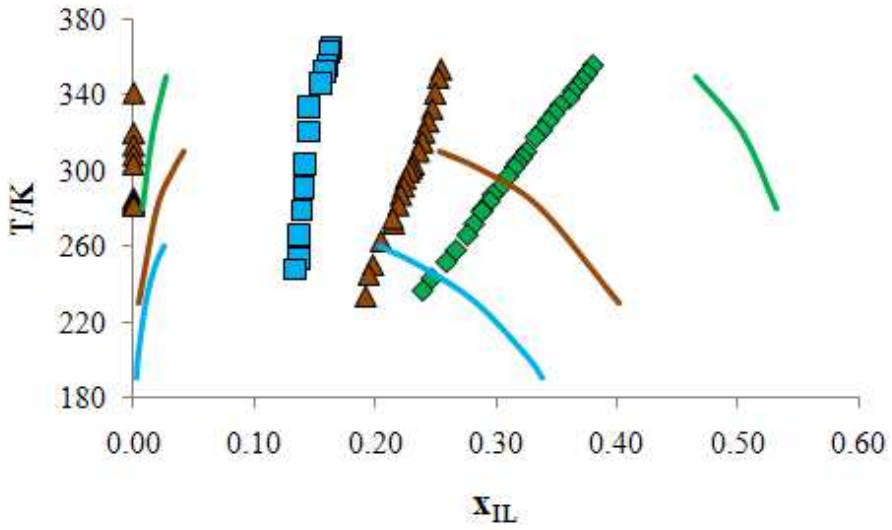

Figure 3.6: Liquid–liquid phase diagram for $[C_2mim][SCN]$ (◆), $[C_4mim][SCN]$ (▲) and $[C_6mim][SCN]$ (■) with TP. The single symbols and the lines represent respectively the literature experimental data[35] and the COSMO-RS calculations performed in this work.

As already discussed above, the results obtained for the COSMO-RS calculations of the TP and $[SCN]^-$-based ILs binary systems confirm that the predictions of the model for such systems involving TP are not in accordance with the experimental data, probably because of an innapropriate treatment of the π-π interactions which determine the behaviour of these systems. In fact, in order to evaluate the IL-cation family influence, COSMO calculations of the solubility of $[Et_3S][NTf_2]$ and of $[C_4{}^4mpy][NTf_2]$ in TP were performed, but COSMO-RS was not able to simulate neither of these systems. According to the experimental data (Figure 3.8) [35], complete miscibility was observed up to the low mole fraction of the IL for mixtures of $[Et_3S][NTf_2]$ and TP, determined by strong interactions between the S-atom of the IL cation and/or $[NTf_2]^-$ and the S-atom in TP. Complete miscibility above low mole fraction of the IL was also found in ($[C_4{}^4mpy][NTf_2]$ + TP) systems (Figure 3.7 and Figure 3.8) [35], where the π-π interactions between the aromatic ring of TP and the pyridinium-based IL are not adequately taken into account in COSMO-RS calculations. Therefore, the model does not seem to properly account these type of interactions.

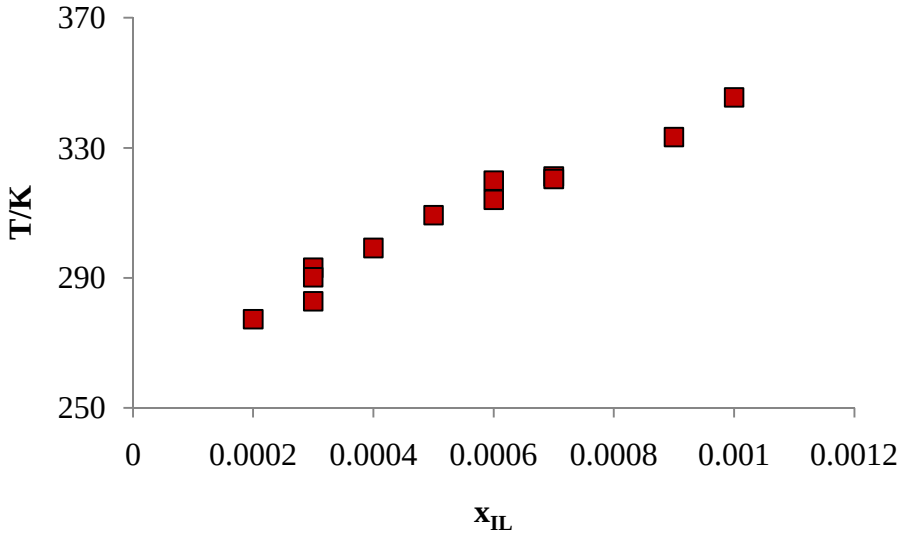

Figure 3.7: Experimental liquid–liquid phase diagram for $[C_4{}^4mpy][NTf_2]$ (■), with TP. [35] .

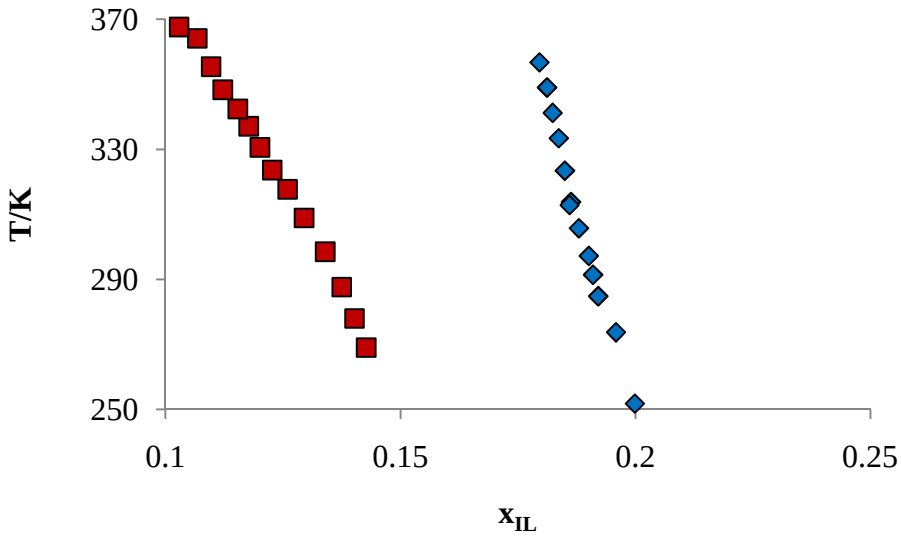

Figure 3.8: Experimental liquid–liquid phase diagram for $[C_4{}^4mpy][NTf_2]$ (■) and $[Et_3S][NTf_2]$ (◆) with TP. [35] .

3.4.2. Effect of the anion family

The comparison of the experimental and predicted data for the solubility of TP in imidazolium based-ILs with the same cation and different anions, presented in Figure 3.9 and Figure 3.10, suggests that COSMO-RS fails in the prediction of the anion effect on the IL-TP mutual solubility.

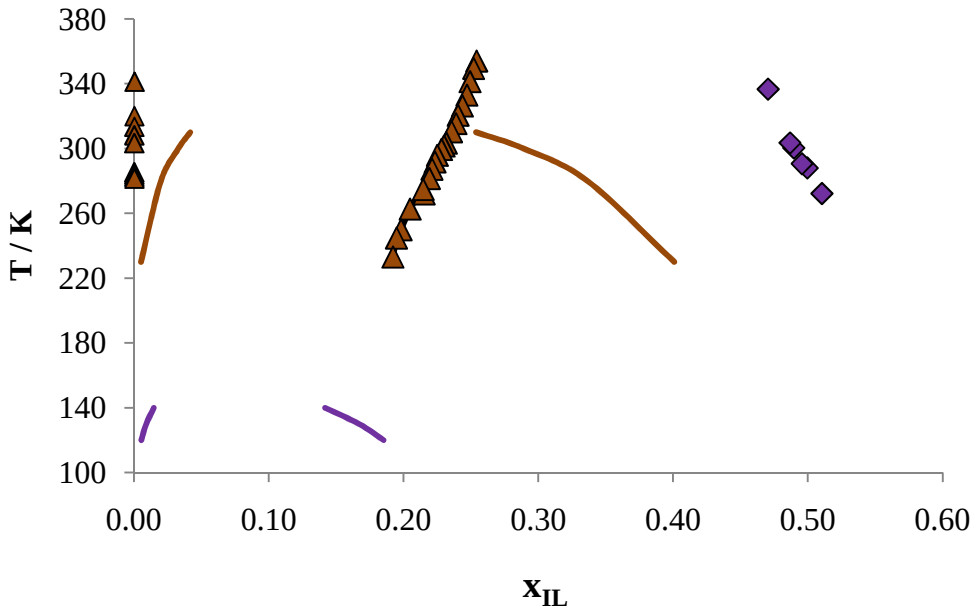

Figure 3.9: Liquid–liquid phase diagram for [C_4mim][NTf_2] (this work) (◆) and [C_4mim][SCN][35] (▲) with TP. The single symbols and the lines represent, respectively, the experimental data and the COSMO-RS calculations performed in this work.

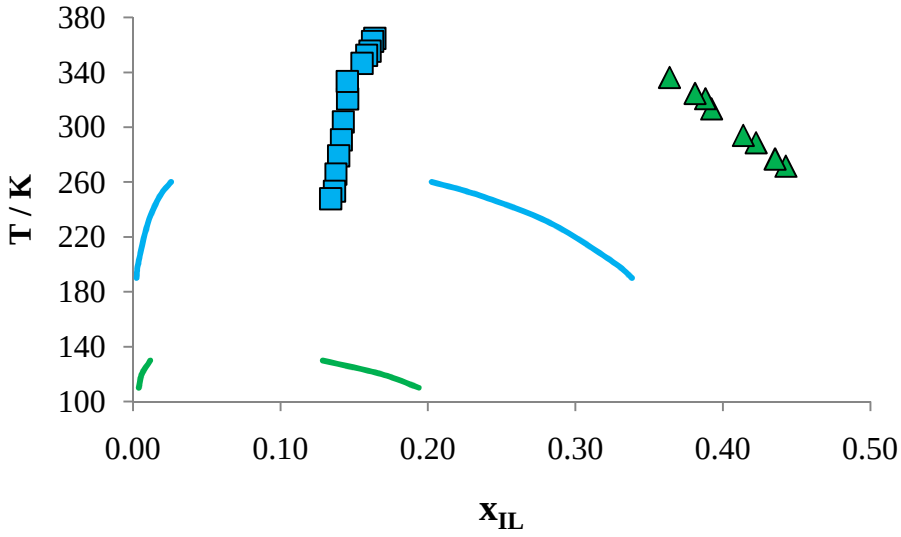

Figure 3.10: Liquid–liquid phase diagram for [C_6mim][NTf_2] (this work) (▲) and [C_6mim][SCN] [35](■) with TP. The single symbols and the lines represent, respectively, the experimental data and the COSMO-RS calculations performed in this work.

The model can qualitatively describe the behaviour of the systems comprising [NTf_2]$^-$-based ILs, but incorrectly predicts the LLE phase diagrams when the anion of the IL is changed to [SCN]$^-$, predicting UCST for both systems, which is not experimentally observed in the case of the latest, as discussed above. This suggests that COSMO-RS is

much less reliable in the description of the phase behaviour of mixtures of TP with $[SCN]^-$-based ILs than of ($[NTf_2]^-$-based ILs + TP) systems.

According to the results obtained with COSMO-RS, the change of the IL anion from $[Tf_2N]^-$ to $[SCN]^-$, maintaining the cation, originates a decrease of the IL-TP mutual solubility, an increase in the immiscibility area and a higher UCST. However, it is experimentally observed that $[SCN]^-$-based ILs [35] have higher solubility in TP when compared with the solubility of $[NTf_2]^-$-based (ILs + TP) systems experimentally determined in this work. A possible explanation is the fact that $[SCN]^-$ is a smaller anion with no sterical shielding effects and thus establishes stronger interactions with TP, which COSMO-RS does not properly treat.

The scarceness of available data makes it difficult to evaluate the anion effect on the mutual solubilities between the compounds of the type of systems under study. Nevertheless, both IL cation and IL anion nature are known to have a significant influence on the phase behaviour and their particular combination is determinant for the IL selectivity for S-compounds [126-127].

3.5 Conclusions

From the analysis of the results obtained in this work and of the literature available data, it can be seen that the liquid phase behaviour of (IL + TP) binary systems depends on different factors such as the cation alkyl chain length and cations/anions families of the ILs.

It was experimentally observed that when the cation chain length of imidazolium-based ILs with the same anion is increased, the solubility of the IL increases. The COSMO-RS model can qualitatively predict this trend for $[NTf_2]^-$ imidazolium-based ILs, but not quantitatively.

In general, a poor qualitative and/or quantitative agreement was found between the data predicted with COSMO-RS and the experimental data available in literature.

COSMO-RS does not provide a good description of the LLE in binary mixtures involving TP and imidazolium $[SCN]^-$-based ILs and completely fails on the prediction of the effect of the IL anion on the phase behaviour of the (IL + TP) systems under study. Nevertheless, since experimental studies on the anion effect are still scarce, further investigation on this subject is needed.

According to the experimental results obtained, the ILs investigated in this work could be effective entrainers for the separation of S-compounds from n-alkanes, since they can be dissolved, for example, in equimolar mixtures at temperatures around 100 ºC.

4. LLE in Ternary Systems

4.1 Introduction

As mentioned in previous chapters, the crucial issue in the design of an EDS process using ILs as solvents is to find an IL that selectively removes the S-compounds, without affecting the concentration of other components such as aliphatic and aromatic HCs because these are important for maintaining octane number in fuels. Therefore, for an IL to be a good extracting agent, the solubility of HCs in the IL must be low and the solubility of S-compounds in the IL high. Moreover, it is desirable that the problem of cross-contamination (presence of the IL in the raffinate and extraction of HCs together with S-compounds) is avoided and thus the IL should additionally have a poor solubility in the HCs. In fact, the complete absence of the IL in the HC rich-phase is desirable in order to avoid the use of a solvent recovering unit in the process. Furthermore, because when considering desulfurization processes in combination with HDS, more reactions than the removal of S-compounds are involved, it is important to analyse the ability of the ILs not only to desulfurizate, but also to denitrogenate. LLE data on ternary systems involving ILs, aliphatic and aromatic HCs, and S- and N-containing compounds are thus essential to identify the best IL to be used and enhance the efficiency of the desulfurization processes.

There are many data on the LLE of ternary systems involving ILs, S- or N-compounds, aromatics and HCs in literature. Some were correlated by the NRTL and UNIQUAC models [3, 10, 23, 36, 48, 94, 96, 100, 102, 104, 128-133] and a few modelled with COSMO-RS [134].

A review on the LLE experimental data of (ILs + S- or N-compounds + alkanes) / (ILs +S-compounds + aromatics) ternary systems relevant to desulfurization or denitrogenation and accessible on the literature is compiled in Table 4.1. As can be seen, there is already a good number of ILs studied, comprising cations of different families and anions of diverse nature. Nevertheless, in face of the large number of cation and anion combinations in ILs, the information available is still not enough and satisfactory. Since a screening of the various possible ILs is essential to an adequate selection of the solvent and experimental studies for all the possible combinations are not possible, COSMO-RS may be a useful tool for this purpose. However, systematic investigations on the performance of COSMO-RS model on the description of ternary systems involved in desulfurization/ denitrogenation processes have seldom been reported [134].

Table 4.1: LLE experimental data of (ILs + S- or N-compounds+ alkanes) / (ILs + S- compounds + aromatics) ternary systems, analytical tecnique and model applied.

Ionic Liquid	**Hydrocarbon**	**S- or N-compound**	**Analitical tecnique**	**Model**	**Reference**
$[C_2mim][EtSO_4]$	*n*-Hexane *n*-Heptane *n*-Dodecane *n*-Hexadecane	TP	Gas Chromatography	NRTL UNIQUAC	[100]
$[C_2mim][EtSO_4]$	2,2,4-Trimethylpentane				[3]
$[C_2mim][EtSO_4]$	Toluene	TP			[3]
$[C_1mim][MP]$	*n*-Heptane	TP	Gas Chromatography Density measurements		[128]
$[C_4mim][SCN]$	*n*-Heptane				
$[C_4mim][BF_4]$	*n*-Heptane				
$[C_8mim][BF_4]$	*n*-Hexane Cyclohexane		Gas Chromatography	NRTL	[23]
$[C_8mim][BF_4]$	*n*-Heptane *n*-Dodecane *n*-Hexadecane			NRTL	[10]
$[C_8mim][BF_4]$	2,2,4-Trimethylpentane			NRTL	[48]
$[C_8mim][BF_4]$	Methylcyclohexane			NRTL	[104]
$[C_8mim][BF_4]$	Toluene	TP		NRTL	[48]
$[C_8mim][BF_4]$	*n*-Hexane	TP		COSMO-RS	[134]
$[C_2mim][EtSO_4]$	*n*-Hexane	Py	Gas Chromatography	NRTL	[129]
$[C_8mim][BF_4]$					
$[C_8mim][NTf_{2]}$					

Ionic Liquid	Hydrocarbon	S- or N-compound	Analytical tecnique	Model	Reference
$[C_2mim][NTf_2]$	*n*-Heptane	TP	Gas Chromatography	NRTL	[130]
$[C_8mim][NTf_2]$	2,2,4-Trimethylpentane			NRTL UNIQUAC	[94]
$[C_8mim][NTf_2]$	Toluene	TP		NRTL UNIQUAC	[94]
$[C_8mim][NTf_2]$	*n*-Hexane *n*-Heptane *n*-Hexadecane	TP		NRTL	[102]
$[C_8mim][NTf_2]$	*n*-Dodecane Cyclohexane			NRTL	[36]
$[C_8mim][NTf_2]$	Methylcyclohexane			NRTL	[104]
$[C_6^{3,5}dmpy][NTf_2]$	*n*-Hexane *n*-Dodecane *n*-Hexadecane			NRTL UNIQUAC	[96]
$[C_6^{3,5}dmpy][NTf_2]$	*n*-Heptane				[135]
$[C_6^{3,5}dmpy][NTf_2]$	2,2,4-Trimethylpentane				
$[C_6^{3,5}dmpy][NTf_2]$	Toluene	TP			[135]
$[C_6^{3,5}dmpy][NTf_2]$	*n*-Hexane	Py			[96]
$[C_2mim][EtSO_4]$	*n*-Dodecane	DBT	Refractometry	NRTL	[131]
$[C_2mim][DEPO_4]$		DBT			
$[C_2mim][EtSO_4]$		4-MDBT			[133]
$[C_2mim][DEPO_4]$		4-MDBT			
$[C_2mim][EtSO_4]$		4,6-DMDBT			[132]
$[C_2mim][DEPO_4]$		4,6-DMDBT			

In this work, experimental LLE data taken from literature of (ILs + S- or N-compounds+ alkanes) / (ILs+ S- compounds + aromatics) ternary systems were modelled with COSMO-RS. The performance of the model on the prediction of the effect of the structural characteristics of the ILs, S- or N-compounds and HCs or aromatics on the mutual solubilities between these compounds was evaluated and the best ILs to be used as extracting solvents for the desulfurization of transportation fuels were identified.

4.2 Modeling

COSMO-RS calculations were performed as described in the previous chapter . All simulations were carried out at 298.15 K, or in some cases at 313.15 K, and at atmospheric pressure. The LLE was calculated for (ILs + S- or N-compounds + alkanes) / (ILs + S-compounds + aromatics) ternary systems combining different IL families and typical compounds that are usually found in transportation fuel formulations like aliphatic, cyclic and aromatic HCs, S-compounds, namely TP and DBT-derivatives, and N-compounds. All the ternary diagrams in this section are presented in molar fraction.

The chemical structure of the cations and anions composing the ILs considered in the simulations, and of the other compounds under study are shown in Figure 4.1 and Figure 4.2, respectively.

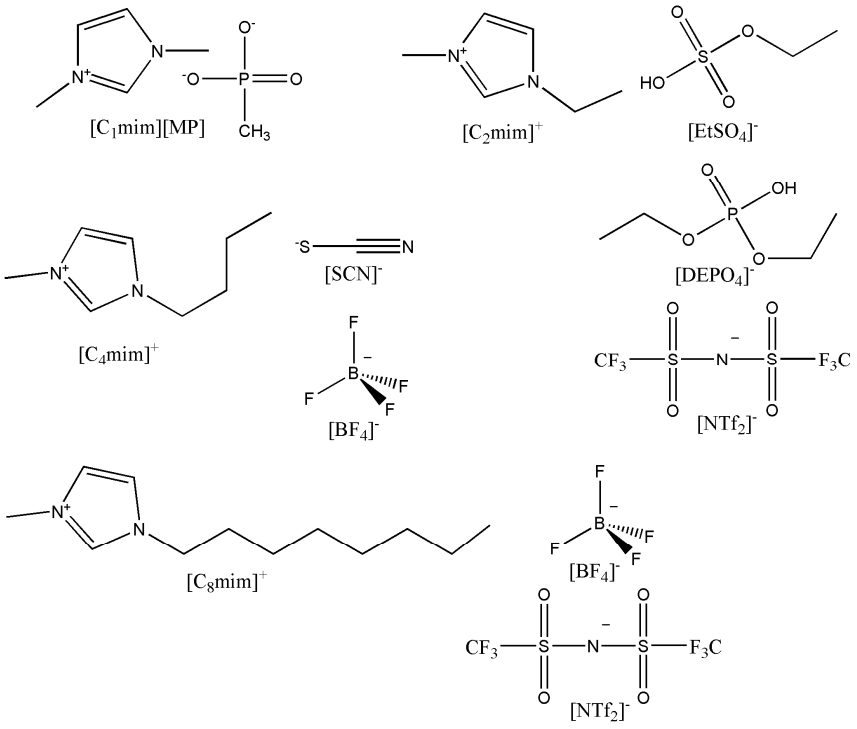

Figure 4.1: Chemical structure of the ILs ions studied.

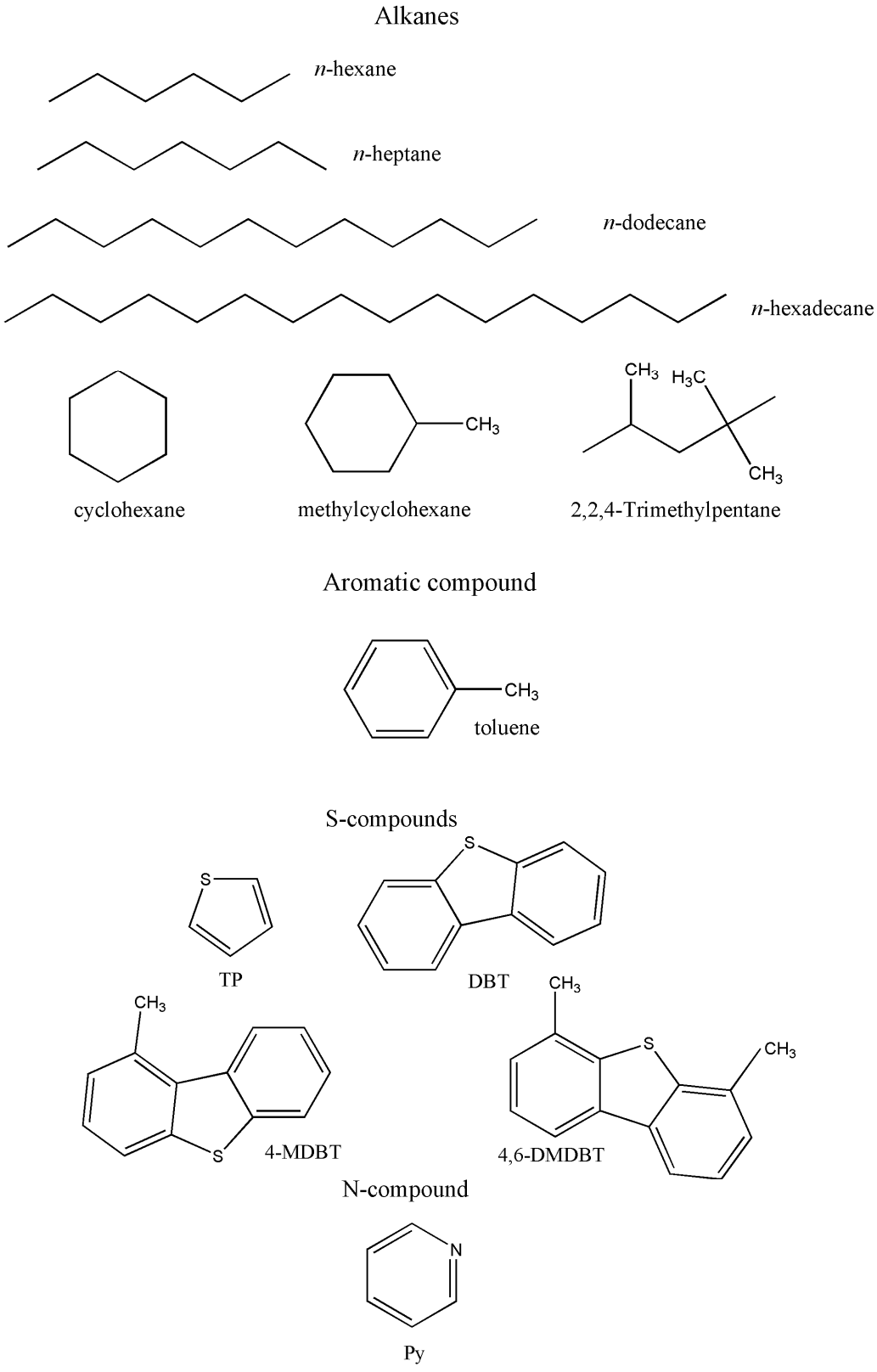

Figure 4.2: Chemical structure of the molecular compounds studied.

4.3. Results and Discussion

The COSMO-RS results obtained in this work, together with the comparison with literature experimental data are presented in Figure 4.3 to Figure 4.36.

From the analysis of the LLE data it is clear that the phase behaviour of the ternary systems, as well as the quality of the COSMO-RS predictions, is dependent on the structural characteristics of the HCs, of the TP and DBT-derivatives and of the cation and anion of the IL.

4.3.1 Effect of the alkanes

In order to evaluate the influence of the structural characteristics of the alkanes on the mutual solubilities, LLE results obtained from the COSMO-RS calculations performed in this work, together with the experimental data are represented in triangular diagrams for the following ternary systems - ([C_2mim][$EtSO_4$] + TP +alkane), ([C_8mim][BF_4] + TP + alkane), ([C_8mim][NTf_2] + TP + alkane) and ([$C_6^{3,5}$dmpy][NTf_2] + TP + alkane), shown in Figure 4.3-Figure 4.10. To make the analysis easier, these systems will be considered in groups in which the IL and TP are fixed and the nature of the alkane is varied (*n*-alkanes with different chain lengths, branched alkanes and cycloalkanes).

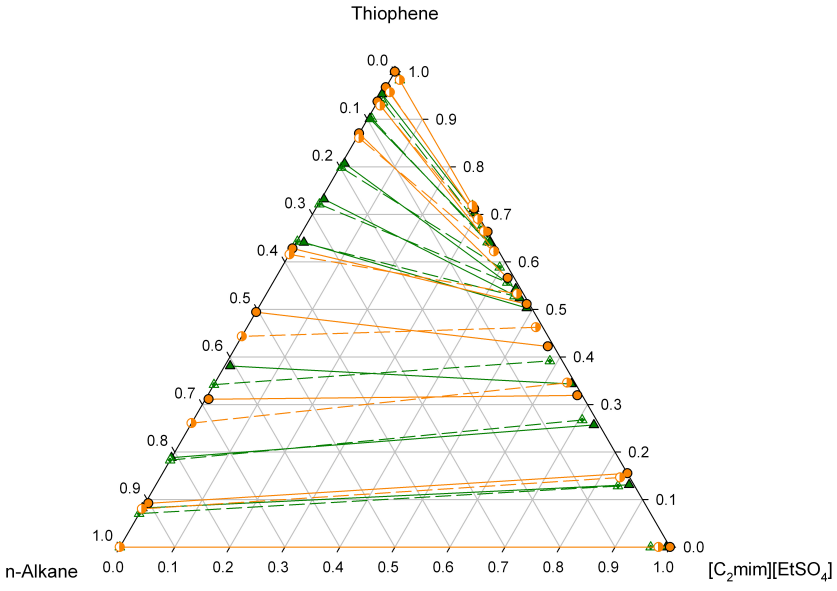

Figure 4.3: Experimental tie-lines for the LLE of the ternary systems {[C_2mim][$EtSO_4$] + TP + *n*-hexane} (▲,solid line) and {[C_2mim][$EtSO_4$] + TP + *n*-heptane}(●, solid line) at 298.15K [100] , and correspondent COSMO-RS predicted tie-lines (◬, ◑, dash lines).

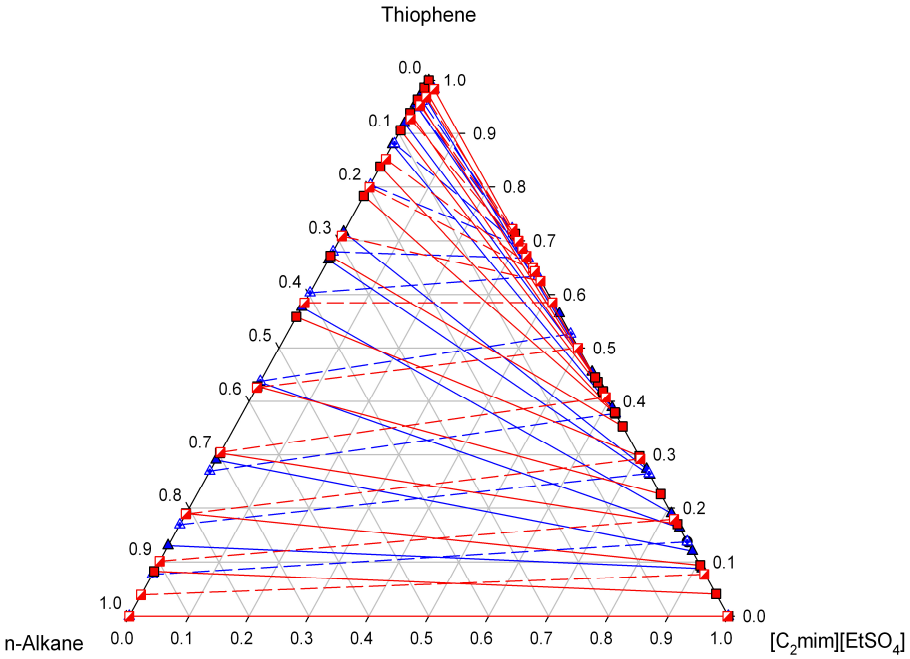

Figure 4.4**:** Experimental tie-lines for the LLE of the ternary systems {[C_2mim][$EtSO_4$] + TP + *n*-dodecane} (■,solid line) and {[C_2mim][$EtSO_4$] + TP + *n*-hexadecane}(▲, solid line) at 298.15K [100], and correspondent COSMO-RS predicted tie-lines (◪, ◬, dash lines).

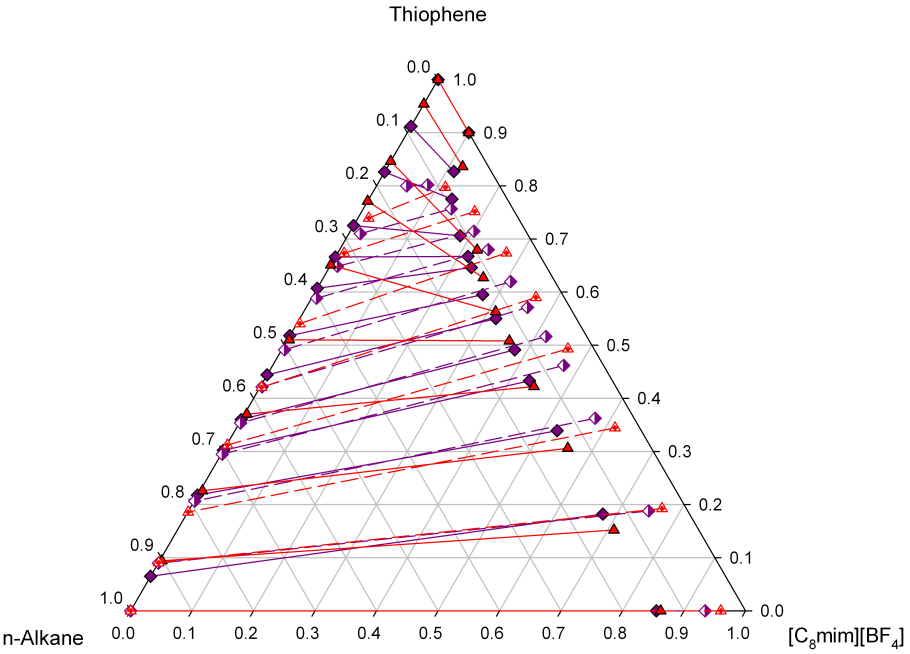

Figure 4.5: Experimental tie-lines for the LLE of the ternary systems {[C_8mim][BF_4] + TP + *n*-hexane}[23] (◆,solid line) and {[C_8mim][BF_4] + TP + *n*-heptane} [10] (▲, solid line) at 298.15K, and correspondent COSMO-RS predicted tie-lines (⬗,◬, dash lines).

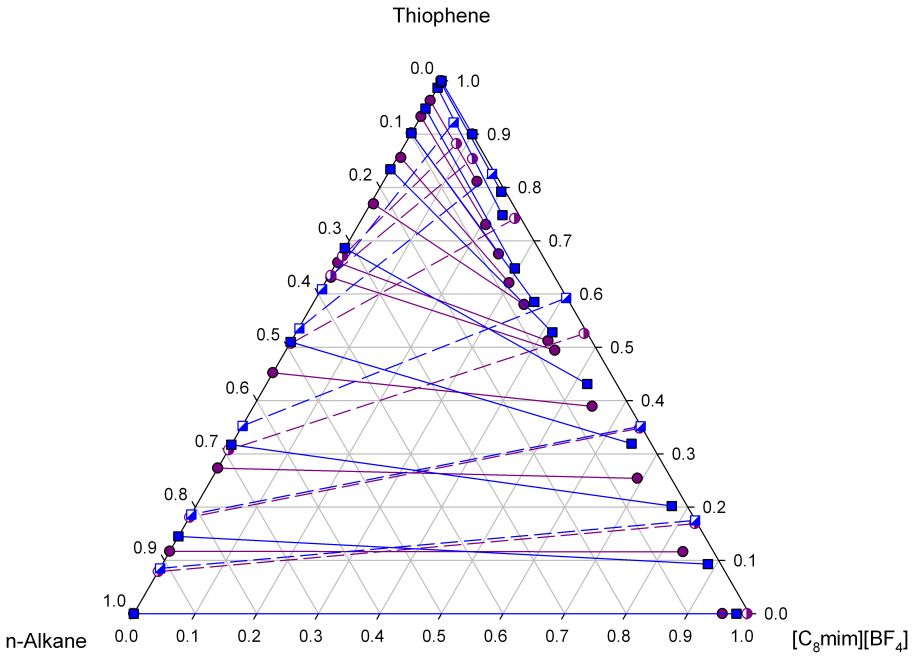

Figure 4.6: Experimental tie-lines for the LLE of the ternary systems {[C_8mim][BF_4] + TP + *n*-dodecane} (●,solid line) and {[C_8mim][BF_4] + TP + *n*-hexadecane}(■, solid line) at 298.15K [10], and correspondent COSMO-RS predicted tie-lines (◑,◪, dash lines).

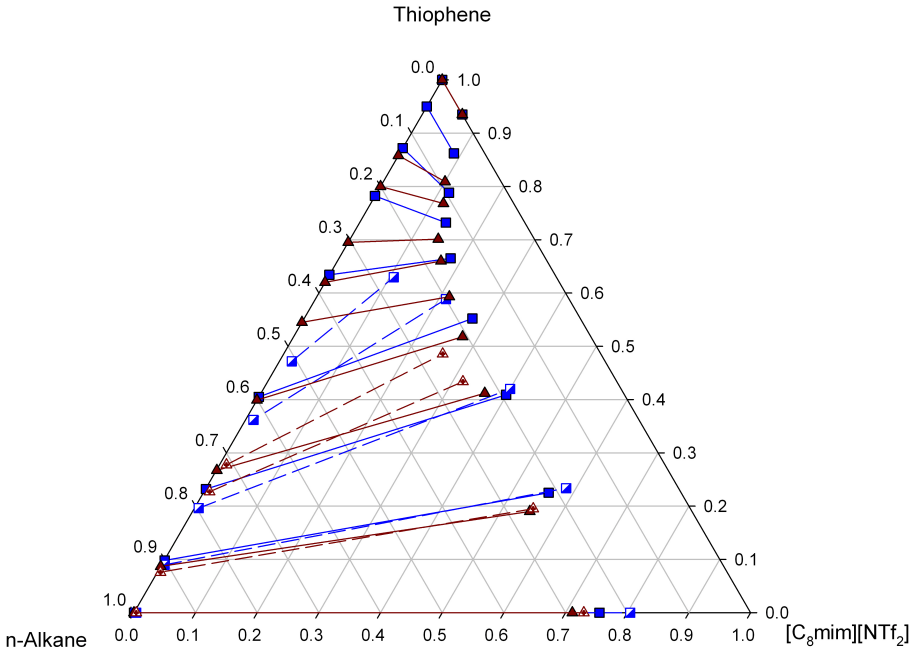

Figure 4.7: Experimental tie-lines for the LLE of the ternary systems {[C_8mim][NTf_2] + TP + *n*-hexane} (▲, solid line) and {[C_8mim][NTF_2] + TP + *n*-heptane}(■, solid line) at 298.15K [102] , and correspondent COSMO-RS predicted tie-lines (◬,◪, dash lines).

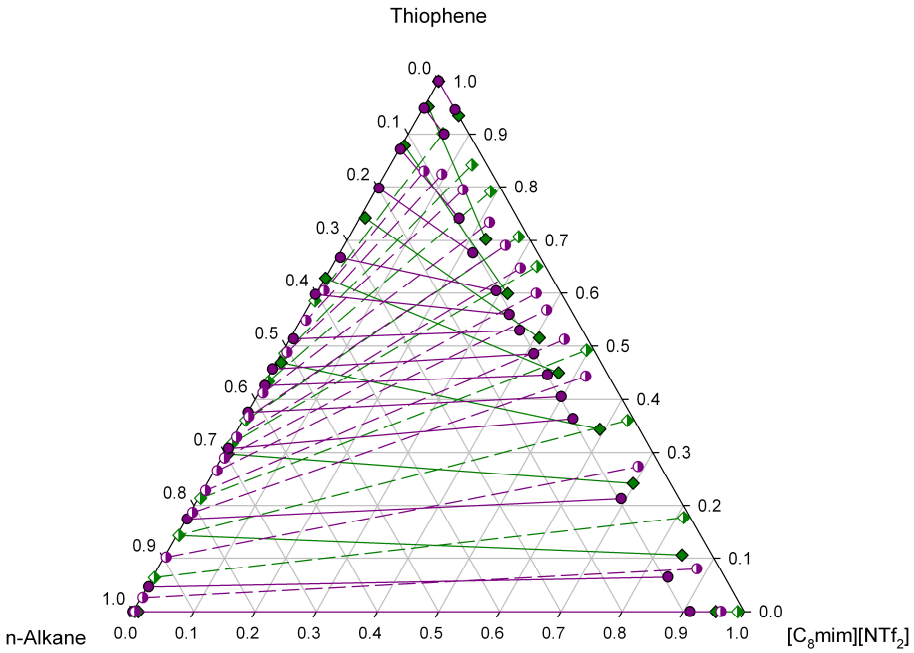

Figure 4.8: Experimental tie-lines for the LLE of the ternary systems {[C_8mim][NTf_2] + TP + *n*-dodecane}[36] (●, solid line) and {[C_8mim][NTf_2] + TP + *n*-hexadecane}[102] (◆, solid line) at 298.15K, and correspondent COSMO-RS predicted tie-lines (◑,◈, dash lines).

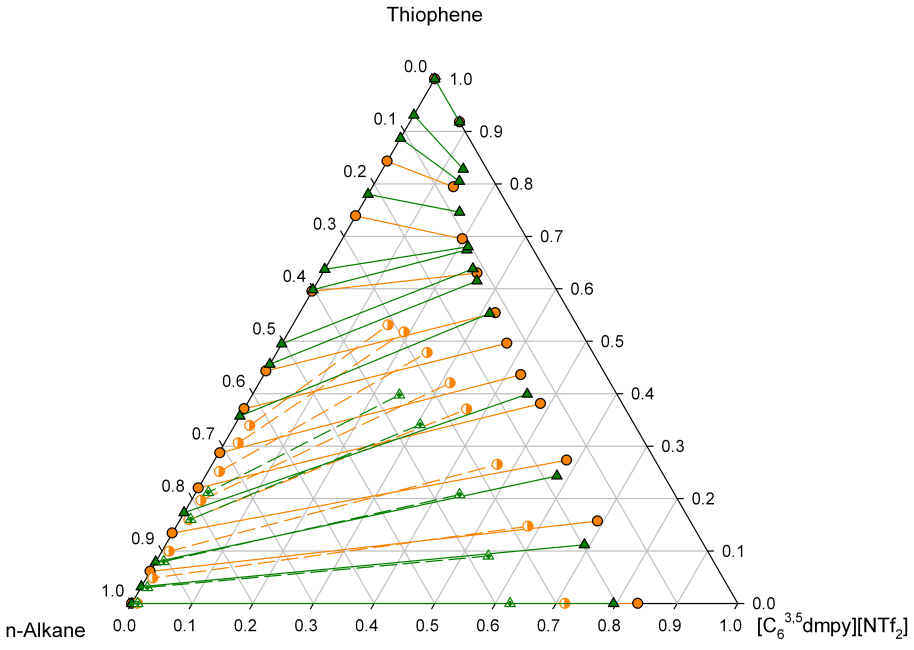

Figure 4.9: Experimental tie-lines for the LLE of the ternary systems {[$C_6^{3,5}$dmpy][NTf_2] + TP + *n*-hexane} (▲, solid line)[96] and {[$C_6^{3,5}$dmpy][NTf_2] + TP + *n*-heptane}[135] (●, solid line) at 298.15K, and correspondent COSMO-RS predicted tie-lines (◬,◑, dash lines).

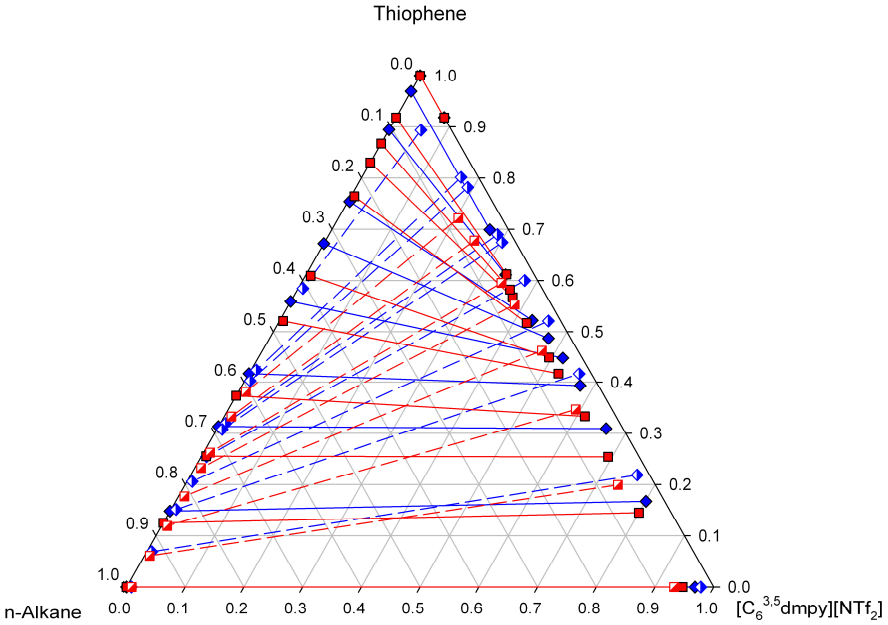

Figure 4.10: Experimental tie-lines for the LLE of the ternary systems {[$C_6^{3,5}$dmpy][NTf_2] + TP + *n*-dodecane} (■, solid line) and {[$C_6^{3,5}$dmpy][NTf_2] + TP + *n*-hexadecane}(◆, solid line) at 298.15K [96], and correspondent COSMO-RS predicted tie-lines (◪,◈, dash lines).

Globally, the main features and quality of the COSMO-RS predictions for the effect of the alkyl chain length of the n-alkane on the LLE are similar for all the ternary systems (IL+TP+n-alkane) studied.

As it can be seen, all the ternary systems predicted with COSMO-RS show Type 2 behaviour, with two of their constituent pairs exhibiting partial immiscibility in good agreement with what is observed experimentally.

In general, COSMO-RS can describe better the tie-lines of the ternary systems containing HCs with small alkyl chains (*n*-hexane and *n*-heptane) than with higher alkyl chain lengths. For the former systems, good predictions are obtained for the lowest part of the diagrams, where the predicted tie-lines have (positive) slopes in good agreement with the experimental data. However, in terms of the binodal curves, better results are obtained for the systems containing HCs with longer alkyl chains. For medium concentrations of TP, however, COSMO-RS provides a less accurate description of the tie-lines, predicting in some cases an inversion of the sloping behaviour experimentally observed. In the case of the ternary systems containing HCs with longer alkyl chains, the model completely fails on the description of the experimental tie-lines in the whole range of TP concentrations These trends are observed for the COSMO-RS predictions of the LLE in the ternary systems ([C_2mim][$EtSO_4$] + TP + *n*-alkane), ([C_8mim][BF_4] + TP + *n*-alkane),

([C_8mim][NTf_2] + TP + *n*-alkane) and ([$C_6^{3,5}$dmpy][NTf_2] + TP + *n*-alkane). For the last two systems mentioned, COSMO-RS was not able to calculate the region of high TP concentrations when small *n*-alkanes were considered, while for the former two systems, a good description of the tie-lines located in the top of the diagrams is obtained. Nevertheless, since the sulfur content in fuels is very low, this region is not of interest for the application of desulfurization processes in practical terms and the lowest parts of the diagrams are actually the ones which must be considered.

Regarding the shape and size of the immiscibility region, the model provides an acceptable qualitative agreement with the experimental data, predicting that increasing the alkyl chain length of aliphatic HCs, the zone of heterogeneity increases, as observed experimentally. Consistently with the experimental results this increase is less notorious in the case of ([C_2mim][$EtSO_4$] + TP + *n*-alkane) systems, but significant for the other ILs considered. In general, the increase in the immiscibility region with increasing alkane chain length predicted by COSMO-RS is in good qualitative agreement with the experimental data, but, from a quantitative point of view, the calculated binodals reasonably deviate from the experimentally determined. As far as the IL concentration in the HC-rich phase is concerned, the results obtained with COSMO-RS show no detectable concentration of IL in the HC-rich phase for all the systems except for ([C_8mim][NTf_2] + TP + *n*-heptane/*n*-hexadecane) and [$C_6^{3,5}$dmpy][NTf_2] ternary mixtures for which very low amounts of IL in the alkane-rich phase are predicted. However, no detectable concentrations of IL in the HC-rich phases has been experimentally found for any of the systems considered. In sum, all these results suggest that for regions of low concentration of TP (which in practice are those of interest) and for systems comprising *n*-alkanes with small alkyl chains, the LLE description of COSMO-RS is good, with the predicted slopes of the tie lines similar to those observed experimentally. For mixtures containing longer chain alkanes, the model fails, probably due to more complex interactions, shielding effects present in those systems, which COSMO-RS cannot properly account for. A possible explanation for the deviations from the experimental data when using cations and HCs with long alkyl chains can be the formation of microaggregates of ILs, which is not taken into account by the COSMO-RS calculations. This fact was verified in a previous study on binary systems concerning ILs and alcohols [117] with the gradual decrease of the quality of the predictions when cations with long alkyl chain lengths are considered. Although the quantitative predictions reasonably deviate from the experimental data, the

model can qualitatively describe the experimentally observed increase in the immiscibility region with the increase of the size of the *n*-alkane chain.

The slope of the tie lines, the shape and extension of the heterogeneous region, and the concentration of TP in the HC-rich phase are crucial aspects to take into account when considering the extraction process in practical terms. Larger immiscibility regions indicate a better selectivity of the solvent (the IL extracts TP and not the alkanes), which is observed for HCs with higher alkyl chain length. In addition, it is desirable to have an undetectable concentration of IL in the HC- rich phase to avoid further separations. Therefore, despite the limitations of the COSMO-RS predictions, the model can correctly predict that the extractions from systems constituted by the largest chain alkanes will be more efficient.

Comparing the phase diagram of the ([C_8mim][BF_4] + TP + n-hexane) ternary system calculated in this work with the one reported in the literature [134], it can be seen that although a better description of the model is obtained in the interest zone for the latest, since the slope of the predicted tie-lines are in very good accordance with the experimental data, a closer global description is obtained for the first diagram. A possible explanation can be the version of the COSMO-RS model and the type of the quantum chemical calculation adopted for each simulation, since it was used a more recent version and the Turbomole program in this work and the Gaussian 03 for the ternary system referenced in the literature. In both cases, the extension of the immiscibility region is not quantitatively well described, since COSMO-RS predicts larger immiscibility regions than those observed experimentally and the calculated binodals reasonably deviate from the experimentally determined.

Regarding the effect of branched chains and of cyclic alkanes, the quality of the COSMO-RS predictions for the systems ([C_8mim][BF_4] + TP + alkane) is similar to that discussed for linear alkanes, but the description of the LLE of ([C_8mim][NTf_2] + TP + alkane) is poorer. As it can be seen from the data presented in Figure 4.11, good descriptions are obtained for low TP concentrations, but, while the immiscibility gap experimentally observed is similar in the phase diagrams of the mixtures containing cyclohexane and methylcyclohexane, wider in *n*-hexane systems and even wider in the branched systems, the model predicts an immiscibitity gap with similar extension for both n-hexane and methylcyclohexane

Although the extension of the immiscibility region for the branched-alkane system is not quantitatively well described since the model predicts a slightly larger immiscibility

region than that observed experimentally, it can be seen that this system is the one which exhibits the larger immiscibility gap which is in accordance with the COSMO-RS calculations. For the systems containing [C_8mim][NTf_2] (Figure 4.12), a reasonable description of the phase behaviour is observed in the lowest part of the diagram, but the model cannot simulate the regions of intermediate and high TP concentration. Also herein, the model can predict that the ternary diagram involving the branched alkane is the one which presents the larger immiscibility gap.

To further study the influence of the branched alkanes on the LLE, the phase diagram of a system containing another IL, [C_2mim][$EtSO_4$], was addionally calculated (Figure 4.13). It can be seen that the quality of the COSMO-RS predictions is similar to that of the ternary systems ([C_2mim][$EtSO_4$] + TP + HCs with higher alkyl chain lengths) previously discussed, *i.e*, the model provides an incorrect description of the experimental tie-lines at low and medium TP concentrations and a good description of the experimental tie-lines situated in the top of the diagram. Indeed, the experimental tie-lines slopes in the lowest part of the diagram are slightly negative, but COSMO-RS predicts an opposite behaviour.

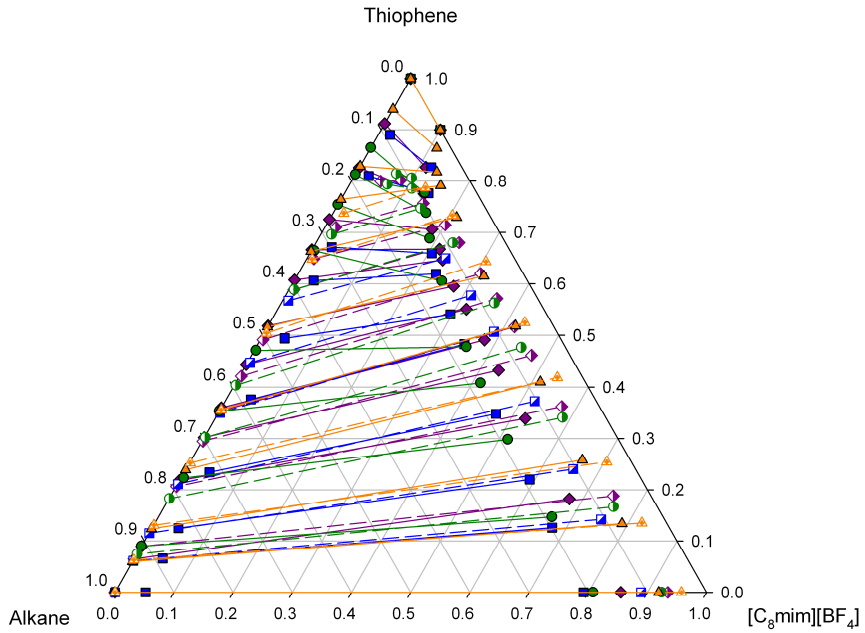

Figure 4.11: Experimental tie-lines for the LLE of the ternary systems {[C_8mim][BF_4] + TP + *n*-hexane}[23] (◆, solid line), {[C_8mim][BF_4] + TP + cyclohexane}[23] (■, solid line), {[C_8mim][BF_4] + TP + methylcyclohexane}[104](●, solid line) and {[C_8mim][BF_4] + TP + 2,2,4-Trimethylpentane} (▲, solid line) at 298.15K, and correspondent COSMO-RS predicted tie-lines (⬗, ◪, ◑, ◬, dash lines).

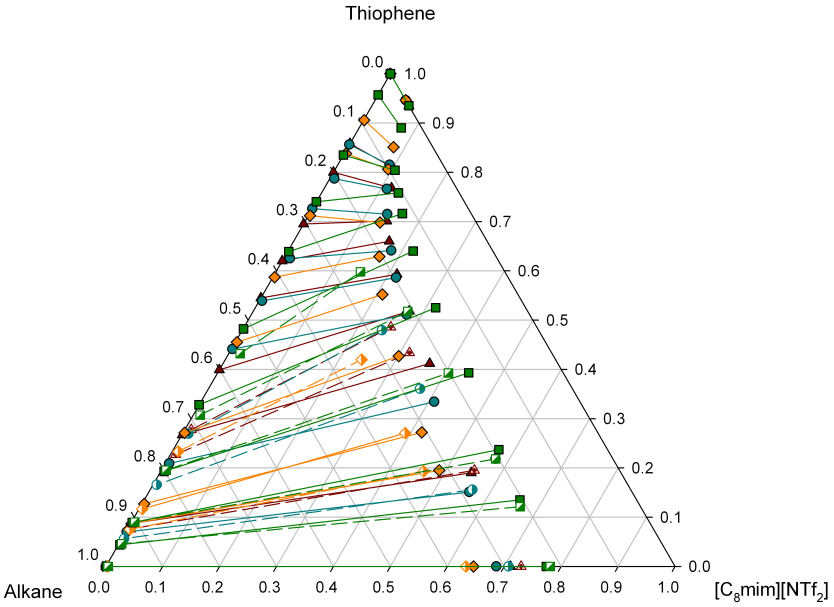

Figure 4.12: Experimental tie-lines for the LLE of the ternary systems {[C_8mim][NTf_2] + TP + *n*-hexane}[102](▲, solid line), {[C_8mim][NTf_2]+ TP + cyclohexane}[36] (◆, solid line), {[C_8mim][NTf_2] + TP + methylcyclohexane}[104](●,solid line) and {[C_8mim][NTf_2] + TP+ 2,2,4-Trimethylpentane} (■, solid line)at 298.15K, and correspondent COSMO-RS predicted tie-lines (◬, ◆, ◑, ◪, dash lines).

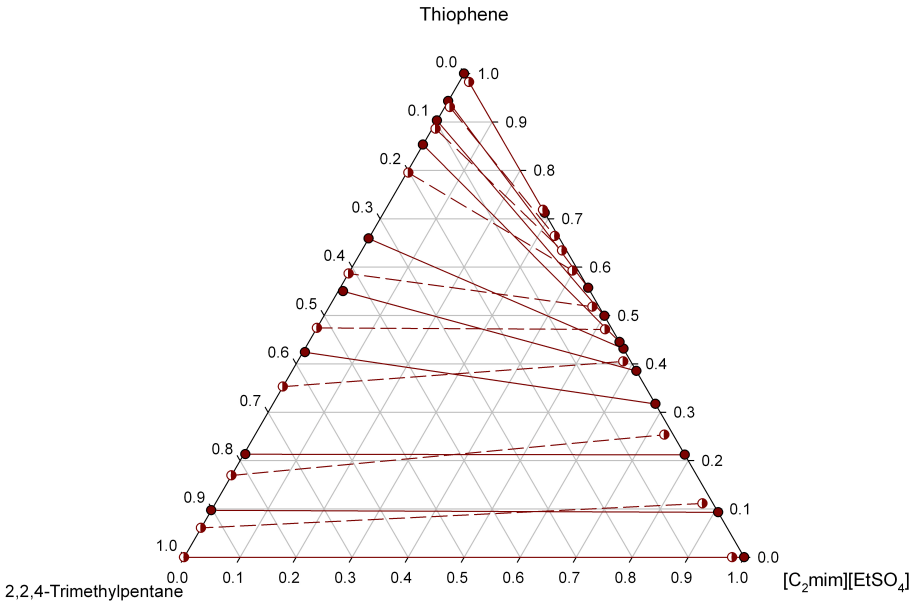

Figure 4.13: Experimental tie-lines for the LLE of the ternary system {[C_2mim][$EtSO_4$] + TP + 2,2,4-Trimethylpentane} [3] (●, solid line) at 298.15K, and correspondent COSMO-RS predicted tie-lines (◑, dash lines).

Comparing the experimental ternary diagrams involving branched and cyclic alkanes, the most favorable extractive system is ([C_2mim][$EtSO_4$] +TP + 2,2,4-Trimethylpentane), since it is the one with larger immiscibility region. Although COSMO-RS globally fails in the qualitative and quantitative description of the LLE experimental

data of systems comprising branched and cyclic alkanes, probably due to the existence of shielding effects in those system for which the model cannot properly account, COSMO-RS can qualitatively predict which are the most convenient systems. Nevertheless, in general terms, it is rather difficult, based on the results obtained, to infer about the quality of the COSMO-RS predictions as far as these alkane effects are concerned.

4.3.2 Effect of the alkyl chain length of the IL cation

The influence of the alkyl chain length of the IL cation on the LLE (IL+TP +alkane) systems and the ability of COSMO-RS to predict this effect was assessed by the inspection of the experimental and calculated phase diagrams of ternary mixtures where the S-compound, the alkane and the IL anion were fixed and the alkyl chain length of the imidazolium cations was varied. For that purpose, the phase diagrams of two groups of systems - ([$C_n$mim][NTf_2] + TP + *n*-heptane), *n* = 2,8 and ([$C_n$mim][NTf_2]+ TP + *n*-heptane), *n* = 2,4 - presented in Figure 4.14 and Figure 4.15 were considered. Since it was observed in the previous section that better COSMO-RS descriptions are obtained for low TP concentrations, and those are, in practical terms, the regions of interest, it will be focused the following discussion on the lower parts of the diagrams.

In the region of interest, better predictions are obtained for the systems comprising cations with smaller alkyl chains, independently of the anion nature. In fact, while for ([C_2mim][NTf_2] + TP + *n*-heptane) and ([C_4mim][BF_4] + TP + *n*-heptane) systems, a good qualitative and quantitative agreement with the experimental data is found for both the tie-lines and the binodals, for the ternary mixtures containing the $[C_8mim]^+$ cation, the slopes of the tie-lines and in particular the extension of the immiscibility region is not quantitatively well described, with COSMO-RS predicting larger immiscibility regions than those observed experimentally.

A possible explanation for these results is an inappropriate treatment of the π-π interactions established between TP and the IL cation. For the reasons discussed in a previous chapter, the longer the alkyl chain of the IL cation, the stronger are those interactions and therefore the worst are the calculated data.

According to the experimental LLE data, an increase in the size of the cation alkyl chain originates a decrease in the extension of the immiscibility region caused, as discussed before, by the enhancement of the π-π interactions between the S-compound and the imidazolium ring of the cation. This qualitative trend is correctly predicted by COSMO-RS model.

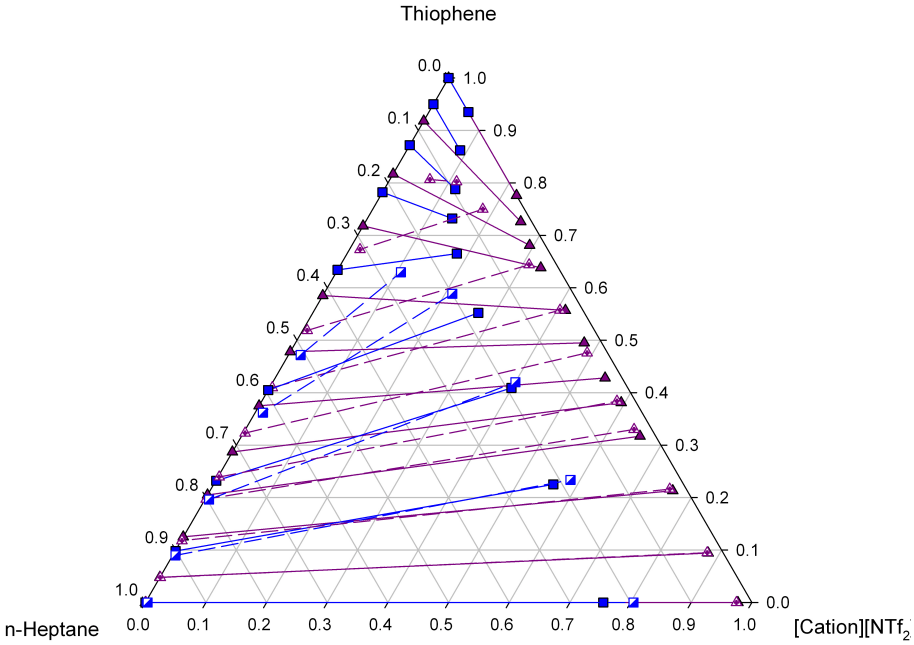

Figure 4.14: Experimental tie-lines for the LLE of the ternary systems {[C_2mim][NTf_2] + TP + *n*-heptane}[130] (▲, solid line) and {[C_8mim][NTf_2] + TP + *n*-heptane}[102] (■, solid line) at 298.15K, and correspondent COSMO-RS predicted tie-lines (◬, ◪, dash lines).

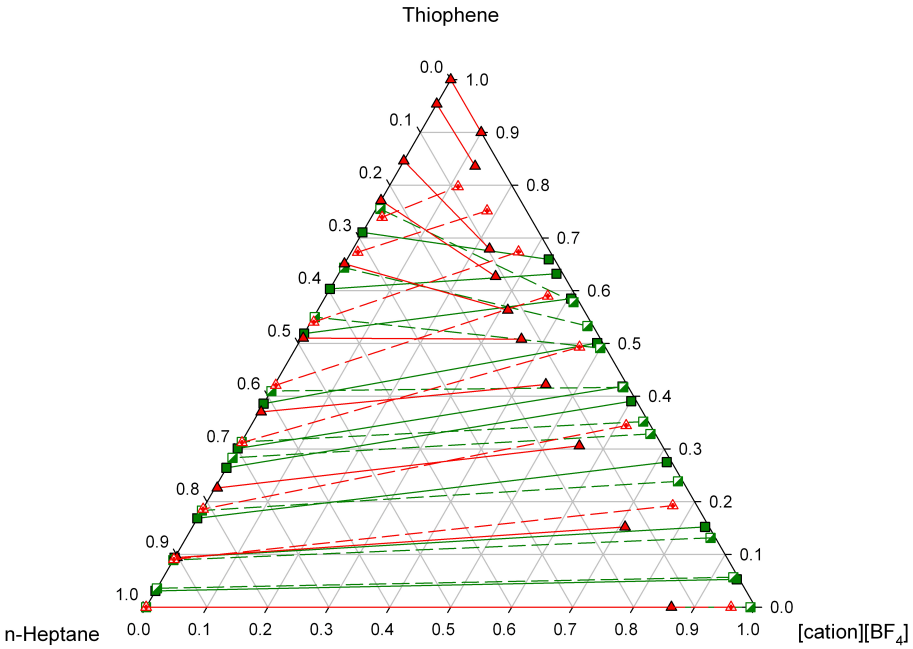

Figure 4.15: Experimental tie-lines for the LLE of the ternary systems {[C_4mim][BF_4] + TP + n-heptane}[128] (■, solid line) and {[C_8mim][BF_4] + TP + n-heptane}[10] (▲, solid line) at 298.15K, and correspondent COSMO-RS predicted tie-lines (◪, ◬,dash lines).

Taking into account these results, the most attractive ILs for a selective extraction of TP (avoiding the extraction of HCs), are the ones which comprise cations with small alkyl chains, since these exhibit higher immiscibility with HCs.

4.3.3 Effect of the cation family

To evaluate the influence of the cation type, and the ability of COSMO-RS to predict this effect, Figure 4.16 and Figure 4.17 show the experimental and COSMO-RS LLE data for ternary systems containing two common classes of IL cations - imidazolium- and pyridinium, maintaining the anion and the alkane.

As observed and discussed before for imidazolium-based ILs systems, COSMO-RS also provides an incorrect description of the experimental tie-lines for medium concentrations of TP in the case of systems containing pyridinium-based ILs. In addition, the model cannot simulate the region which corresponds to high TP concentration.

As it can be seen from the data presented in Figure 4.16, for low TP concentrations, the model correctly describes the tie-lines sloping behaviour, providing reasonable qualitative and quantitative predictions for both types of cations. As far as the immiscibility gap is concerned, there is a good quantitative agreement with the experimental data for imidazolium-based ILs systems, but a poor quantitative description of the binodals for pyridinium-based ILs mixtures, in such a way that the trend predicted by COSMO-RS for the effect of the cation family is the opposite of that experimentally observed. According to experimental data, there is an increase in the immiscibility region when going from imidazolium- to pyridinium- based ILs, indicating a higher selectivity of the latest to the S-compounds, due to stronger π-π interactions established between TP and the aromatic ring of the pyridinium cation than between the S-compound and the imidazolium cation. These stronger interactions might justify the less accurate description of the binodal curves in the case of ternary systems containing pyridinium-based ILs. This type of behaviour is also found in the results presented in Figure 4.17.

Although more data on ternary systems involving more types of cations would be needed to conclude about the ability of COSMO-RS to predict the influence of cation family on the LLE, from the results obtained in this work it might be inferred that the model cannot still be safely used as an *a priori* method for the selection of the IL cation for desulfurization purposes.

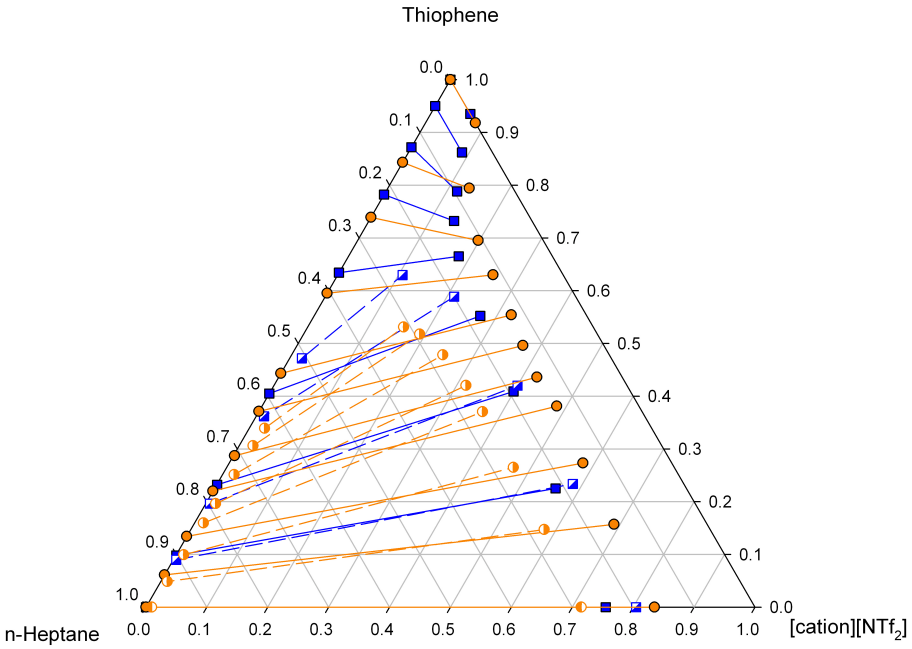

Figure 4.16: Experimental tie-lines for the LLE of the ternary systems {[$C_6^{3,5}$dmpy][NTf_2] + TP + *n*-heptane}[135] (●, solid line) and {[C_8mim][NTf_2] + TP + *n*-heptane}[102] (■, solid line) at 298.15 K, and correspondent COSMO-RS predicted tie-lines (◑, ◪, dash lines).

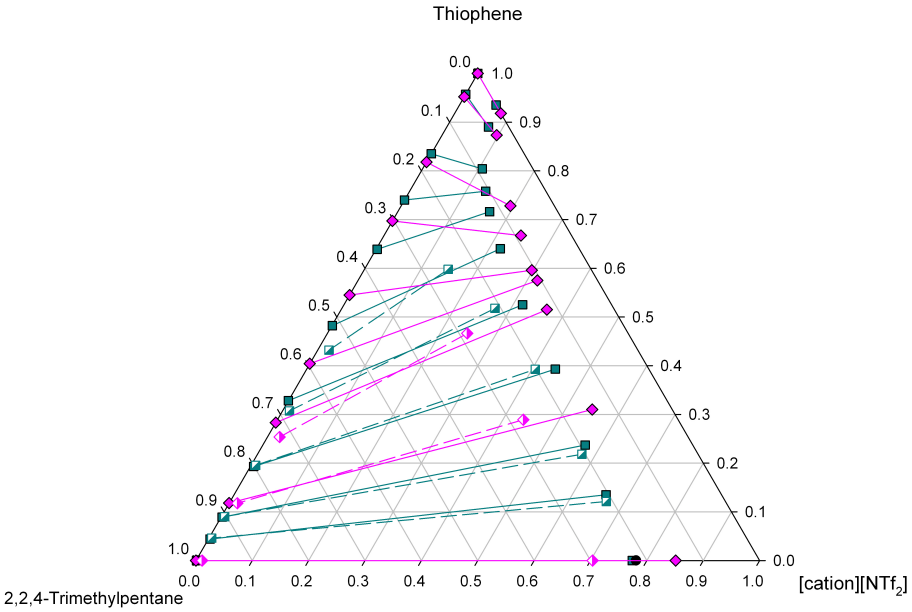

Figure 4.17: Experimental tie-lines for the LLE of the ternary systems {[$C_6^{3,5}$dmpy][NTf_2] + TP + 2,2,4-Trimethylpentane}[135](◆, solid line) and {[C_8mim][NTf_2] + TP + 2,2,4-Trimethylpentane }[94](■, solid line) at 298.15 K, and correspondent COSMO-RS predicted tie-lines (◈, ◪, dash lines).

4.3.4 Effect of the anion family

The influence of the IL anion was examined by changing its nature on a number of systems, while maintaining the cation, S-compound and alkane. Figure 4.18-Figure 4.24 present the experimental and COSMO-RS LLE data for the ([$C_n$mim][anion]+TP+alkane), n = 2,4,8 ternary systems with the following anions: $[EtSO_4]^-$, $[SCN]^-$, $[BF_4]^-$and $[NTf_2]^-$.

In general, in the regions of low TP concentrations, good qualitative predictions are obtained for all the systems considered. For all the systems studied, COSMO-RS correctly predicts larger immiscibility regions for $[BF_4]^-$ than for $[NTf_2]^-$, although for the former anion the extension of the immiscibility region is not quantitatively well described. For the $[SCN]^-$ anion, a good agreement with the experimental data is only observed for very low concentrations of TP. On the basis of the results obtained, COSMO-RS seems thus to be less reliable in the description of the phase behaviour of mixtures containing $[BF_4]^-$- and $[SCN]^-$-based ILs than of those comprising hydrophobic anions, such as $[NTf_2]^-$-based ILs. A possible reason for this fact is the absence of sterical shielding effects around the $[BF_4]^-$ and $[SCN]^-$, which implies stronger interactions with TP which COSMO-RS does not properly treat. A similar interpretation has been suggested in a previous chapter to explain the less reliable prediction of the phase behaviour of binary mixtures containing $[SCN]^-$-based ILs when compared to $[NTf_2]^-$ systems.

The simulation of ternary mixtures involving other anions, namely ([C_1mim][MP] + TP + *n*-heptane), was also performed in this work, but the model was not capable to calculate the LLE of such system. A possible explanation can be the existence of more complex interactions between the IL and the S-compound in those type of systems, which the model is not able to properly account for.

According to the results, (Figure 4.18 and Figure 4.19), the best IL anions to successfully extract the S-compounds are the $[EtSO_4]^-$, and also $[SCN]^-$ and $[BF_4]^-$, since, when combined with a cation like $[C_4mim]^+$, present phase diagrams with larger immiscibility zones.

Although some features of the anion influence can be pointed out the results obtained in this section are still scarce to infer about the COSMO-RS ability to describe the effect of the anions on the LLE. The data suggests, however, that the quality of the COSMO-RS predictions is more dependent on the alkane and IL cation characteristics than on the IL anion nature.

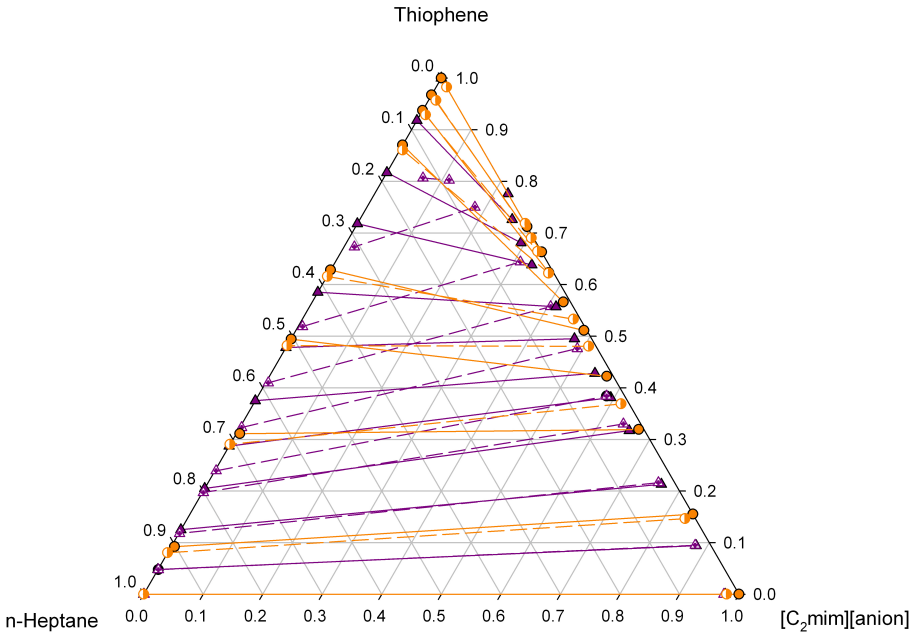

Figure 4.18: Experimental tie-lines for the LLE of the ternary systems {[C_2mim][$EtSO_4$] + TP + *n*-heptane} (●, solid line)[100] and {[C_2mim][NTf_2] + TP + *n*-heptane}[130] (▲, solid line) at 298.15 K, and correspondent COSMO-RS predicted tie-lines (◑, ◬, dash lines).

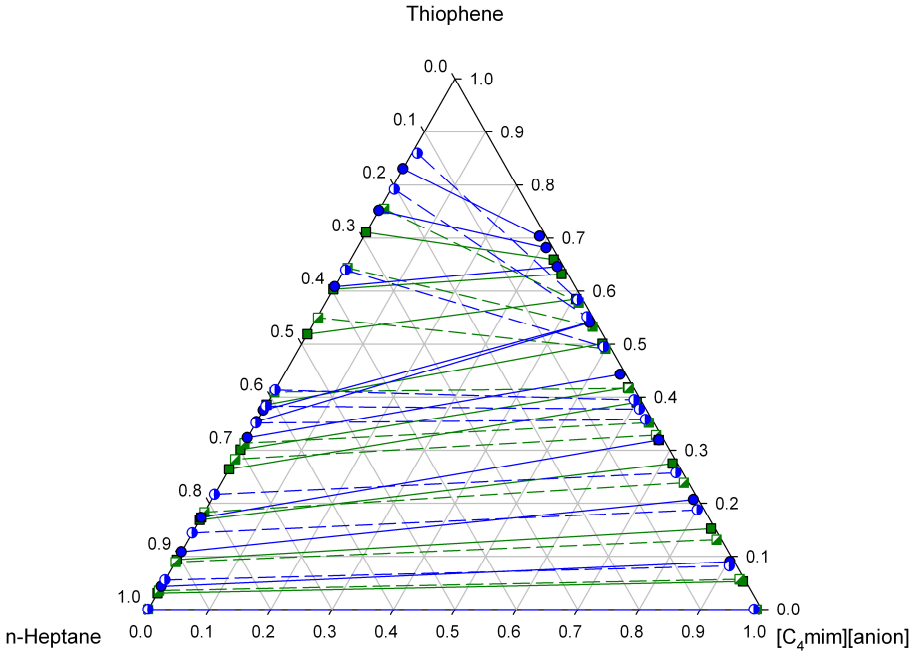

Figure 4.19: Experimental tie-lines for the LLE of the ternary systems {[C_4mim][BF_4] + TP + *n*-heptane} (■, solid line) and {[C_4mim][SCN] + TP + *n*-heptane}(●, solid line) at 298.15 K [128], and correspondent COSMO-RS predicted tie-lines (◪, ◑, dash lines).

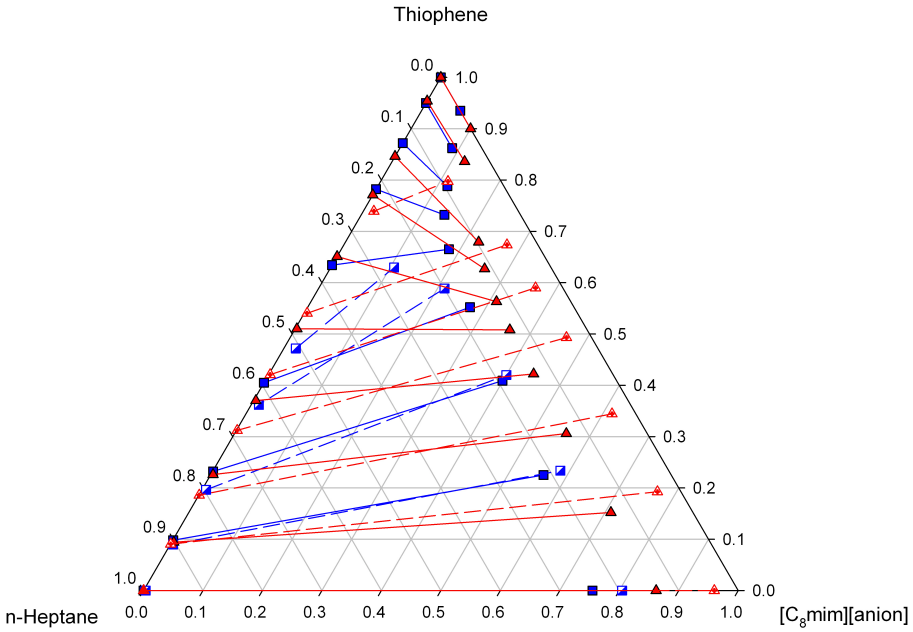

Figure 4.20: Experimental tie-lines for the LLE of the ternary systems {[C_8mim][BF_4] + TP + *n*-heptane}[10] (▲, solid line) and {[C_8mim][NTf_2] + TP + *n*-heptane}[102] (■, solid line) at 298.15 K, and correspondent COSMO-RS predicted tie-lines (◬, ◪, dash lines).

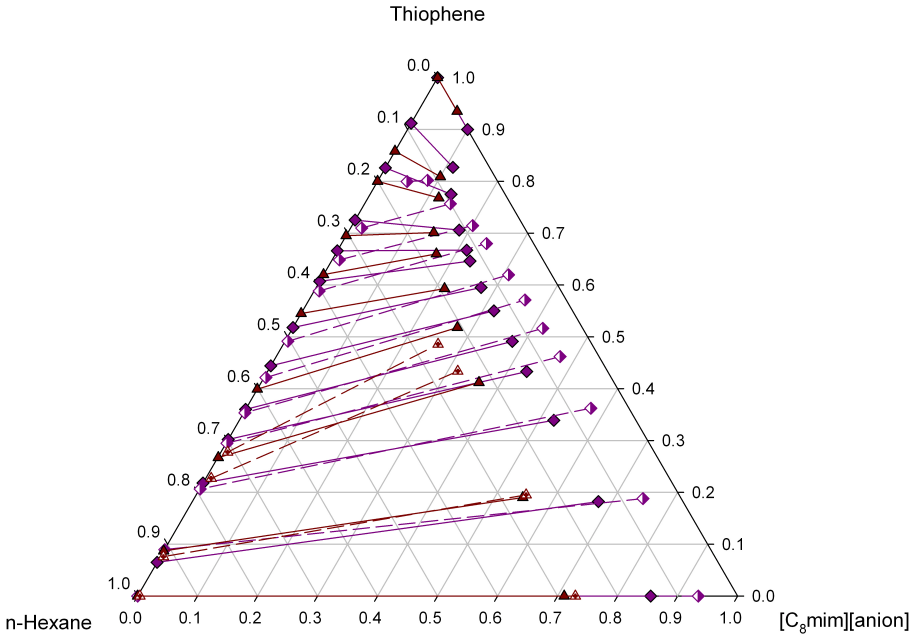

Figure 4.21: Experimental tie-lines for the LLE of the ternary systems {[C_8mim][BF_4] + TP + *n*-hexane}[23] (◆, solid line) and {[C_8mim][NTf_2] + TP + *n*-hexane}[102] (▲, solid line) at 298.15 K, and correspondent COSMO-RS predicted tie-lines (⬗, ◬, dash lines).

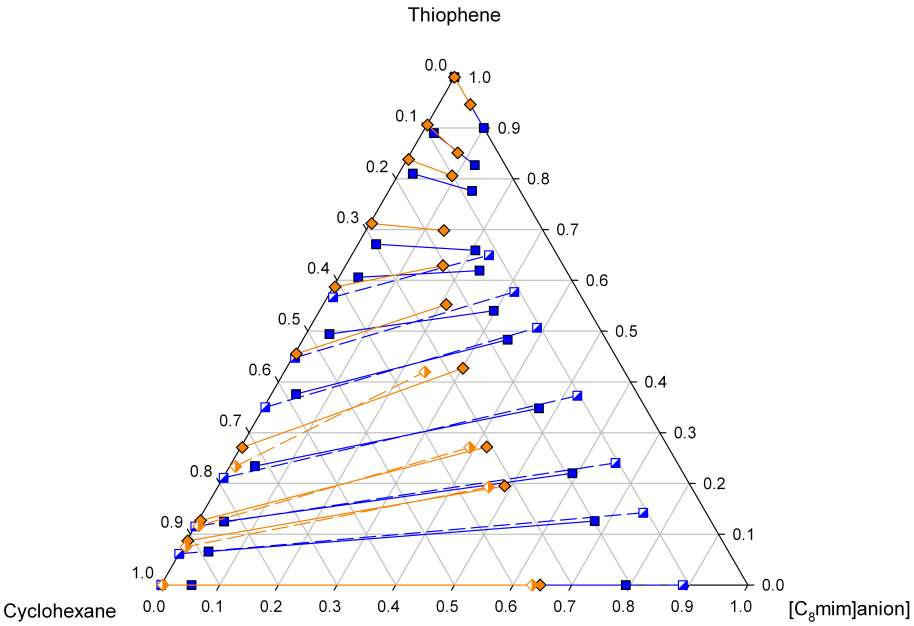

Figure 4.22: Experimental tie-lines for the LLE of the ternary systems {[C_8mim][BF_4] + TP + cyclohexane[23] (■, solid line) and {[C_8mim][NTf_2] + TP + cyclohexane } [36] (◆, solid line) at 298.15 K and correspondent COSMO-RS predicted tie-lines (◪, ◆, dash lines).

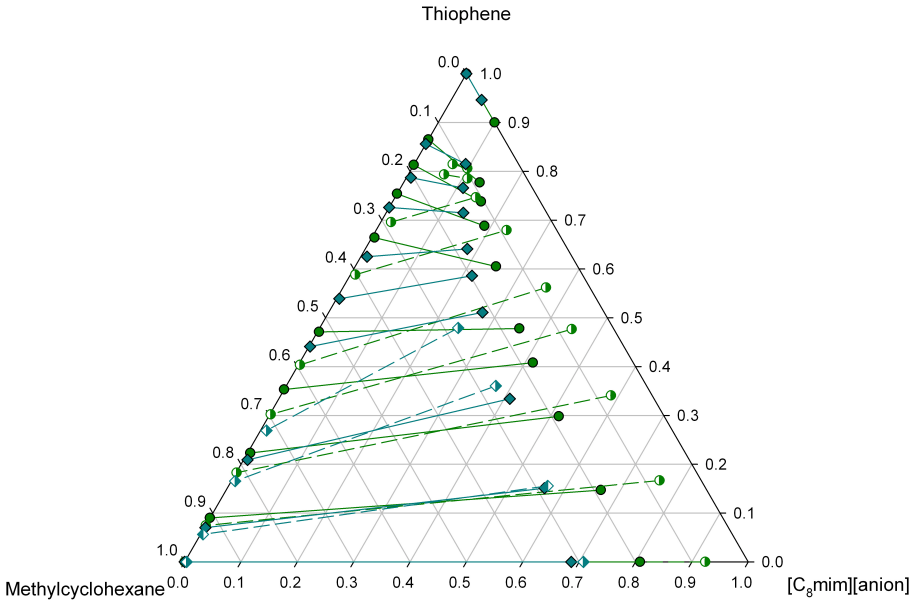

Figure 4.23: Experimental tie-lines for the LLE of the ternary systems {[C_8mim][BF_4] + TP + methylcyclohexane} (●, solid line) and {[C_8mim][NTf_2] + TP + methylcyclohexane}(◆, solid line) at 298.15 K [104], and correspondent COSMO-RS predicted tie-lines (◑, ◆, dash lines).

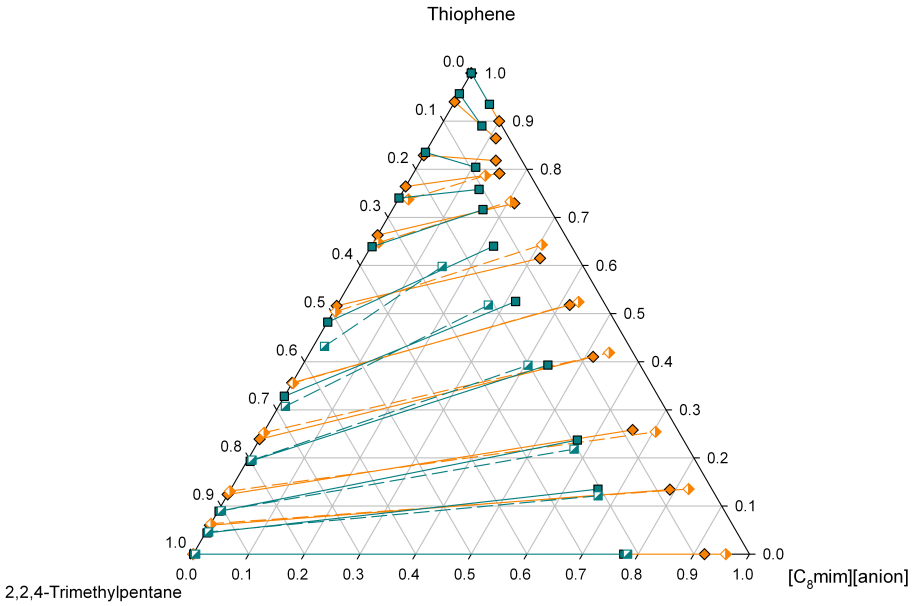

Figure 4.24: Experimental tie-lines for the LLE of the ternary systems {[C_8mim][BF_4] + TP + 2,2,4-Trimethylpentane}[48] (◆, solid line) and {[C_8mim][NTf_2] + TP + 2,2,4-Trimethylpentane }[94] (■, solid line) at 298.15 K, and correspondent COSMO-RS predicted tie-lines (◆, ◪, dash lines).

4.3.5 Effect of the S-compounds

Although TP is usually taken as model S-compound, the fuel is a complex mixture containing other S-species whose structural characteristics will influence the selectivity exhibited by the ILs to organic sulfur.

Figure 4.25 show the influence of different S-compounds that can be found in transportation fuels in the phase diagrams of ternary systems containing [C_2mim][$EtSO_4$] and *n*-dodecane. Regarding the ternary phase diagrams presented above, it can be seen that a good qualitative and quantitative agreement is found between the data predicted with COSMO-RS and the experimental data, in the region of low concentrations of S-species, for all the DBT-derivatives considered. However, incorrect descriptions are obtained when the S-compound is TP (Figure 4.4). It has been suggested that the most likely mechanism for the extraction of S-compounds with imidazolium and pyridinium-based ILs is the formation of liquid clathrates due to the π-π interactions between the aromatic structures of S-compounds and the imidazolium/pyridinium rings [22, 44, 99, 106]. It has also been further proved that molecules with highly polarizable π-electron density preferably insert into the molecular structure of the ILs and that S-compounds with a higher density of aromatic π electrons are favorably absorbed by ILs [22, 44, 47, 99]. Otsuki et al. [72] reported that the electron density on the S atom is 5.760 for 4,6-DMDBT, 5.758 for DBT and 5.696 for TP and therefore stronger interactions are established in the systems containing DBT-derivatives.

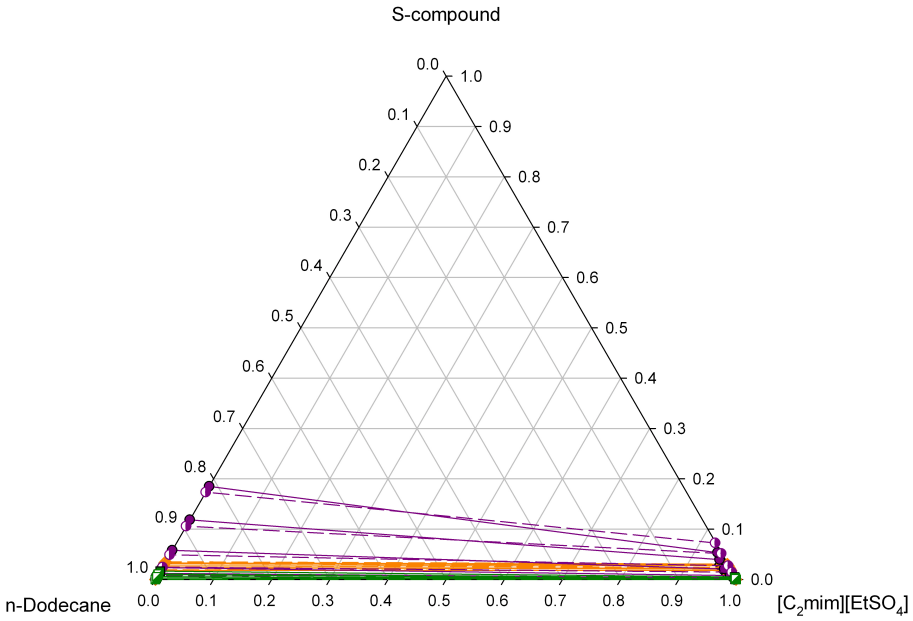

Figure 4.25: Experimental tie-lines for the LLE of the ternary system {[C_2mim][$EtSO_4$] + DBT + *n*-dodecane}[131] (◆, solid line), {[C_2mim][$EtSO_4$] + 4-MDBT + *n*-dodecane}[133] (●, solid line) and {[C_2mim][$EtSO_4$] + 4,6-DMDBT + *n*-dodecane}[132] (■, solid line) at 298.15 K, and correspondent COSMO-RS predicted tie-lines (◆, ◑, ◪, dash lines).

Since, as discussed above, some interactions, namely the π-π interactions between the aromatic ring of S-compounds and the IL, are not adequately taken into account or properly treated by COSMO-RS, better descriptions would be expected for TP (weaker π-π interactions) and for 4,6-DMDBT (the steric hinderance due to methyl substitution weakens the π-π interactions). From the results here obtained this is, however, not observed. Not only it is rather difficult to conclude about the effect of the nature of the DBT-derivatives on the quality of the COSMO-RS predictions, but also incorrect descriptions are obtained for TP. It has been reported that the presence of an additional aromatic ring in DBT hinders the π-π interaction established with the IL cation, and thus, the interaction mainly occurs via CH-π bond and H-bond formation [126]. This fact can justify the better agreement observed between experimental and calculated data of systems involving DBT derivatives, since the model is more reliable in the description of the latest interactions, i.e., H-bond formation, but naturally, other factors must be taken into account. Other simulations of analogous systems concerning another anion, namely ([C_2mim][$DEPO_4$] + DBT + *n*-dodecane), ([C_2mim][$DEPO_4$] + 4-MDBT + *n*-dodecane) and ([C_2mim][$DEPO_4$] + 4,6-DMDBT + *n*-dodecane) have been performed, but the model was not capable to calculate any of the correspondent phase diagrams, clearly due to the type of IL anion considered. Since the $[DEPO_4]^-$ has a hydroxyl group, it is able to establishe H bonds with the DBT-derivatives. Because the interactions involved are so

strong, the model is not able to properly account for them. Rather than conclusions on the S-compound effect, the results presented in this section further confirm conclusions derived in previous sections. The ability of the model to correctly predict the LLE in these type of systems will therefore be dependent on the particular combination of species present, because these determine the strength and type of interactions established.

4.3.6 Effect of other aromatics: toluene

The problem of cross-contamination (presence of IL in the raffinate and extraction of HCs together with the S-compounds) is frequently pointed out for desulfurization since the composition and quality of fuel can be affected by the cross solubility of ILs and fuel components. Thus, it is essential to study not only the IL selectivity for TP and its derivatives but also for the different HCs which compose the fuels. Aromatic HCs, for instance, are an important class of fuel components because they enhance the octane number, but their content is also limited by regulations. Therefore, care must be taken for the extension of the extraction of these compounds by ILs in desulfurization processes.

In order to account for this problem, it was tested the ability of COSMO-RS to predict the LLE of (IL + TP + toluene) mixtures, taking toluene as model compound, representative of the aromatics present in fuels. Figure 4.26 and Figure 4.27 show the experimental LLE data for the ternary systems ([C_2mim][$EtSO_4$] or [C_8mim][BF_4] + TP + toluene) respectively, and the correspondent COSMO-RS calculations.

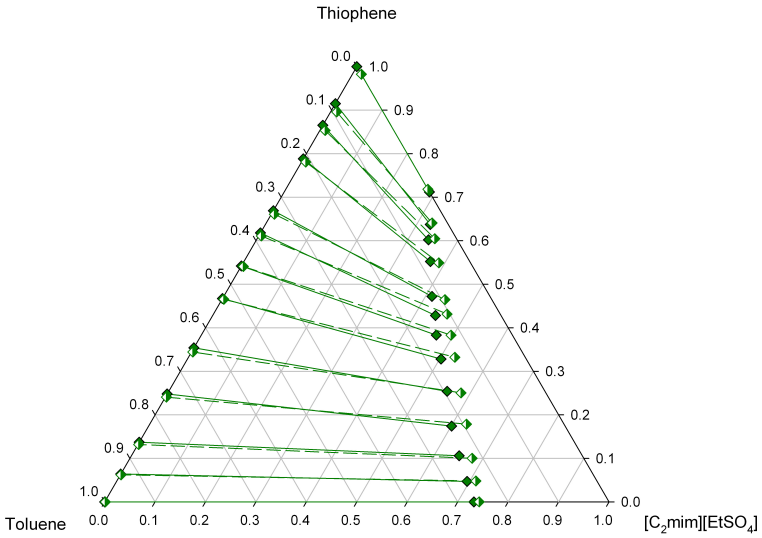

Figure 4.26: Experimental tie-lines for the LLE of the ternary system {[C_2mim][$EtSO_4$] + TP + toluene}[3] (◆, solid line) at 298.15 K, and correspondent COSMO-RS predicted tie-lines (◇, dash lines).

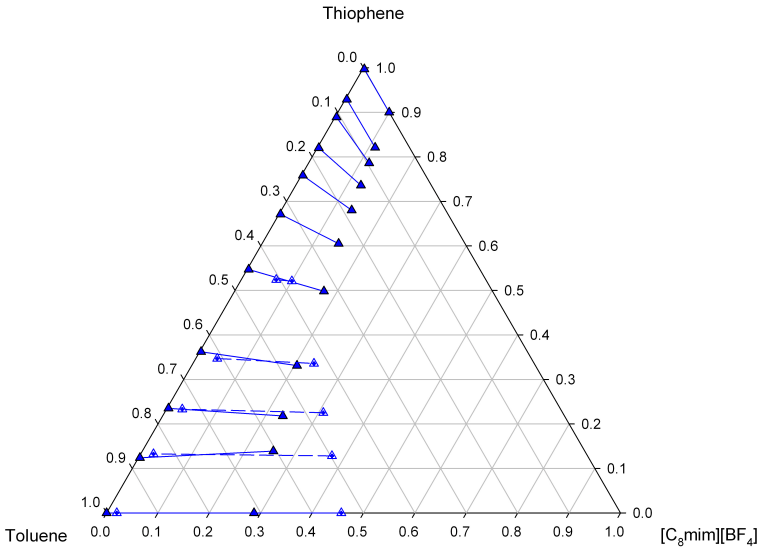

Figure 4.27: Experimental tie-lines for the LLE of the ternary system {[C8mim][BF4] + TP + toluene}[48] (▲, solid line) at 298.15 K, and correspondent COSMO-RS predicted tie-lines (◬, dash lines).

The results illustrated in Figure 4.27 reveal a less accurate COSMO-RS description of the LLE of ([C_8mim][BF_4] + TP + toluene). The model predicts a larger immiscibility gap when compared to experimental data for the lowest part of the diagram and cannot calculate the regions of medium and high TP concentration. Moreover, according to the COSMO-RS results, some IL is present in the toluene-rich phase, while no significant amount is found experimentally. In addition, the experimental data shows a high solubility of toluene in [C_8mim][BF_4] and a poor solubility of the IL in the HC, suggesting that generally aromatic compounds would also be extracted, at least to some extent. COSMO-RS calculations are not, however, in good quantitative agreement with these results.

The results obtained in this section are not enough and sufficiently conclusive to infer about the COSMO-RS ability to describe the LLE involving ILs, S-compounds and aromatics. The simulation of other systems involving toluene, namely ([C_8mim][NTf_2] + TP + toluene) and ([$C_6^{3,5}$dmpy][NTf_2] + TP + toluene), was also performed in this work, but the model was not capable to calculate any of the diagrams, since it assumes a complete miscibility. The main interactions involved are π-π interactions, which are overestimated by the model. Toluene is, like TP, an aromatic compound which establishes π-π interactions with the S-compound and the IL cation, for which COSMO-RS is not always able to properly account. The performance of the model will be dependent on the number and strength of those interactions, which, for its turn, are dependent on the type of species involved. For systems comprising long chain IL cations, anions such as $[BF_4]^-$ and $[NTf_2]^-$, TP and aromatics, the predictions are thus likely to be less accurate or even not

possible. Further studies on these type of systems are nevertheless needed before conclusions can be taken.

4.3.7 Effect of the temperature

Since the extraction temperature is also a factor that influences the extraction ability of the ILs [131-133], this effect was as well evaluated. Figure 4.28-Figure 4.33 present the experimental data and COSMO-RS calculations for ([C_2mim][$EtSO_4$] + S-compound + *n*-dodecane) ternary systems, at 298.15 K and 313.15 K.

The results obtained for the phase diagrams suggest that the temperature does not have, *a priori*, a significant influence on the quality of the predictions of the model, since similar results are obtained for both temperatures studied. As a result, COSMO-RS is able to describe the phase behavior and their dependence on the temperature.

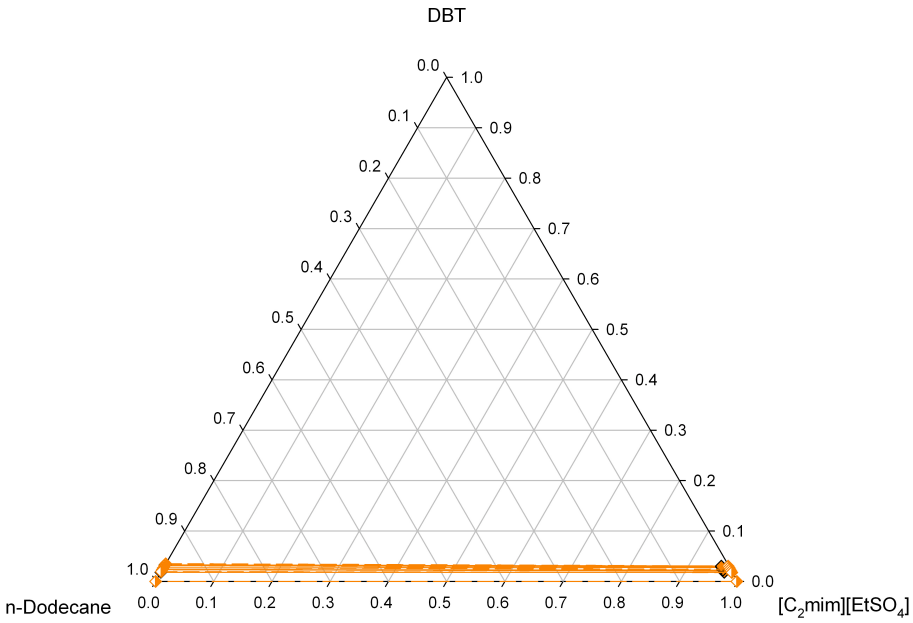

Figure 4.28: Experimental tie-lines for the LLE of the ternary system {[C_2mim][$EtSO_4$] + DBT + *n*-dodecane}[131] (◆, solid line) at 298.15 K, and correspondent COSMO-RS predicted tie-lines (◆, dash lines).

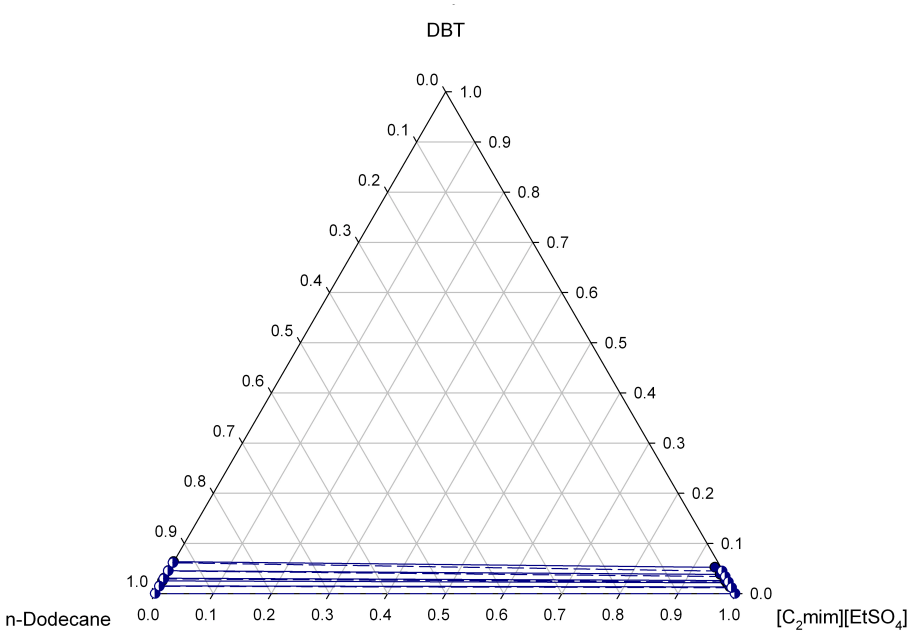

Figure 4.29: Experimental tie-lines for the LLE of the ternary system {[C_2mim][$EtSO_4$] + DBT + *n*-dodecane}[131] (●, solid line) at 313.15 K, and correspondent COSMO-RS predicted tie-lines (◑, dash lines).

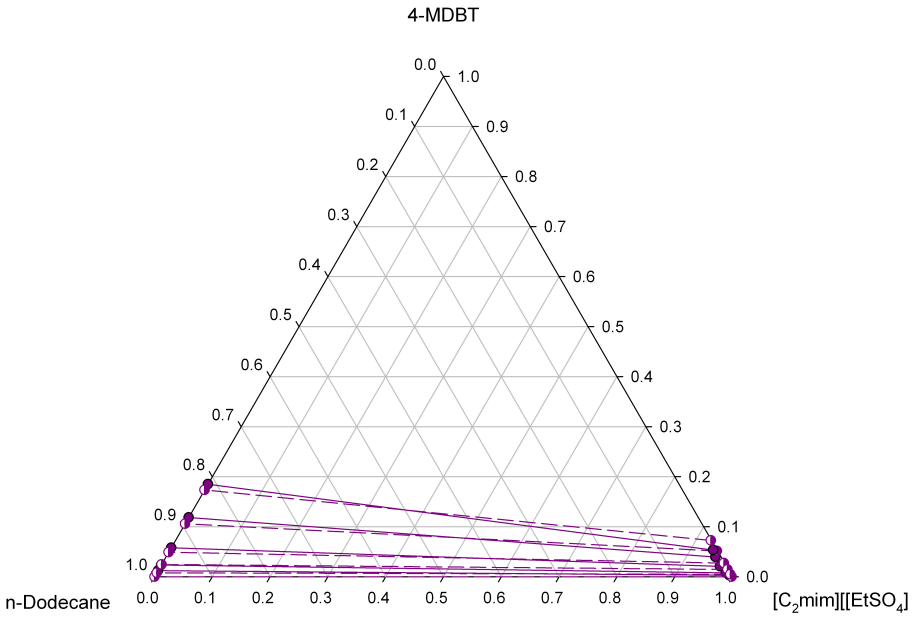

Figure 4.30: Experimental tie-lines for the LLE of the ternary system {[C_2mim][$EtSO_4$] + 4-MDBT + *n*-dodecane}[133] (●, solid line) at 298.15 K, and correspondent COSMO-RS predicted tie-lines (◑, dash lines).

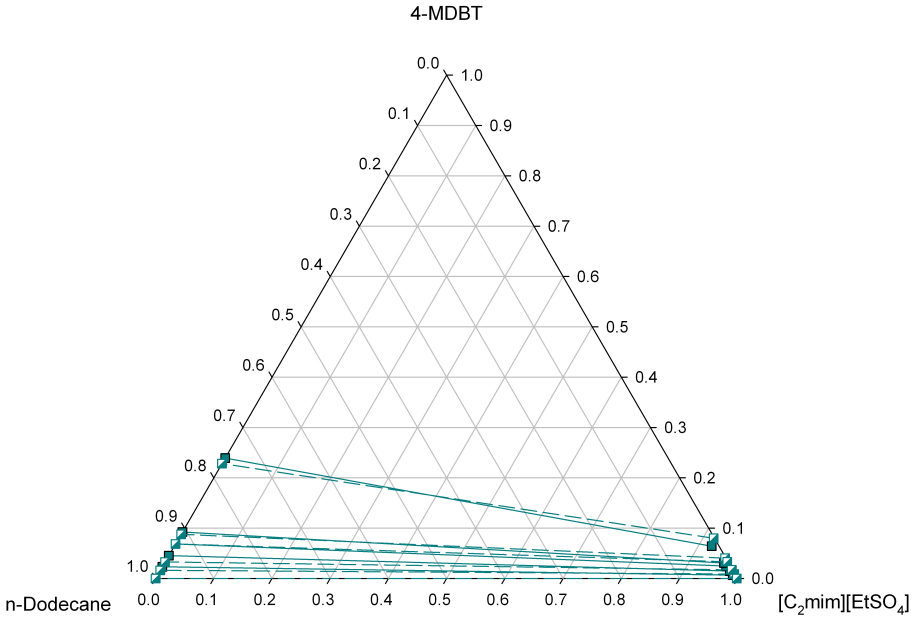

Figure 4.31: Experimental tie-lines for the LLE of the ternary system {[C_2mim][$EtSO_4$] + 4-MDBT + *n*-dodecane} [133] (■, solid line) at 313.15 K, and correspondent COSMO-RS predicted tie-lines (◪, dash lines).

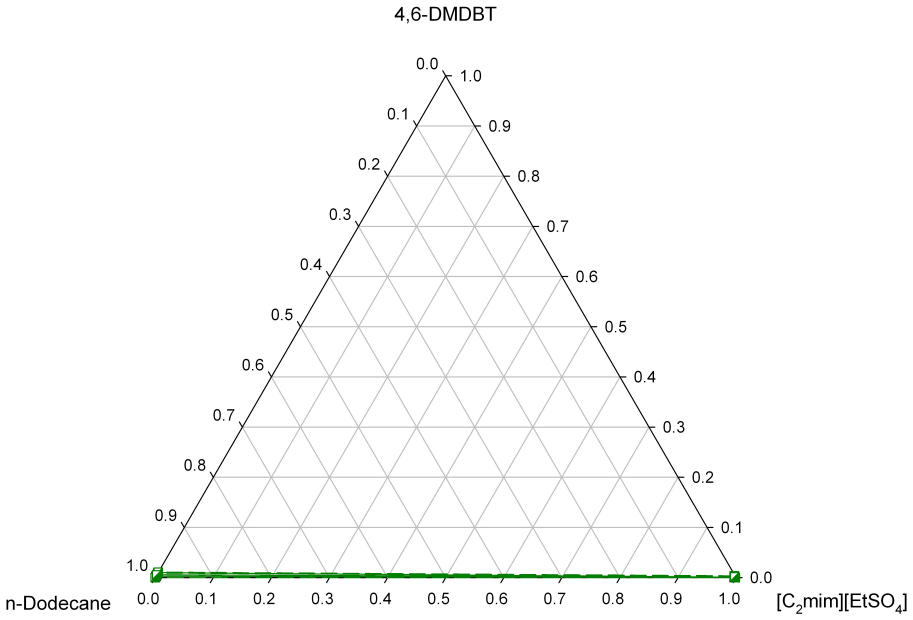

Figure 4.32: Experimental tie-lines for the LLE of the ternary system {[C_2mim][$EtSO_4$] + 4,6-DMDBT + *n*-dodecane}[132] (■, solid line) at 298.15 K, and correspondent COSMO-RS predicted tie-lines (◪, dash lines).

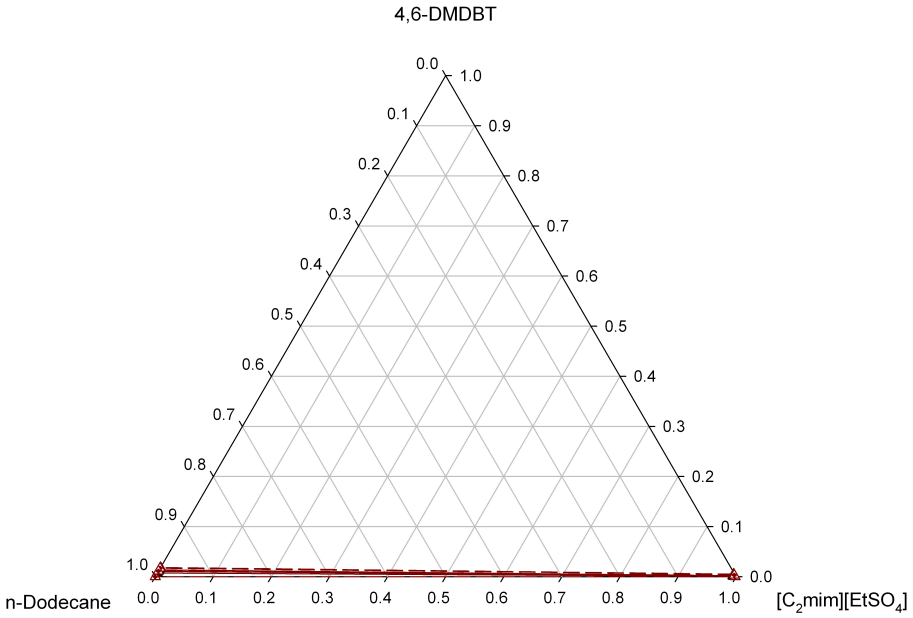

Figure 4.33: Experimental tie-lines for the LLE of the ternary system {[C_2mim][$EtSO_4$] + 4,6-DMDBT + *n*-dodecane}[132] (▲, solid line) at 313.15 K and correspondent COSMO-RS predicted tie-lines (⚠, dash lines).

4.4 Results and discussion of the LLE in ternary systems containing pyridine

Since desulfurization processes involve more reactions than just the removal of S-compounds, it is important to analyze the ability of the ILs to extract other compounds besides S-derivatives. Therefore, it is essential to evaluate the performance of the ILs not only in the desulfurization and dearomatization, but also in the denitrogenation because the effectiveness of these three processes has to be balanced when selecting the best solvent. For this reason, it was additionally tested the ability of COSMO-RS to predict the LLE of ternary systems containing an alkane, the model N-compound pyridine (Py) and different ILs- [C_8mim][NTf_2], [C_8mim][BF_4], [C_2mim][$EtSO_4$] and [$C_6^{3,5}$dmpy][NTf_2] - which have shown to be suitable as extraction solvents for the desulfurization and denitrogenation of fuel oils. The LLE results obtained from the COSMO-RS calculations performed in this work, together with the literature experimental data are represented in triangular diagrams shown in Figure 4.34 to Figure 4.36.

In order to evaluate the influence of the structural characteristics of the cation/anion of the IL on the mutual solubilities groups of systems in which pyridine and the alkane are fixed and the cation/anion nature of the IL is varied have been considered. As it can be seen in Figure 4.34 and Figure 4.35, unlike TP ternary mixtures, all the ternary systems

concerning Py correspond to Type 1 category, with only one pair exhibiting partial miscibility. Moreover, the slope of the tie-lines is positive in all the concentration regions considered. The model is able to describe qualitatively this behavior, in spite of being unable to calculate the superior tie-lines. The other main characteristics of the COSMO-RS predictions pointed out before for the (IL + TP + *n*-alkane) systems are also observed when the N-derivative is the target compound.

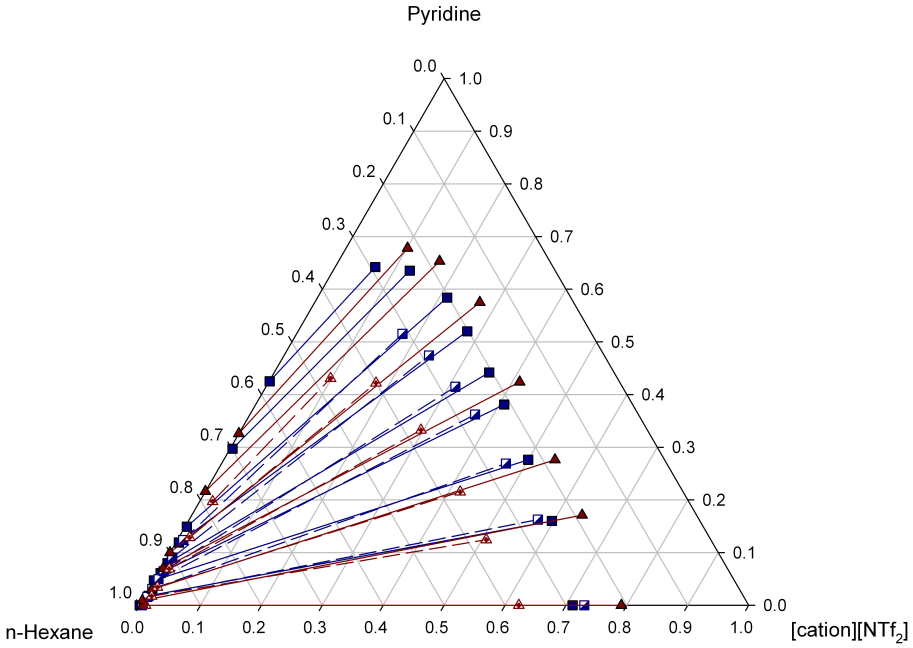

Figure 4.34: Experimental tie-lines for the LLE of the ternary systems {[$C_6^{3,5}$dmpy][NTf_2] + pyridine + *n*-hexane}[96] (▲, solid line) and {[C_8mim][NTf_2] + pyridine + *n*-hexane}[129] (■, solid line) at 298.15 K, and correspondent COSMO-RS predicted tie-lines (◬, ◪, dash lines).

Actually, as far as the IL cation effect is concerned, the data presented in Figure 4.34 show as well a good quantitative and qualitative agreement with the experimental tie-lines for both cations, but much better quantitative descriptions of the binodals for the imidazolium ion than for the pyridinium, and an incorrect prediction of the effect of the cation on the extension of the immiscibility region.

From the comparison between the experimental and calculated LLE of systems concerning an imidazolium-based cation in combination with two different anions, $[BF_4]^-$ and $[NTf_2]^-$ (Figure 4.35), it can be seen that a good qualitative description of the tie lines and a reasonable quantitative prediction of the extension of the heterogeneity zone is found for both systems, in the interest zone. Moreover, COSMO-RS is able to predict the increase in the immiscibility area observed experimentally when the anion of the IL is changed from $[NTf_2]^-$ to $[BF_4]^-$, although a slightly better quantitative agreement is obtained in the case of the former anion.

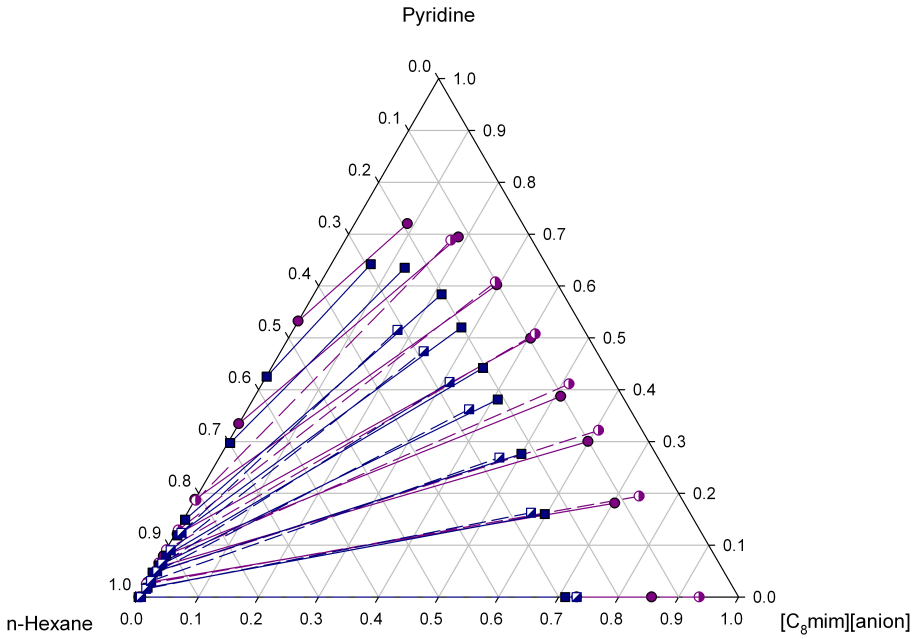

Figure 4.35: Experimental tie-lines for the LLE of the ternary systems {[C_8mim][BF_4] + pyridine + *n*-hexane} (●, solid line) and {[C_8mim][NTf_2] + pyridine + *n*-hexane}(■, solid line) at 298.15 K[129], and correspondent COSMO-RS predicted tie-lines (◑, ◪, dash lines).

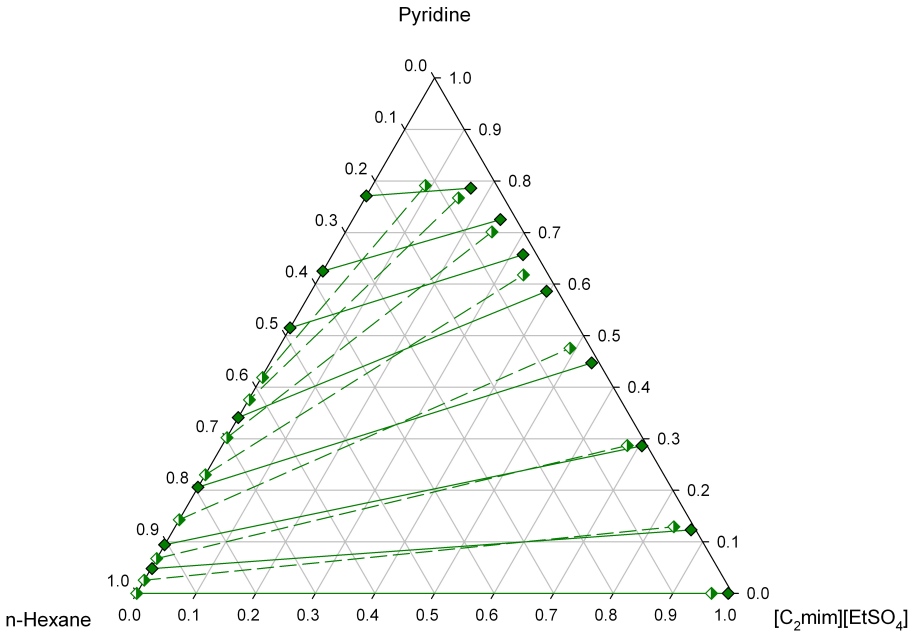

Figure 4.36: Experimental tie-lines for the LLE of the ternary systems {[C_2mim][$EtSO_4$] + pyridine + *n*-hexane}[129] (◆, solid line) at 298.15 K, and correspondent COSMO-RS predicted tie-lines (⬗, dash lines).

The quality of the COSMO-RS predictions is similar for both systems, with a good description of the sloping behaviour and a reasonable quantitative agreement of the binodals (only) for the lowest part of the diagrams.

The similarity observed in the quality and main features of the COSMO-RS descriptions of the phase diagrams of the ternary systems involving Py and of those containing TP suggests that the same type of effects, or, in other words, the same factors are on the basis of the accuracy level that is possible to achieve in the LLE data calculated by the model. Indeed, being Py and TP aromatic compounds with a somehow similar structure, it is expected that the main interactions governing the solubility behaviour of (IL + Py + *n*-alkane) systems are as well π-π interactions established between the aromatic rings of the cation and of the N-derivative. Moreover, the extraction capability of the ILs under study has shown to be identical for TP and Py, which also supports a common molecular mechanism [96, 100, 129]. For these reasons, the discussion performed in previous sections for the LLE of TP systems is also valid for the Py mixtures and the results obtained for the latest constitute additional evidence for the fact that the intensity of the π-π interactions established in these systems is determinant for the accuracy of COSMO-RS predictions.

4.5 Conclusions

Good COSMO-RS descriptions of the LLE of the ternary systems are obtained for low concentrations of TP, but the model fails on the prediction of the phase diagrams for medium and high concentrations of solute.

Better agreement with the experimental LLE data is found for systems containing alkanes with small alkyl chains, short chain IL cations and the $[NTf_2]^-$ anion. Good descriptions are also obtained for other IL anions such as $[EtSO_4]^-$ and $[BF_4]^-$ and worst results for $[SCN]^-$.

The results obtained for the IL cation family, nature of S-compounds and temperature influences on the accuracy of the COSMO-RS predictions are not conclusive, and the main features of the predictive data have shown to be identical for TP and Py.

The quality of the simulations of the LLE is dependent on the type of interactions that are established between the compounds. COSMO-RS cannot simulate or correctly predict the LLE of ternary systems whose behaviour is determined by strong π-π interactions because the model cannot properly take them into account.

The ability of the model to simulate the LLE is dependent on the particular combination of species present in the systems since these will be determinant for the type and strength of the interactions established. To derive well supported conclusions, however, further investigation is needed.

5. Final Remarks

5.1 General Conclusions

In this work, LLE data have been provided for (imidazolium-based ILs + TP) binary systems and the ability of COSMO-RS to describe and predict the phase behaviour of binary and ternary systems involved in desulfurization processes has been tested.

It was experimentally observed that the phase behaviour of the binary systems studied depends on different factors, such the nature of the cation and of the anion of the ILs. In general, a poor qualitative and/or quantitative agreement was found between the data predicted with COSMO-RS and the experimental data of binary systems available in literature. The model completely fails on the prediction of the IL anion effect, providing a poor description of the LLE of systems involving $[SCN]^-$ imidazolium-based ILs. However, the model can qualitatively predict the phase behaviour of ($[NTf_2]^-$ imidazolium-based ILs + TP) mixtures, but not quantitatively. Nevertheless, since experimental studies on the anion effect are still scarce, further investigation on this subject is needed.

Regarding ternary systems, COSMO-RS proved to be a useful tool in the prediction of the LLE data in the region of low concentrations of TP, since, in general, a good qualitative and/or quantitative agreement was found between the data predicted with this model and the experimental data available in literature. Globally, poor descriptions of the model are obtained for the top of the diagrams. Because, for practical applications, the region of low TP concentrations is the interest zone, this evidence is promissory.

COSMO-RS has shown potential to be used as *an a priori* method to predict the LLE data of ternary systems containing alkanes with small alkyl chains, short chain IL cations and the $[NTf_2]^-$ anion.

According to the results, the most attractive ILs for a selective extraction of S-compounds are the ones which comprise cations with small alkyl chains combined with the anions such $[EtSO_4]^-$, $[SCN]^-$, $[BF_4]^-$ and $[NTf_2]^-$, since these exhibit higher immiscibility with HCs.

Although COSMO-RS has shown potentialities, due to the scariness of data and to several inconclusive results obtained, the model should be still used with precaution as a previous and alternative method to predict the phase behaviour and to identify the ILs with better selectivities for S- and N-compounds, before further studies are performed.

5.2 Future work

In the future, it would be interesting to measure the S-partition coefficients between the ILs and oils in order to evaluate the desulfurization performance of the former, as well as the solubility of ILs in alkanes.

To better evaluate the effect of the IL anion family on the LLE of (IL+TP) binary mixtures, it would be important to extend the study to more systems beyond those considered here, by performing experimental measurements of the LLE of systems concerning other type of anions, and its modeling with the COSMO-RS.

It would also be of utmost importance to perform further experimental measurements of the LLE of more ternary systems to compare with the COSMO-RS predictions.

6. Bibliographic References

1. Nie, Y., Li, C.X., and Wang, Z.H., *Extractive desulfurization of fuel oil using alkylimidazole and its mixture with dialkylphosphate ionic liquids.* Industrial & Engineering Chemistry Research, 2007. **46**(15): p. 5108-5112.
2. Lo, W.H., Yang, H.Y., and Wei, G.T., *One-pot desulfurization of light oils by chemical oxidation and solvent extraction with room temperature ionic liquids.* Green Chemistry, 2003. **5**(5): p. 639-642.
3. Alonso, L., Arce, A., Francisco, M., and Soto, A., *Liquid-liquid Equilibria of ([C2mim][EtSO4] + Thiophene + 2,2,4-Trimethylpentane) and ([C2mim][EtSO4] + Thiophene + Toluene): Experimental Data and Correlation.* Journal of Solution Chemistry, 2008. **37**(10): p. 1355-1363.
4. Ma, X.L., Zhou, A.N., and Song, C.S., *A novel method for oxidative desulfurization of liquid hydrocarbon fuels based on catalytic oxidation using molecular oxygen coupled with selective adsorption.* Catalysis Today, 2007. **123**(1-4): p. 276-284.
5. Campos-Martin, J.M., Capel-Sanchez, M.C., and Fierro, J.L.G., *Highly efficient deep desulfurization of fuels by chemical oxidation.* Green Chemistry, 2004. **6**(11): p. 557-562.
6. Ma, X.L., Sun, L., and Song, C.S., *A new approach to deep desulfurization of gasoline, diesel fuel and jet fuel by selective adsorption for ultra-clean fuels and for fuel cell applications.* Catalysis Today, 2002. **77**(1-2): p. 107-116.
7. Deng, Z., Wang, T., and Wang, Z., *Hydrodesulfurization of diesel in a slurry reactor*. Chemical Engineering Science, 2010. **65**(1): p. 480-486.
8. *http://www.epa.gov/otaq/regs/fuels/diesel/diesel.htm*. , acessed March 2010.
9. *http://www.dieselnet.com/standards/eu/fuel.php*. , acessed March 2010.
10. Alonso, L., Arce, A., Francisco, M., and Soto, A., *Solvent extraction of thiophene from n-alkanes (C7, C12, and C16) using the ionic liquid [C8mim][BF4]*. The Journal of Chemical Thermodynamics, 2008. **40**(6): p. 966-972.
11. He, L.N., Li, H.M., Zhu, W.S., Guo, J.X., Jiang, X., Lu, J.D., and Yan, Y.S., *Deep oxidative desulfurization of fuels using peroxophosphomolybdate catalysts in ionic liquids.* Industrial & Engineering Chemistry Research, 2008. **47**(18): p. 6890-6895.
12. Esser, J., Wasserscheid, P., and Jess, A., *Deep desulfurization of oil refinery streams by extraction with ionic liquids.* Green Chemistry, 2004. **6**(7): p. 316-322.
13. *http://apps.isiknowledge.com*. , acessed May 2010.
14. Olivier-Bourbigou, H., Magna, L., and Morvan, D., *Ionic liquids and catalysis: Recent progress from knowledge to applications.* Applied Catalysis A: General, 2010. **373**(1-2): p. 1-56.
15. Olivier-Bourbigou, H. and Magna, L., *Ionic liquids: perspectives for organic and catalytic reactions.* Journal of Molecular Catalysis A: Chemical, 2002. **182-183**: p. 419-437.
16. Sheldon, R., *Catalytic reactions in ionic liquids.* Chemical Communications, 2001(23): p. 2399-2407.
17. Przybysz, K., Drzewinska, E., Stanislawska, A., Wysocka-Robak, A., Cieniecka-Roslonkiewicz, A., Foksowicz-Flaczyk, J., and Pernak, J., *Ionic Liquids and Paper.* Industrial & Engineering Chemistry Research, 2005. **44**(13): p. 4599-4604.
18. Huo, Y., Xia, S.Q., Yi, S.Z., and Ma, P.S., *Measurement and correlation of vapor pressure of benzene and thiophene with BMIM PF6 and BMIM BF4 ionic liquids.* Fluid Phase Equilibria, 2009. **276**(1): p. 46-52.

19. Tomé, L.I.N., Catambas, V.R., Teles, A.R.R., Freire, M.G., Marrucho, I.M., and Coutinho, J.A.P., *Tryptophan extraction using hydrophobic ionic liquids.* Separation and Purification Technology, 2010. **72**(2): p. 167-173.
20. Wasserscheid, P. and Keim, W., *Ionic Liquids - New Solutions for Transition Metal Catalysis.* Angewandte Chemie, 2000. **39**(21): p. 3772-3789.
21. Welton, T., *Room-Temperature Ionic Liquids. Solvents for Synthesis and Catalysis.* Chemical Reviews, 1999. **99**(8): p. 2071-2084.
22. Zhang, S.G. and Zhang, Z.C., *Novel properties of ionic liquids in selective sulfur removal from fuels at room temperature.* Green Chemistry, 2002. **4**(4): p. 376-379.
23. Alonso, L., Arce, A., Francisco, M., Rodríguez, O., and Soto, A., *Liquid−Liquid Equilibria for Systems Composed by 1-Methyl-3-octylimidazolium Tetrafluoroborate Ionic Liquid, Thiophene, and n-Hexane or Cyclohexane.* Journal of Chemical & Engineering Data, 2007. **52**(5): p. 1729-1732.
24. Macaev, F., Stingaci, E., and Munteanu, V., *Design of New "Ionic Liquids" for Liquid/Liquid Extraction of Persistent Toxic Substances*, in *Soil Chemical Pollution, Risk Assessment, Remediation and Security*, L. Simeonov and V. Sargsyan, Editors. 2008, Springer Netherlands. p. 223-228.
25. Camper, D., Scovazzo, P., Koval, C., and Noble, R., *Gas Solubilities in Room-Temperature Ionic Liquids.* Industrial & Engineering Chemistry Research, 2004. **43**(12): p. 3049-3054.
26. Li, Z., Jia, Z., Luan, Y., and Mu, T., *Ionic liquids for synthesis of inorganic nanomaterials.* Current Opinion in Solid State and Materials Science, 2008. **12**(1): p. 1-8.
27. Liu, H., Liu, Y., and Li, J., *Ionic liquids in surface electrochemistry.* Physical Chemistry Chemical Physics, 2010. **12**(8): p. 1685-1697.
28. Carlin, R.T. and Wilkes, J.S., *Complexation of Cp2MCl2 in a chloroaluminate molten salt: relevance to homogeneous Ziegler-Natta catalysis.* Journal of Molecular Catalysis, 1990. **63**(2): p. 125-129.
29. Stepnowski, P., Müller, A., Behrend, P., Ranke, J., Hoffmann, J., and Jastorff, B., *Reversed-phase liquid chromatographic method for the determination of selected room-temperature ionic liquid cations.* Journal of Chromatography A, 2003. **993**(1-2): p. 173-178.
30. Branco, L.C., Crespo, J.G., and Afonso, C.A.M., *Studies on the Selective Transport of Organic Compounds by Using Ionic Liquids as Novel Supported Liquid Membranes.* Chemistry – A European Journal, 2002. **8**(17): p. 3865-3871.
31. Wasserscheid, P., Hal, R.v., and Bösmann, A., *1-n-Butyl-3-methylimidazolium ([bmim]) octylsulfate—an even'greener' ionic liquid.* Green Chemistry, 2002. **4**(4): p. 400-404.
32. Ventura, S.P.M., Gonçalves, A.M.M., Gonçalves, F., and Coutinho, J.A.P., *Assessing the toxicity on [C3mim][Tf2N] to aquatic organisms of different trophic levels.* Aquatic Toxicology, 2010. **96**(4): p. 290-297.
33. Couling, D.J., Bernot, R.J., Docherty, K.M., Dixon, J.K., and Maginn, E.J., *Assessing the factors responsible for ionic liquid toxicity to aquatic organisms via quantitative structure-property relationship modeling.* Green Chemistry, 2006. **8**(1): p. 82-90.
34. Jastorff, B., Molter, K., Behrend, P., Bottin-Weber, U., Filser, J., Heimers, A., Ondruschka, B., Ranke, J., Schaefer, M., Schroder, H., Stark, A., Stepnowski, P., Stock, F., Stormann, R., Stolte, S., Welz-Biermann, U., Ziegert, S., and Thoming,

J., *Progress in evaluation of risk potential of ionic liquids-basis for an eco-design of sustainable products.* Green Chemistry, 2005. **7**(5): p. 362-372.
35. Domanska, U., Królikowski, M., and Slesinska, K., *Phase equilibria study of the binary systems (ionic liquid + thiophene): Desulphurization process.* The Journal of Chemical Thermodynamics, 2009. **41**(11): p. 1303-1311.
36. Alonso, L., Arce, A., Francisco, M., and Soto, A., *(Liquid + liquid) equilibria of [C8mim][NTf2] ionic liquid with a sulfur-component and hydrocarbons.* The Journal of Chemical Thermodynamics, 2008. **40**(2): p. 265-270.
37. Walden, P., *Bulletin de l'Académie Impériale des Sciences de St.-Pétersbourg.* 1914. **8**: p. 405-422.
38. Gujar, A.C. and White, M.G., *Ionic liquids as catalysts, solvents and conversion agents.* The Royal Society of Chemistry, 2009. **21**: p. 154-190.
39. Carmichael, A.J. and Seddon, K.R., *Polarity study of some 1-alkyl-3-methylimidazolium ambient-temperature ionic liquids with the solvatochromic dye, Nile Red.* Journal of Physical Organic Chemistry, 2000. **13**(10): p. 591-595.
40. Wishart, J.F., *Energy applications of ionic liquids.* Energy & Environmental Science, 2009. **2**(9): p. 956-961.
41. Kumar, V. and Malhotra Sanjay, V., *Ionic Liquids as Pharmaceutical Salts: A Historical Perspective*, in *Ionic Liquid Applications: Pharmaceuticals, Therapeutics, and Biotechnology*. 2010, American Chemical Society. p. 1-12.
42. Bosmann, A., Datsevich, L., Jess, A., Lauter, A., Schmitz, C., and Wasserscheid, P., *Deep desulfurization of diesel fuel by extraction with ionic liquids.* Chemical Communications, 2001(23): p. 2494-2495.
43. Huang, C., Chen, B., Zhang, J., Liu, Z., and Li, Y., *Desulfurization of Gasoline by Extraction with New Ionic Liquids.* Energy & Fuels, 2004. **18**(6): p. 1862-1864.
44. Zhang, S.G., Zhang, Q.L., and Zhang, Z.C., *Extractive desulfurization and denitrogenation of fuels using ionic liquids.* Industrial & Engineering Chemistry Research, 2004. **43**(2): p. 614-622.
45. Jiang, X., Nie, Y., Li, C., and Wang, Z., *Imidazolium-based alkylphosphate ionic liquids - A potential solvent for extractive desulfurization of fuel.* Fuel, 2008. **87**(1): p. 79-84.
46. Nie, Y., Li, C., Sun, A., Meng, H., and Wang, Z., *Extractive Desulfurization of Gasoline Using Imidazolium-Based Phosphoric Ionic Liquids.* Energy & Fuels, 2006. **20**(5): p. 2083-2087.
47. Gao, H.S., Li, Y.G., Wu, Y., Luo, M.F., Li, Q., Xing, J.M., and Liu, H., *Extractive Desulfurization of Fuel Using 3-Methylpyridinium-Based Ionic Liquids.* Energy & Fuels, 2009. **23**(5): p. 2690-2694.
48. Alonso, L., Arce, A., Francisco, M., Rodríguez, O., and Soto, A., *Gasoline desulfurization using extraction with [C8min][BF4] ionic liquid.* AIChE Journal, 2007. **53**(12): p. 3108-3115.
49. Jian-long, W., Zhao, D.-s., Zhou, E.-p., and Dong, Z., *Desulfurization of gasoline by extraction with N-alkyl-pyridinium-based ionic liquids.* Journal of Fuel Chemistry and Technology, 2007. **35**(3): p. 293-296.
50. Ko, N.H., Lee, J.S., Huh, E.S., Lee, H., Jung, K.D., Kim, H.S., and Cheong, M., *Extractive Desulfurization Using Fe-Containing Ionic Liquids.* Energy & Fuels, 2008. **22**(3): p. 1687-1690.

51. Gao, H., Luo, M., Xing, J., Wu, Y., Li, Y., Li, W., Liu, Q., and Liu, H., *Desulfurization of Fuel by Extraction with Pyridinium-Based Ionic Liquids.* Industrial & Engineering Chemistry Research, 2008. **47**(21): p. 8384-8388.
52. Nie, Y., Li, C., Meng, H., and Wang, Z., *N,N-dialkylimidazolium dialkylphosphate ionic liquids: Their extractive performance for thiophene series compounds from fuel oils versus the length of alkyl group.* Fuel Processing Technology, 2008. **89**(10): p. 978-983.
53. Planeta, J., Karasek, P., and Roth, M., *Distribution of sulfur-containing aromatics between hmim Tf2N and supercritical CO2: a case study for deep desulfurization of oil refinery streams by extraction with ionic liquids.* Green Chemistry, 2006. **8**(1): p. 70-77.
54. Sevignon, M., Macaud, M., Favre-Reguillon, A., Schulz, J., Rocault, M., Faure, R., Vrinat, M., and Lemaire, M., *Ultra-deep desulfurization of transportation fuels via charge-transfer complexes under ambient conditions.* Green Chemistry, 2005. **7**(6): p. 413-420.
55. Zhu, W.S., Li, H.M., Hang, X., Yan, Y.S., Lu, H.D., and Xia, J.X., *Oxidative desulfurization of fuels catalyzed by peroxotungsten and peroxomolybdenum complexes in ionic liquids.* Energy & Fuels, 2007. **21**: p. 2514-2516.
56. Wang, J., Zhao, D., and Li, K., *Oxidative Desulfurization of Dibenzothiophene Using Ozone and Hydrogen Peroxide in Ionic Liquid.* Energy & Fuels, 2010. **24**(4): p. 2527-2529.
57. Zhang, J.T., Zhu, W.S., Li, H.M., Jiang, W., Jiang, Y.Q., Huang, W.L., and Yan, Y.S., *Deep oxidative desulfurization of fuels by Fenton-like reagent in ionic liquids.* Green Chemistry, 2009. **11**(11): p. 1801-1807.
58. Babich, I.V. and Moulijn, J.A., *Science and technology of novel processes for deep desulfurization of oil refinery streams: A review.* Fuel, 2003. **82**(6): p. 607-631.
59. Kabe, T., Ishihara, A., and Tajima, H., *Hydrodesulfurization of sulfur-containing polyaromatic compounds in light oil.* Industrial & Engineering Chemistry Research, 1992. **31**(6): p. 1577-1580.
60. Isoda, T., Nagao, S., Ma, X., Korai, Y., and Mochida, I., *Hydrodesulfurization of Refractory Sulfur Species. 2. Selective Hydrodesulfurization of 4,6-Dimethyldibenzothiophene in the Dominant Presence of Naphthalene over Ternary Sulfides Catalyst.* Energy & Fuels, 1996. **10**(2): p. 487-492.
61. Song, C., *An overview of new approaches to deep desulfurization for ultra-clean gasoline, diesel fuel and jet fuel.* Catalysis Today, 2003. **86**(1-4): p. 211-263.
62. Mochida, I., Sakanishi, K., Ma, X., Nagao, S., and Isoda, T., *Deep hydrodesulfurization of diesel fuel: Design of reaction process and catalysts.* Catalysis Today, 1996. **29**(1-4): p. 185-189.
63. Seeberger, A. and Jess, A., *Desulfurization of diesel oil by selective oxidation and extraction of sulfur compounds by ionic liquids-a contribution to a competitive process design.* Green Chemistry, 2010. **12**(4): p. 602-608.
64. Knudsen, K.G., Cooper, B.H., and Topsøe, H., *Catalyst and process technologies for ultra low sulfur diesel.* Applied Catalysis A: General, 1999. **189**(2): p. 205-215.
65. Ma, X., Sakanishi, K., and Mochida, I., *Hydrodesulfurization reactivities of various sulfur compounds in diesel fuel.* Industrial & Engineering Chemistry Research, 1994. **33**(2): p. 218-222.

66. Hernández-Maldonado, A.J. and Yang, R.T., *Desulfurization of Commercial Liquid Fuels by Selective Adsorption via π-Complexation with Cu(I)−Y Zeolite.* Industrial & Engineering Chemistry Research, 2003. **42**(13): p. 3103-3110.
67. Kim, J.H., Ma, X.L., Zhou, A.N., and Song, C.S., *Ultra-deep desulfurization and denitrogenation of diesel fuel by selective adsorption over three different adsorbents: A study on adsorptive selectivity and mechanism.* Catalysis Today, 2006. **111**(1-2): p. 74-83.
68. Kirimura, K., Furuya, T., Nishii, Y., Ishii, Y., Kino, K., and Usami, S., *Biodesulfurization of dibenzothiophene and its derivatives through the selective cleavage of carbon-sulfur bonds by a moderately thermophilic bacterium Bacillus subtilis WU-S2B.* Journal of Bioscience and Bioengineering, 2001. **91**(3): p. 262-266.
69. Kirimura, K., Furuya, T., Sato, R., Ishii, Y., Kino, K., and Usami, S., *Biodesulfurization of naphthothiophene and benzothiophene through selective cleavage of carbon-sulfur bonds by Rhodococcus sp strain WU-K2R.* Applied and Environmental Microbiology, 2002. **68**(8): p. 3867-3872.
70. Bhatia, S. and Sharma, D.K., *Biodesulfurization of dibenzothiophene, its alkylated derivatives and crude oil by a newly isolated strain Pantoea agglomerans D23W3.* Biochemical Engineering Journal, 2010. **50**(3): p. 104-109.
71. Shiraishi, Y., Tachibana, K., Taki, Y., Hirai, T., and Komasawa, I., *A Novel Desulfurization Process for Fuel Oils Based on the Formation and Subsequent Precipitation of S-Alkylsulfonium Salts. 2. Catalytic-Cracked Gasoline.* Industrial & Engineering Chemistry Research, 2001. **40**(4): p. 1225-1233.
72. Otsuki, S., Nonaka, T., Takashima, N., Qian, W., Ishihara, A., Imai, T., and Kabe, T., *Oxidative Desulfurization of Light Gas Oil and Vacuum Gas Oil by Oxidation and Solvent Extraction.* Energy & Fuels, 2000. **14**(6): p. 1232-1239.
73. Yazu, K., Yamamoto, Y., Furuya, T., Miki, K., and Ukegawa, K., *Oxidation of Dibenzothiophenes in an Organic Biphasic System and Its Application to Oxidative Desulfurization of Light Oil.* Energy & Fuels, 2001. **15**(6): p. 1535-1536.
74. Al-Shahrani, F., Xiao, T., Llewellyn, S.A., Barri, S., Jiang, Z., Shi, H., Martinie, G., and Green, M.L.H., *Desulfurization of diesel via the H2O2 oxidation of aromatic sulfides to sulfones using a tungstate catalyst.* Applied Catalysis B: Environmental, 2007. **73**(3-4): p. 311-316.
75. Shiraishi, Y., Hirai, T., and Komasawa, I., *Identification of desulfurization products in the photochemical desulfurization process for benzothiophenes and dibenzothiophenes from light oil using an organic two-phase extraction system.* Industrial & Engineering Chemistry Research, 1999. **38**(9): p. 3300-3309.
76. Te, M., Fairbridge, C., and Ring, Z., *Oxidation reactivities of dibenzothiophenes in polyoxometalate/H2O2 and formic acid/H2O2 systems.* Applied Catalysis A: General, 2001. **219**(1-2): p. 267-280.
77. Zhu, W.S., Li, H.M., Hang, X., Yan, Y.S., Lu, H.D., and Xia, J.X., *Oxidative desulfurization of fuels catalyzed by peroxotungsten and peroxomolybdenum complexes in ionic liquids.* Energy & Fuels, 2007. **21**(5): p. 2514-2516.
78. Xu, D., Zhu, W.S., Li, H.M., Zhang, J.T., Zou, F., Shi, H., and Yan, Y.S., *Oxidative Desulfurization of Fuels Catalyzed by V2O5 in Ionic Liquids at Room Temperature.* Energy & Fuels, 2009. **23**: p. 5929-5933.

79. Lu, L., Cheng, S., Gao, J., Gao, G., and He, M.-y., *Deep Oxidative Desulfurization of Fuels Catalyzed by Ionic Liquid in the Presence of H2O2.* Energy & Fuels, 2006. **21**(1): p. 383-384.
80. Li, H.M., He, L.N., Lu, J.D., Zhu, W.S., Jiang, X., Wang, Y., and Yan, Y.S., *Deep Oxidative Desulfurization of Fuels Catalyzed by Phosphotungstic Acid in Ionic Liquids at Room Temperature.* Energy & Fuels, 2009. **23**(3): p. 1354-1357.
81. Zhu, W.S., Li, H.M., Jiang, X., Yan, Y.S., Lu, J.D., He, L.N., and Xia, J.X., *Commercially available molybdic compound-catalyzed ultra-deep desulfurization of fuels in ionic liquids.* Green Chemistry, 2008. **10**(6): p. 641-646.
82. Chen, L., Guo, S., and Zhao, D., *Oxidation of Thiophenes over Silica Gel in Hydrogen Peroxide/Formic Acid System.* Chinese Journal of Chemical Engineering, 2006. **14**(6): p. 835-838.
83. Collins, F.M., Lucy, A.R., and Sharp, C., *Oxidative desulphurisation of oils via hydrogen peroxide and heteropolyanion catalysis.* Journal of Molecular Catalysis A: Chemical, 1997. **117**(1-3): p. 397-403.
84. Komintarachat, C. and Trakarnpruk, W., *Oxidative Desulfurization Using Polyoxometalates.* Industrial & Engineering Chemistry Research, 2006. **45**(6): p. 1853-1856.
85. Li, H.M., Zhu, W.S.A., Wang, Y., Zhang, J.T., Lu, J.D., and Yan, Y.S., *Deep oxidative desulfurization of fuels in redox ionic liquids based on iron chloride.* Green Chemistry, 2009. **11**(6): p. 810-815.
86. Viveros-García, T., Ochoa-Tapia, J.A., Lobo-Oehmichen, R., de los Reyes-Heredia, J.A., and Pérez-Cisneros, E.S., *Conceptual design of a reactive distillation process for ultra-low sulfur diesel production.* Chemical Engineering Journal, 2005. **106**(2): p. 119-131.
87. Wu, Z. and Ondruschka, B., *Ultrasound-assisted oxidative desulfurization of liquid fuels and its industrial application.* Ultrasonics Sonochemistry, 2010. **17**(6): p. 1027-1032.
88. Dai, Y., Qi, Y., and Zhao, D., *A Novel Technology for Desulfurization of FCC Diesel Fuels: Combination of Hydrogenation and Oxidation-assisted Ultrasound.* Petroleum Science and Technology, 2010. **28**(2): p. 146-154.
89. Shiraishi, Y., Tachibana, K., Hirai, T., and Komasawa, I., *Photochemical Production of Biphenyls from Oxidized Sulfur Compounds Obtained by Oxidative Desulfurization of Light Oils.* Energy & Fuels, 2002. **17**(1): p. 95-100.
90. Shiraishi, Y., Hirai, T., and Komasawa, I., *Novel desulfurization and simultaneous denitrogenation processes for fuel oils by alkylation and precipitation.* Kagaku Kogaku Ronbunshu, 2002. **28**(3): p. 231-240.
91. Kulkarni, P.S. and Afonso, C.A.M., *Deep desulfurization of diesel fuel using ionic liquids: current status and future challenges.* Green Chemistry, 2010. **12**(7): p. 1139-1149.
92. Lin, L., Zhang, Y., and Li, H., *Pervaporation and sorption behavior of zeolite-filled polyethylene glycol hybrid membranes for the removal of thiophene species.* Journal of Colloid and Interface Science, 2010. **350**(1): p. 355-360.
93. Agarwal, P. and Sharma, D.K., *Comparative Studies on the Bio-desulfurization of Crude Oil with Other Desulfurization Techniques and Deep Desulfurization through Integrated Processes.* Energy & Fuels, 2010. **24**(1): p. 518-524.

94. Alonso, L., Arce, A., Francisco, M.a., and Soto, A., *Liquid−Liquid Equilibria for [C8mim][NTf2] + Thiophene + 2,2,4-Trimethylpentane or + Toluene.* Journal of Chemical & Engineering Data, 2008. **53**(8): p. 1750-1755.
95. Schmidt, R., *[bmim]AlCl4 Ionic Liquid for Deep Desulfurization of Real Fuels.* Energy & Fuels, 2008. **22**(3): p. 1774-1778.
96. Francisco, M., Arce, A., and Soto, A., *Ionic liquids on desulfurization of fuel oils.* Fluid Phase Equilibria, 2010. **294**(1-2): p. 39-48.
97. Mochizuki, Y. and Sugawara, K., *Removal of Organic Sulfur from Hydrocarbon Resources Using Ionic Liquids.* Energy & Fuels, 2008. **22**(5): p. 3303-3307.
98. Gao, H.S., Xing, J.M., Li, Y.G., Li, W.L., Liu, Q.F., and Liu, H.Z., *Desulfurization of Diesel Fuel by Extraction with Lewis-Acidic Ionic Liquid.* Separation Science and Technology, 2009. **44**(4): p. 971-982.
99. Su, B.-M., Zhang, S., and Zhang, Z.C., *Structural Elucidation of Thiophene Interaction with Ionic Liquids by Multinuclear NMR Spectroscopy.* The Journal of Physical Chemistry B, 2004. **108**(50): p. 19510-19517.
100. Alonso, L., Arce, A., Francisco, M., and Soto, A., *Thiophene separation from aliphatic hydrocarbons using the 1-ethyl-3-methylimidazolium ethylsulfate ionic liquid.* Fluid Phase Equilibria, 2008. **270**(1-2): p. 97-102.
101. Wang, Y., Li, H., Zhu, W., Jiang, X., He, L., Lu, J., and Yan, Y., *The Extractive Desulfurization of Fuels Using Ionic Liquids Based on FeCl3.* Petroleum Science and Technology, 2010. **28**(12): p. 1203-1210.
102. Alonso, L., Arce, A., Francisco, M., and Soto, A., *Phase behaviour of 1-methyl-3-octylimidazolium bis[trifluoromethylsulfonyl]imide with thiophene and aliphatic hydrocarbons: The influence of n-alkane chain length.* Fluid Phase Equilibria, 2008. **263**(2): p. 176-181.
103. Cassol, C., Umpierre, A., Ebeling, G., Ferrera, B., Chiaro, S., and Dupont, J., *On the Extraction of Aromatic Compounds from Hydrocarbons by Imidazolium Ionic Liquids.* International Journal of Molecular Sciences, 2007. **8**(7): p. 593-605.
104. Alonso, L., Arce, A., Francisco, M., and Soto, A., *Measurement and Correlation of Liquid−Liquid Equilibria of Two Imidazolium Ionic Liquids with Thiophene and Methylcyclohexane.* Journal of Chemical & Engineering Data, 2007. **52**(6): p. 2409-2412.
105. Asumana, C., Yu, G., Li, X., Zhao, J., Liu, G., and Chen, X., *Extractive desulfurization of fuel oils with low-viscosity dicyanamide-based ionic liquids.* Green Chemistry, 2010. **12**(11): p. 2030-2037.
106. Holbrey, J.D., Reichert, W.M., Nieuwenhuyzen, M., Sheppard, O., Hardacre, C., and Rogers, R.D., *Liquid clathrate formation in ionic liquid-aromatic mixtures.* Chemical Communications, 2003(4): p. 476-477.
107. Holbrey, J.D., Lopez-Martin, I., Rothenberg, G., Seddon, K.R., Silvero, G., and Zheng, X., *Desulfurisation of oils using ionic liquids: selection of cationic and anionic components to enhance extraction efficiency.* Green Chemistry, 2008. **10**(1): p. 87-92.
108. Diedenhofen, M. and Klamt, A., *COSMO-RS as a tool for property prediction of IL mixtures--A review.* Fluid Phase Equilibria, 2010. **294**(1-2): p. 31-38.
109. Eckert, F. and Klamt, A., *Fast solvent screening via quantum chemistry: COSMO-RS approach.* AIChE Journal, 2002. **48**(2): p. 369-385.

110. Klamt, A., *Conductor-like Screening Model for Real Solvents: A New Approach to the Quantitative Calculation of Solvation Phenomena.* The Journal of Physical Chemistry, 1995. **99**(7): p. 2224-2235.
111. Klamt, A., *"COSMO-RS from quantum chemistry to fluid phase thermodynamics and drug design.* Amsterdam Elsevier 2005.
112. Klamt, A. and Eckert, F., *COSMO-RS: a novel and efficient method for the a priori prediction of thermophysical data of liquids.* Fluid Phase Equilibria, 2000. **172**(1): p. 43-72.
113. Klamt, A., Eckert, F., and Arlt, W., *COSMO-RS: An Alternative to Simulation for Calculating Thermodynamic Properties of Liquid Mixtures.* Annual Review of Chemical and Biomolecular Engineering, 2010. **1**(1): p. 101-102.
114. Eckert, F.K., A., *COSMOtherm. Version C2.1, Release 01.05.* COSMOlogic GmbH & Co. Kg: Leverkusen, Germany, 2005.
115. Eckert, F., *COSMOtherm user's manual version C2.1, Release 01.05.* COSMOlogic GmbH & Co. Kg: Leverkusen, Germany, 2005.
116. Diedenhofen, M., Eckert, F., and Klamt, A., *Prediction of Infinite Dilution Activity Coefficients of Organic Compounds in Ionic Liquids Using COSMO-RS†.* Journal of Chemical & Engineering Data, 2003. **48**(3): p. 475-479.
117. Freire, M.G., Santos, L.M.N.B.F., Marrucho, I.M., and Coutinho, J.A.P., *Evaluation of COSMO-RS for the prediction of LLE and VLE of alcohols + ionic liquids.* Fluid Phase Equilibria, 2007. **255**(2): p. 167-178.
118. Marsh, K., Deev, A., Wu, A., Tran, E., and Klamt, A., *Room temperature ionic liquids as replacements for conventional solvents – A review.* Korean Journal of Chemical Engineering, 2002. **19**(3): p. 357-362.
119. Domanska, U., Pobudkowska, A., and Eckert, F., *Liquid-liquid equilibria in the binary systems (1,3-dimethylimidazolium, or 1-butyl-3-methylimidazolium methylsulfate + hydrocarbons).* Green Chemistry, 2006. **8**(3): p. 268-276.
120. Domanska, U., Pobudkowska, A., and Eckert, F., *(Liquid + liquid) phase equilibria of 1-alkyl-3-methylimidazolium methylsulfate with alcohols, or ethers, or ketones.* The Journal of Chemical Thermodynamics, 2006. **38**(6): p. 685-695.
121. Najdanovic-Visak, V., Esperança, J.M.S.S., Rebelo, L.P.N., Nunes da Ponte, M., Guedes, H.J.R., Seddon, K.R., de Sousa, H.C., and Szydlowski, J., *Pressure, Isotope, and Water Co-solvent Effects in Liquid−Liquid Equilibria of (Ionic Liquid + Alcohol) Systems.* The Journal of Physical Chemistry B, 2003. **107**(46): p. 12797-12807.
122. Freire, M.G., Carvalho, P.J., Gardas, R.L., Marrucho, I.M., Santos, L.M.N.B.F., and Coutinho, J.A.P., *Mutual Solubilities of Water and the [Cnmim][Tf2N] Hydrophobic Ionic Liquids.* The Journal of Physical Chemistry B, 2008. **112**(6): p. 1604-1610.
123. Schafer, A., Klamt, A., Sattel, D., Lohrenz, J.C.W., and Eckert, F., *COSMO Implementation in TURBOMOLE: Extension of an efficient quantum chemical code towards liquid systems.* Physical Chemistry Chemical Physics, 2000. **2**(10): p. 2187-2193.
124. Ahlrichs, R., Bär, M., Häser, M., Horn, H., and Kölmel, C., *Electronic structure calculations on workstation computers: The program system turbomole.* Chemical Physics Letters, 1989. **162**(3): p. 165-169.

125. Schafer, A., Huber, C., and Ahlrichs, R., *Fully optimized contracted Gaussian-basis sets of triple zeta valence quality for atoms Li to Kr.* Journal of Chemical Physics, 1994. **100**(8): p. 5829-5835.
126. Anantharaj, R. and Banerjee, T., *COSMO-RS based predictions for the desulphurization of diesel oil using ionic liquids: Effect of cation and anion combination.* Fuel Processing Technology, 2011. **92**(1): p. 39-52.
127. Banerjee, T., Verma, K.K., and Khanna, A., *Liquid–liquid equilibrium for ionic liquid systems using COSMO-RS: Effect of cation and anion dissociation.* AIChE Journal, 2008. **54**(7): p. 1874-1885.
128. Revelli, A.-L., Mutelet, F., and Jaubert, J.-N.l., *Extraction of Benzene or Thiophene from n-Heptane Using Ionic Liquids. NMR and Thermodynamic Study.* The Journal of Physical Chemistry B, 2010. **114**(13): p. 4600-4608.
129. Alonso, L., Arce, A., Francisco, M.a., and Soto, A., *Extraction Ability of Nitrogen-Containing Compounds Involved in the Desulfurization of Fuels by Using Ionic Liquids.* Journal of Chemical & Engineering Data, 2010. **55**(9): p. 3262-3267.
130. Rodríguez, H., Francisco, M., Soto, A., and Arce, A., *Liquid-liquid equilibrium and interfacial tension of the ternary system heptane + thiophene + 1-ethyl-3-methylimidazolium bis(trifluoromethanesulfonyl)imide.* Fluid Phase Equilibria, 2010. **298**(2): p. 240-245.
131. Oliveira, L.H.D. and Aznar, M.N., *Phase equilibria in ionic liquids + dibenzothiophene + n-dodecane systems.*, in preparation.
132. Oliveira, L.H.D. and Aznar, M.N., *Liquid-liquid equilibria for {1-ethyl-3-methylimidazolium diethylphosphate or 1-ethyl-3-methylimidazolium ethylsulfate} + 4,6-dimethyldibenzothiophene + dodecane systems at 298.15 and 313.15 K*, in preparation.
133. Oliveira, L.H.D. and Aznar, M.N., *Liquid−Liquid Equilibrium Data in Ionic Liquid + 4-Methyldibenzothiophene + n-Dodecane Systems.* Industrial & Engineering Chemistry Research, 2010. **49**(19): p. 9462-9468.
134. Kumar, A.A.P. and Banerjee, T., *Thiophene separation with ionic liquids for desulphurization: A quantum chemical approach.* Fluid Phase Equilibria, 2009. **278**(1-2): p. 1-8.
135. Arce, A., Francisco, M., and Soto, A., *Evaluation of the polysubstituted pyridinium ionic liquid [hmmpy][Ntf2] as a suitable solvent for desulfurization: Phase equilibria.* The Journal of Chemical Thermodynamics, 2010. **42**(6): p. 712-718.